

PART - II

CHAPTER - IV

MICROHARDNESS OF CRYSTALS (GENERAL)

CHAPTER - IV

MICROHARDNESS OF CRYSTALS (GENERAL)

	<u>PAGE</u>
4.1 Introduction	77
4.2 Definition and Measurements	77
4.3 General Information on Hardness	83
4.4 Variation of hardness with load	87

REFERENCES

4.1 INTRODUCTION

Of all the mechanical properties of materials, hardness is least understood. It may be broadly defined as the ability of one body to resist penetration by another. It is by definition a relative property of a material and depends on the elastic and plastic properties of both the penetrated body and the penetrator. In addition, the comparative hardness of different materials is strongly dependent upon the method of measurement. All hardness tests measure some combination of various material properties, namely elastic modulus, yield stress (which denotes the onset of plastic behaviour or permanent distortion), physical imperfection, impurities and workhardening capacity. The latter is a measure of the increase in stress to continue plastic flow as strain increases. Since each hardness test measures a different combination of these properties, hardness itself is not an absolute quantity and, to be meaningful, any statement of hardness of a body must include the method used for measurements.

4.2 DEFINITIONS AND MEASUREMENTS

From time to time many definitions have been given for hardness but none has been found to be satisfactory for quantitative interpretation of the processes taking

place in indented materials. Tuckerman¹ explained hardness as a hazily conceived aggregate or conglomeration of properties of a material more or less related to each other. The best general definition is given by Ashby² "Hardness is a measure of the resistance to permanent deformation or damage". The general definition of indentation hardness which is related to the various forms of the indenters is the ratio of load applied to the surface area of the indentation. Meyer³ proposed that hardness should be defined as the ratio of load to the projected area of the indentation. Hence the hardness has the dimensions of stress. Spaeth⁴ suggested that hardness should not be defined as stress but as the resistance to indentation in the form of the ratio of the specific surface load to the unrecovered deformation. In short, the hardness of a solid is defined by the resistance function of inner atomic forces (Tertsch⁵). Attempts towards a physical definition of hardness were made by Friedrich⁶, Goldschmidt⁷ and Chatterjee⁸.

Chatterjee⁸ defined indentation hardness as the work done per unit volume of the indentation in a static indentation test for a definite angle of indentation. On the basis of this definition and Meyer's law $P = ad^n$ for spherical indenters, he derived a formula for measurement of hardness. According to Plendl and Gielisse⁹

hardness can be defined as pressure or force per square centimeter, and thus it can be conceived as an energy per unit volume, e.g. the ratio between the input energy and volume of indentation. They have concluded that resistance is a function of the lattice energy per unit volume and called it volumetric lattice energy (U/V) having the dimension ergs/c.c. U is the total cohesive energy of the lattice per mole and V is the molecular volume defined as M/S where M is a molecular weight and S is specific heat. The hardness was thus considered to be the absolute overall hardness. Matkin and Caffyn¹⁰ from their studies on hardness of sodium chloride single crystals containing divalent impurities, correlated hardness with the dislocation theory. They redefined hardness in terms of generation and/or movement of dislocations associated with indentation. It is the measure of the rate at which the dislocations dissipate energy when moving through a crystal lattice. It is now realized that (Westbrook and Conrad¹¹) hardness is not a single property but rather a whole complex of mechanical properties and at the same time a measure of the intrinsic bonding of the material.

Hardness measurements

There are basically four methods to determine hardness of materials. They are as follows :

- (i) Scratch hardness tester,
- (ii) Abrasive method,
- (iii) Dynamic method and
- (iv) Static indentation method.

They are briefly reviewed here.

(i) Scratch hardness

An early method of measuring scratch hardness still in wide use today by mineralogists was developed by Friedrich Mohs in 1822. This gives a relative ranking of minerals based simply on their ability to scratch one another. The Mohs method is not suitable for a general use with materials of hardness greater than 4. Since in this range the intervals are rather closely and unevenly spaced. The modification of this method were overshadowed by other sensitive methods and experiments.

(ii) Abrasive hardness

Abrasive hardness is defined as the resistance to mechanical wear, a measure of which is the amount of material removed from the surface under specific condition. The hardness may be found by the depth of penetration.

(iii) Dynamic hardness

The hardness measurement in this method involves the dynamic deformation of specimen under study and is determined by following different considerations :

- (a) Here a steel sphere or a diamond - tipped hammer is dropped from a given height, and the height to which the ball or hammer rebounds is read on a scale. This is taken to be the measure of hardness. The kinetic energy of a ball or hammer is used up partly in plastically deforming the specimen surface by creating a slight impression and partly in rebound. This test is sometimes referred as 'dynamic rebound test'.
- (b) Here a steel sphere or a diamond - tipped hammer is dropped from a given height, the depth and size of the impression produced and the energy of impact gives ratio of the energy of impact to the volume of the indentation mark.
- (c) Chalmers¹² assessed the surface hardness in terms of the reduction in optical reflectivity when a known amount of sand was allowed to impinge on the surface under standard conditions.

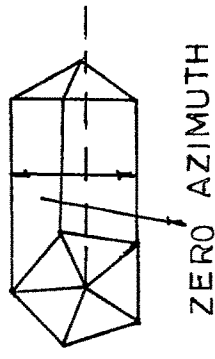
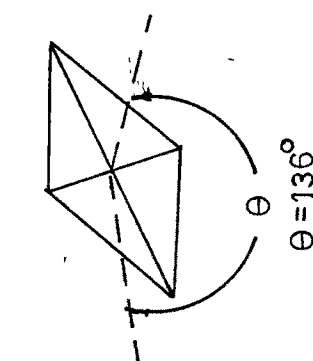
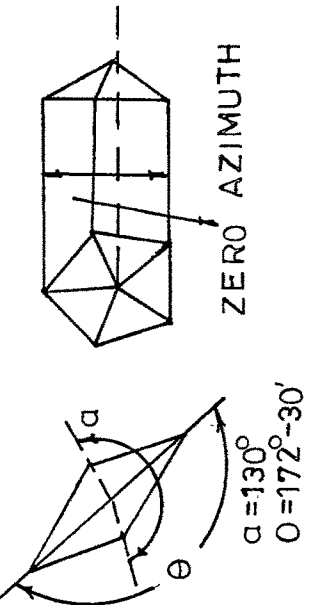
(iv) Static indentation hardness

The most widely used method of hardness testing is the static indentation method. This is the simplest and a very sensitive method in which a hard indenter (e.g. diamond) is applied slowly, and after a certain time of application, carefully removed, leaving behind a permanent indentation mark on the surface of specimen. Measurement is made either of the size of the indentation resulting from a fixed load on the indenter or the load necessary to force the indenter down to predetermined depth and the hardness of material is then defined as the ratio of the load to the area of the indentation mark. The hardness values so obtained vary with the indenter geometry and with the method of calculations.

Many combinations of indenter, load, loading procedure, and means of indentation measurement are used among the various tests in order to accommodate various shapes, sizes and hardness of specimens, and this has resulted in a proliferation of hardness scales. The most commonly used indenters are described in table 4.1. Diamond indenters must be used for hard materials in order to minimize errors due to elastic distortion of the indenter. In case ball indenters are used, the hardness number will be independent of load only when the ratio of load to indenter diameter is held constant. For cone and pyramidal

Table 4.1

	Brinell	Rockwell	Vickers	Knoop	Brookes & Moxley
Material of which indenter is made	Diamond	Hardened steel	Diamond	Diamond	Diamond
Shape of indenter	Sphere	Cone	Sphere	Sphere	Sphere
Dimensions of indenter	$D = 10 \text{ MM}$	$\theta = 120^\circ$	$D = 10 \text{ MM}$	$D = 10 \text{ MM}$	$D = 10 \text{ MM}$
Characteristics	1. Geometrically similar impressions are not obtained	1. Prepares the surface upon which the further penetration due to major load is based 2. Hardness is read directly on the dial gauge 3. Hardness value may be appreciable in error due to large amount of recovery along depth	1. Geometrically similar impressions are obtained	1. Hardness of uppermost surface layers can be found 2. Sensitive to anisotropy of crystals. 3. Shorter diagonal undergoes recovery	1. Eliminates the anisotropy normally observed in hardness with all other indenters.



indenters, hardness number will be independent of load for all loads above a certain minimum value depending upon specimen material.

4.3 GENERAL INFORMATION ON HARDNESS

The hardness study undertaken, so far for studying the strength of solids and the effect of various treatments on the hardness of a solid, have proved somewhat useful. Most of the work has been reported on alkali halides and metals. Previously, hardness studies were made only from the view of materials research but as the expansion in the field of scientific research increased, the study on hardness helped in understanding various other mechanical properties of solids. Gilman and Roberts¹³ correlated indentation hardness with the elastic modulus by gathering the data for various materials. Their empirical linear relation shows that elastic modulus is an important factor which determines plastic resistivity against the dislocation motion. The behaviour of the indented region during the propagation of stresses which initiate dislocations and their motion is not yet understood clearly. When an indenter is pressed on surface of a solid, the stresses are not simply tensile or compressive in nature. Stresses in various directions are set up and the one should treat the resultant plastic

flow as a result of these combined stresses. It is also observed that the fundamental mechanisms of deformation can be either slip or twin or at times fracture.

- (i) Slip is the most common mode of plastic deformation, which is characterised by the displacement of one part of crystal relative to another along certain definite crystallographic planes. The slip planes are usually of low indices and the slip directions are those of closely packed ones in a crystal structure.

- (ii) Certain crystals may also deform by twinning, a mechanism by means of which a portion of a crystal may change lattice orientation with respect to the other in a definite symmetrical fashion. Schmidt and Boas¹⁴ described the twinning as the simple sliding of one plane of atoms over the next, the extent of the movement of each plane being proportional to its distance from the twinning plane. Partridge¹⁵ studied the microhardness anisotropy of magnesium and zinc crystals. He observed twin in above crystals. and concluded that the resolved shear stress criterion is insufficient to account for the observed distribution of twins and any analysis which attempts to relate deformation twinning with hardness

anisotropy must take into account the dimensional changes which occur during twin deformation. Indenting diamond flats with diamond indenter Phaal¹⁶ reported the slip and twinning of diamonds. Vahldick et al.,¹⁷ studied the slip system and twinning in molybdenum carbide single crystals with the help of Knoop and Vickers indenters. When the indented crystal is etched by a dislocation etchant rosettes are formed on some crystals (usually alkali halide) indicating the dislocation distribution around an indentation. Dislocation loops are also formed around the indentation mark in cesium iodide and sodium chloride (Urusovskaya¹⁸ and Kubo¹⁹).

Many workers have proposed some or other explanation for the microcrack formation during indentation of a crystal surface. Smakula and Klein²⁰ from their punching experiments on a sodium chloride explained the crack formation on the basis of shear on slip planes. Gilman²¹ attributed these microcracks which have a definite crystallographic direction to the piling up of dislocation on the slip plane. Breidith et al.,²² observed that crack formation is less at higher temperature (375°C) than at lower temperature (25°C). The cracks are usually observed to propagate from the corner of the impression.

The interferometric studies of indented surfaces have revealed the nature of deformation and the history of the sample under test. Votava et al.,²³ were the first to study the deformed region on the cleavage faces of mica and sodium chloride. Tolansky and Nickols²⁴ studied the indented surfaces of steel, tin and bismuth. They observed maximum distortion along the medians bisecting sides of the square and minimum along diagonals, showing thereby that no distortion projects beyond the diagonal. They established interferometrically that the symmetry in the fringe pattern is purely crystallographic and depends on the previous history of samples, and has nothing to do with the orientation of the square of indentation mark. They (1949) concluded that the convex sides, corresponding to extended wings in the interference pattern were 'piled-up' regions and concave sides were 'sunked-in' regions. Satyanarayan²⁵ observed barrel or pin-cushion shape of indentation marks interferometrically and gave idea about 'sinking-in' which occurs mostly at faces with very little along the diagonals of the indentation mark.

In crystalline material plastic deformation or slip occurs through the movement of line imperfections called dislocations. As dislocations are multiplied (by one of several mechanisms) during deformation, their spacing

decreases and they interact and impede each other's motion, thus leading to work hardening. The strength of dislocation interference depends on the nature of the crystal and on the ratio of temperature of deformation to the melting point of the crystal.

In general, hardening of crystals can be accomplished by introduction of any barrier to dislocation motion. This can occur by (a) work hardening (b) impurity hardening (impurities tend to segregate to dislocations and pin them) (c) decreasing grain size in a polycrystal (grain boundaries are barriers to dislocation motion) (d) dispersion of fine particles of second phase in the crystal and (e) phase transformations (by quenching).

It can be seen from this brief review that the amount of plastic deformation induced in a material by an indenter under load depends in a complicated way on variety of factors which defy simple analysis.

4.4 VARIATION OF HARDNESS WITH LOAD

For geometrically similar shapes of the indent marks for all loads, it can be shown that the hardness is independent of load. However this is experimentally incorrect for certain ranges of applied load. It is clear that during a hardness test the formation of indentation

mark leads to an increase in effective hardness of the material and so the hardness number obtained is not actual hardness of the material in the initial state. This is mainly due to work hardening of the substance during the process of indentation which will be varying with the load. Attempts have been made to determine the absolute hardness by eliminating work hardening. This can be done only, if the method does not appreciably deform the substance plastically. Absolute hardness was found to be one third of the normal hardness by Harrise.²⁶

A large number of workers have studied the variation of hardness with load and the results given are quite confusing. Their findings are summarised below : Knoop et al.,²⁷ ; Bernhardt²⁸ etc. observed an increase in hardness with the decrease in load whereas Campbell et al.²⁹ Mott et al.,³⁰ etc. observed a decrease in hardness with decrease in load. Some authors e.g. Taylor³¹, Bergsman³² reported no significant change of hardness with load. In view of these different observations it has become rather difficult to establish any definite relationship of general validity between microhardness values and applied load.

There are two ways of studying relation between hardness (H) and applied load (P) or relation between load

and diagonal (d) of the indentation mark. An empirical formula is given by equation,

$$P = ad^n \quad \dots (4.1)$$

where ' a ' and ' n ' are constants of the material under test.

From the definition of hardness number,

$$H = rp/d^2 \quad \dots (4.2)$$

where ' r ' is a constant and depends upon the geometry of the indenter. The combination of the above equations yields,

$$H = a_1 d^{n-2} \quad \dots (4.3)$$

$$H = a_2 p^{n-2/n} \quad \dots (4.4)$$

where, $a_1 = ra \quad \dots (4.5)$

$$a_2 = ra^{2/n} \quad \dots (4.6)$$

It has been shown that in case of Vickers micro-hardness the value of the exponent n is equal to 2 for all indenters that give geometrically similar impressions. This implies a constant hardness value for all loads.

Hanemann and Schulz³³ from their observations concluded that in the low load region ' n ' generally has a

value less than two. Onitsch³⁴ found such low values of n (1 to 2) by observing variation of hardness with load while Grodzinski³⁵ found variation of n values from 1.3 to 4.9 ; the value of n was nearly found to be 1.8. The standard hardness values thus obtained were expected to yield constant results but actual results obtained by different workers revealed disparities amounting to 30 - 50%. Due to this variation in the results, a high load region was selected which led to definition of an independent region of microhardness. The hardness values so obtained for this region again showed scattered results even though the apparatus had a good mechanical precision. The scattered observations may be attributed to the following reasons :

- (1) Equation i.e. $P = ad^n$ is not valid.
- (2) Microstructures exercise a considerable influence on measurements involving very small indentations.
- (3) The experimental errors due to mechanical polishing, preparation of specimen, vibrations, loading rate, shape of indenter, measurement of impercession, affect the hardness measurements considerably.

The term connected with the above test, microhardness means microindentation hardness, as it actually refers to

the hardness measurement on the microscopic scale. Some authors prefer the term low load hardness for the above term. This confusion has arisen because these ranges have not been defined sharply. However, three possible regions can be defined as follows :

- (1) Microhardness : From lowest possible loads upto maximum of 200 gms.
- (2) Low load hardness : Loads from 200 gms to 3 kg.
The most characteristic region comprises of loads from 200 gms. to 1 kg.
- (3) Standard hardness : Loads over 3 kg.

Since the present study is made in the region of microhardness as defined in (1) above ; the following presents a brief review of the work reported on microhardness of various crystals.

In the recent work reported by many workers (1960 onwards) the hardness has been found to be increasing at low loads, then remaining constant for a range of higher loads. Murphy³⁶ studied hardness anisotropy in copper crystal ; the variation in hardness by plastic deformation is shown to be in part due to the escape of primary edge dislocations.

Sugita³⁷ while studying the indentation hardness of Ge crystal, found occurrence of ring cracks and radial cracks and that the load required to produce the observable cracks increased with the temperature. The temperature at which the microscopic slip lines become observable was higher in heavily doped crystals than in high purity crystals, indicating that dislocation multiplication was strongly affected by impurities.

Koserich and Bashmakov³⁸ studied the formation of twins produced in Bi, Sb, Bi-Sb, Bi-Sn and Bi-Pb single crystals under action of concentrated load by diamond pyramid microhardness tester. They showed that the length (l) of twins was proportional to the diagonal (d) of the indentation and the intensity of twinning thus given by the coefficient α in the equation

$$l = a + \alpha d$$

The value of α was more for homogeneous alloys and increased with Sb content and remained constant for higher concentration of Sn and Pb.

The variation of hardness with load was also studied by Shah and Mathai³⁹, who explained hardness in terms of slip taking place due to deformation in the crystal (tellurium). Edelman⁴⁰ showed that microhardness of

InSb and GaSb single crystals decreased exponentially with temperature. The presence of deflection points on the curves at 0.45 - 0.50 T_m indicate the deformation by slip. The activation energy for plastic flow in InSb and GaSb was estimated to be 0.6 ev.

Samsonov et al.,⁴¹ studied temperature-dependence of microhardness of titanium carbide in the homogeneity range and found that the hardness decreases with decrease in carbon content in carbide. They also determined the activation energies of dislocation movement by plastic deformation.

Hardness variation was also studied with respect to the impurity content, dislocation density and the change in mobility of dislocation by various workers. Milvidski et al.,⁴² observed decrease in hardness with increase in concentration of impurity and dislocation density in silicon single crystal. Kuz'menko et al.,⁴³ showed decrease in hardness due to change in mobility of dislocations as a result of excitation of electrons during lighting and their transition to higher energetic zone in titanium iodide and termed this a 'photochemical effect'. Beilin and Vekilov⁴⁴ observed decrease in the hardness upto 60% illumination in Ge and Bi. Decrease in hardness was attributed to the induced photoconductivity,

which altered the widths of the dislocation cores at the sample surface and in turn altered the plasticity.

Westbrook and Gilman⁴⁵ studied electrochemical effect in number of semiconductors. They observed decrease in resistance of semiconducting crystals to mechanical indentations in the presence of a small electric potential (0.05 to 10 V) between the indenter and the crystal surface. This was found to be due to significant enhancement of the surface photovoltage by a longitudinal electric field.

The anisotropic nature of microhardness of semiconductor was studied by Tsinzerling et al.,⁴⁶. They observed that the anisotropy was connected with anisotropic bonding and with the position of the cleavage planes relative to the movement of the indenter.

The variation of hardness in number of semiconductors was studied in terms of concentration of charge carrier mobility and their interaction by many workers. Osvenskii et al.,⁴⁷ observed decrease in microhardness due to increase in carrier concentration for different contents of donor and acceptor impurities for GaAs and InSb semiconductors. In addition to this they also showed that decrease in hardness was independent of the type of carrier. Smirnov et al.,⁴⁸ studied the temperature

dependence of carrier density and mobility of Ga crystals after irradiation with electrons and during various stages of annealing. They observed that the microhardness of such crystals did not recover fully their initial value and this was attributed to the interaction between radiation, defects and dislocations, which could act as sinks or condensations for compounds of Frankel pairs. Seltzer⁴⁹ who studied the influence of charged defects on mechanical properties of lead sulphide found that the rosette wing length and hardness were nearly independent of concentration of free electrons in n-type, while it had marked dependence on concentration of holes in p-type. For a hole concentration about $8 \times 10^{-7} \text{ cm}^{-3}$, rapid hardening was observed with attendant decrease in rosette size. It was suggested that this behaviour results from an e.s. interaction between charged dislocations and acceptor point defects.

Perinova and Urusovskaya⁵⁰ studied the hardening of NaCl single crystals by x-rays and found the increase in microhardness by irradiation due to pinning of dislocations in irradiated samples and that the pinning was not destroyed by illumination. The effect of irradiation was also studied by Berzina and Berman⁵¹ who gave a relationship between the length of rays of etch

figure star and proton irradiation done in LiF, NaCl and KCl single crystal.

Because of substantial effect of surface layers on the microhardness, the increase in the microhardness was observed when applied load was reduced (Upit et al.⁵²) They showed the ratio P/l^2 (where l is the length of rays in dislocation rosette around the indentation mark) was not constant (P against l^2 was not linear) at low loads due to retarding influence of the surface on the motion of dislocations. Further they (1970) estimated the change of the mechanical properties of the crystal as the indentation depth decreased on the basis of correlation between the size of an indentation mark and the length of dislocation beam.

The distribution of dislocations around an indentation mark was studied using chemical etch pit technique by Urusovskaya and Tyagaradzhian⁵³. They found large number of prismatic loops. They examined the process of interaction of dislocations in crystals having CsCl lattice. Shukla and Murthy⁵⁴ also studied the distribution of dislocations in NaCl single crystals. They found increase in the distance travelled by leading dislocations with increase in load. They further observed that impurity had

little effect on the dimensions of the indentation but had a pronounced effect on length of the edge rays of the ' star pattern ' and the ratio of the mean diagonal length to mean length of the edge rays was nearly constant. Matkin and Caffyn⁵⁵ observed increase in the hardness with increase in Ca^{++} concentration in NaCl, while the distance travelled by leading dislocation was observed to decrease.

The effect of impurity on hardness was also studied by various workers. Dryden et al.,⁵⁶ studied the hardness of alkali halides when low concentration of divalent cations are incorporated in the crystal lattice on the basis of dielectric measurement of doped alkali halide crystals. They observed following effect of the state of aggregation of the divalent impurities on the critical resolved shear stress. (1) the increase in critical shear stress was proportional to $C^{2/3}$, where C is the concentration of divalent ionvacancy pairs, (2) there was no increase in hardness as these divalent ion-vacancy pairs aggregate into groups of three (trimers), (3) in $\text{NaCl} : \text{Mn}^{++}$, $\text{KCl} : \text{Sr}^{++}$ and $\text{KCl} : \text{Ba}^{++}$ there was no increase in hardness as these trimers grow into large aggregates, (4) in $\text{LiF} : \text{Mg}^{++}$, there was a large increase in hardness as the trimers grow into larger aggregates and

(5) in NaCl : Ca⁺⁺ the hardness increases as a second region of dielectric absorption appears. They have also concluded that the structure of the trimer was same in all these crystals and the trimer can grow in two ways, one of which produces an increase in the resistance to movement of dislocations. Urusovskaya et al.,⁵⁷ investigated the influence of impurity on the strength of crystals, microhardness, length of dislocation rosette rays and velocity of dislocation movement in CsI crystals. Takeuchi and Kitano⁵⁸ reported the softening of NaCl crystal due to introduction of water molecules. The plastic resistance was almost independent of dislocation velocity except at very high velocities. It was, however, strongly influenced by temperature, impurities, radiation damage and structure of core of dislocation. Gilman⁵⁹ observed a sharp drop in plastic resistance of covalent crystal at roughly about two-third of the melting temperature and suggested that the drop was because the cores of dislocation in covalent crystal 'melt' at this temperature.

Temperature dependence of microhardness was also studied by Sarkozi and Vannay⁶⁰. They concluded that besides thermal stress the observed hardening may be due to dislocations piled-up at various impurities, to complexes in solid solution and vacancy clusters which

were developed at high temperature. And by quenching, the clusters become distributed in the crystals as fine dispersions.

Temperature dependence of microhardness was also studied by Shah⁶¹ who found that hardness of calcite cleavage faces increases with the temperature. Acharya⁶² found that the hardness of Zn and KBr decreases with the quenching temperature while the hardness of TGS increases with the quenching temperature.

Comparative study of Vickers and Knoop hardness numbers has been investigated in detail by Mohrnheim⁶³ on metallic materials. An analysis of Knoop microhardness led Hays and Kendall⁶⁴ to modify Meyer's⁶⁵ law correlating applied load to the long Knoop diagonal by term which accounted for the resistance offered by the test specimens. Results were also discussed for usage of modified Meyer's law to obtain Knoop hardness numbers independent of applied load. Comparative study of Knoop and Vickers hardness numbers was also reported by Tietz and Troger⁶⁶.

The above represents a brief review of the work done on hardness of various crystals. The present work is centred on the study of variation of load with diagonal length of indentation mark, of variation of hardness with

load of synthetic sodium nitrate crystals grown from melt at various quenching temperatures by using Knoop and Vickers diamond pyramidal indenters.

REFERENCES

1. Tuckerman, L.B. Mech. Eng. 47, 53-5, 1925.
2. Ashby, N.A. N.Z. Engng., 6, 33, 1951.
3. Meyer, E.F. Verdt^{eu}sch Ing., 52, 645, 1908.
4. Spaeth, W. Physik and Technique der haetre and Weiche, Berlin, 1940.
5. H. Tertsch. Z. Krist., 92, 39-48, 1935;
Neus Jahrb. Mineral ; Monatsh
73-87, 1951

Neus Jahrb. Mineral.; Monatsh
136-44, 1952.
6. Friedrich, F. Portschrtee Chem. Physik,
18, 5-44, 1926.
7. Goldschmidt, V.M. Norske Voð Akad i Oslo Skr
Mat Nat KI # 8, p.102, 1926.
8. Chatterjee, G.P. Ind. J. Phys., 28, 9-20, 1956.
9. Plendl, J.N. and Gielisse, P.J. Phys. Revi., 125, 828-32, 1962.
10. Matkin, D.I. and Caffyn, J.E. Trans. Britt. Ceram. Soc. 62,
753-61, 1963.
11. Westbrook, J.H. and Conrad, H. 'The Science of hardness and
Its Research Applications'.
American Soc. For Metals,
Ohio, 1973.
12. Chalmers, B. J. Inst. Metals, 67, 295-314,
1941.

13. Gilman, J.J. and Roberts, B.W. J. Appl. Phys., 32, 1405, 1961.
14. Schmidt, E. and Boas, W. Naturwiss., 20, 416, 1955.
15. Partridge, P.W. Nature, 203, 634-5, 1964.
16. Phaal, C. Phil. Mag., 10, 887-91, 1964.
17. Vahldick, F.W. Japan, J. Appl. Phys., 5, 663-70, 1966.
18. Urusovskaya, A.A. Sov. Phys. Cryst. 10, 437-41, 1965.
19. Kubo, K. J. Phys. Soc. Japan, 28, 117-87, 1970.
20. Smakula, A. and Klein, M.W. Phys. Rev., 84, 1056, 1951.
21. Gilman, J.J. Trans, AIME, 212, 783-91, 1958.
22. Breidth, P., Greimer, E.S. and Ellise, W.C. Acta, Met., 5, 60-63, 1957.
23. Votava, B., Amelinckx, S. and Dekeysor, W. Physica, 19, 1163-72, 1953.
24. Tolansky, S. and Nickols, D.G. Nature, 164, 840, 1949.
Phil-Mag., 43, 410, 1952.
25. Satyanarayan, B.S. Can. J. Teck., 3, 375-7, 1956.
26. Harrise, P.W. J. Inst. Metals, 27, 1922.

27. Knoop, F. Tech. Blatter, 27, 472-80, 1937.
28. Bernhardt, E.O. Z. Metalkunde, 33, 135-44, 1941.
29. Campbell, R.F., Henderson, and Donleavy, M.R. Trans. Amer. Soc. Metals, 40, 954, 1948.
30. Mott, B.W. 'Microindentation hardness testing', Butterworths Scientific Publications, London, Ch. 1. 1956.
31. Taylor, E.W. J. Inst. Metals, 74, 493-500, 1948.
32. Bergsman, E.W. Metal Progress, 54, 183-88, 1948.
33. Hanemann, H. and Schultz, F. Z. Metalkunde, 33, 124-34, 1941.
34. Onitsch, E.M. Microscopic, 2, 131-4, 1947.
35. Grodzinski, P. Ind. Diamond Rev., 12, 209, 235, 1952.
36. Murphy, R.J. Scripta Metallurgica, (USA) 3, 905-10, 1969.
37. Sugita, Y. Japan, J. Appl. Phys., 10, 951, 1963.
38. Koserich, V.M. and Bashmakov, V.I. Fiz. Metallovi, Metallevnenie, 9, 288-93, 1960.
39. Shah, B.S. and Mathai, M.B. Current Sci. (India), 38, 4780, 1969.

40. Edelman, F.L. Phys. Statussolidi (Germany), 7, K 65-66, 1964.
41. Samsonov, G.V.,
Kovalchenko, V.V.,
Dzemedinskii and
Upadhyay, G.S. Fiz. Tekh., Paluprevachikov, 3, 1760-5, 1969.
42. Milvidski, M.G.,
Osvenskii, V.B.,
Stolyarov, O.G., &
Shylakov, D.B. Fiz. Metallov, Metallovedenie, 20, 150-1, 1965.
43. Kuz'menko, P.P.,
Novykov, N.N. &
Ya. Horydko, N. Ukvayin, Fiz. Zn. (USSR), 8, 116-20, 1963.
44. Beilin, V.M. and
Vekilov, Yu. Kh. Fiz. Tverdogo, Tela, 5 2372-4, 1963.
45. Westbrook, J.J. &
Gilman J.J. J. Phys. Soc, Japan, 18, 15-19, 1963.
46. Tsinzerling, E.G.,
Berkovich, E.S. &
Shaskol'skaya, M.P. Kristallografiya (USSR), 14, 1037-43, 1969.
47. Osvenskii, V.B.,
Milvidskii, M.G.,
Stolyarov, O.G. &
Ivleva, V.S. Fiz. Tverdo, Tela, 10(9), 2809-11, 1968.
48. Smirnov, L.S.,
Stas, V.F. &
Khainovskaya, V.V. Fiz. Tekh. Paluprevachikov, 3, 1760-5, 1969.
49. Seltzer, M.S. J. Appl. Phys., 37, 4780, 1966
50. Perinova, M. &
Urusovskaya, A.A. Czech. J. Phys. B-6, 791-6, 1966.

51. Berzina, I.G.,
Berman, I.B. &
Savintsev, P.A. Sovt. Phys. Crst., 9, 483,
1965.
52. Upit, G.P.,
Varchomiya, S.A. &
Muktepavel, F.O. Fiz. Tverdo, Tela, 11, 2841-5.
1969.
53. Urusovskaya, A.A. &
Tyagaradzhan, R. Kristallographiya, 9, 531-6,
1965.
54. Shukla, S.K. &
Murthy, T.S. Nucl. Phys. and Solid State
Phys. Symp.; Pawai, Bombay
(India), 1968.
55. Matkin, D.X. &
Caffyn, J.E. Trans. Britt. Ceram. Soc.,
62, 753-61, 1963.
56. Dryden, J.S.,
Morimoto, S. &
Cook, J.S. Phil. Mag. (G.B.), 12, 379-91,
1965.
57. Urusovskaya, A.A.,
Dobrzhanskii, G.F.,
Sizova, N.L. and
Govorkov, V.G. Sovt. Phys. Cryst., 13, 6,
1969.
58. Takeuchi, N. &
Kitano, F. Japan J. Appl. Phys., 10,
951, 1971.
59. Gilman, J.J. Surface Chem. Metals and
Semiconductor Symp. ; John
Wiley & Sons N.Y., 1960.
60. Sarkozi, J. &
Vannay, L. Phys. Status Solidi, A, 6,
(Germany), 39-41, 1971.
61. Shah, R.T. Ph.D. Thesis, M.S. Univ. of
Baroda, Baroda, 1976.

62. Acharya, C.T. Ph.D. Thesis, M.S. Univ. of Baroda, Baroda, 1978.
63. Mohrnheim. Prakt. Metallogr. (Germany), 10, 2, 94-97, 1973.
64. Hays, C. & Kendall, E.G. Metallography (USA), 6, 4, 275-82, 1973.
65. Meyer, L. Quoted in 'The Science of hardness Testing and Its Research Applications', Am. Soc. for Metals, Ohio, 1973.
66. Tietz, H.D. & Troger, A. Feingerate Tech. (Germany), 24, 8, 355-57, 1975.

CHAPTER - V

VARIATION OF LOAD WITH

DIAGONAL LENGTH OF INDENTATION MARK

CHAPTER - V

VARIATION OF LOAD WITH

DIAGONAL LENGTH OF INDENTATION MARK

	<u>PAGE</u>
5.1 Introduction	101
5.2 Experimental	102
5.3 Observations	104
5.4 Results and Discussion	104
5.4.1 Characteristics of two straight line regions in the graph	107
5.5 Conclusions	110

REFERENCES

5.1 INTRODUCTION

A variety of useful tests have been devised wherein some kind of mechanical operation is performed on the surface of a specimen. Quantities measured by these surface tests are generally associated with the term 'hardness'. Hardness as applied to amorphous and crystalline materials has long been the subject of discussion amongst engineers, physicists, metallurgists and mineralogists and there are all sorts of conceptions as to what constitute hardness. The overwhelming difficulty of defining hardness is that it does not appear to be a fundamental property of material. There is no universally accepted single test for hardness applicable to all materials. Thus there is hardness as measured by resistance to cutting, by scratching, by penetration, by electrical and magnetic properties (Mott¹). The fundamental physics of hardness is not yet clearly understood. The present work is taken up with the express purpose of critically reexamining the various formulae connected with hardness by systematically studying 'microhardness' of synthetic single crystals of sodium nitrate (NaNO_3). It is an extension of the work reported earlier (Shah², Acharya³, Bhagia⁴). Further it also aims at comparing the hardness values and behaviour of two types of diamond pyramidal indenters viz. Vickers and Knoop indenters on NaNO_3 cleavages. As far as the author is aware

no such systematic work on NaNO_3 crystals is reported so far. In what follows the terms 'hardness' and 'microhardness' of crystals are used to indicate the same meaning.

5.2 EXPERIMENTAL

Single crystals of sodium nitrate grown from melt and solution by methods described in Chapter II were used for the present study. Small crystal cleavages from a big block of rhombohedral sodium nitrate were used in the present investigation. Every time freshly cleaved crystals of approximately equal sizes are used so that a comparison of treated and untreated samples can be easily made without introducing other factors. Freshly cleaved blocks having dimensions 10 mm x 10 mm x 2 mm were fixed on glass plates with an adhesive. The levelling of the specimens was tested by using a table microscope. The hardness tester described in Chapter II was used to produce indentations on a freshly cleaved surface by using square based Vickers pyramidal and rhomb-based Knoop pyramidal indenters. The filar micrometer eyepiece was used to measure the surface dimensions of the indentation marks. In order to avoid the influence of one indentation mark on the other the distance between two consecutive indentations was maintained at least eight times the diagonal length

of mark ; the indentation time for all specimens was kept 15 seconds. The load was varied from 1.25 gm. to 120 gm. Care was taken to see that errors introduced during the work of indentation marks are avoided or minimized. The indentation marks were produced by diamond indenters on the surface in such a way that one of their diagonals always remained parallel to $[100]$ direction on the crystal surface. Further the indentations were produced by Knoop and Vickers indenters on the same sample to facilitate comparison. Due to non-availability of a hot stage and optical components of microscope to be used with it in hardness tester, the indentation work was carried out at room temperature for annealed and/or quenched crystals for studying the variations of hardness with temperature. For these experiments, crystals of approximately equal sizes were used. They were gradually raised to a desired temperature and kept at this temperature for identical periods running into a few hours (24 hours in the present case). They were then quenched to room temperature. The quenching rates were made as high as possible and were adjusted so that the quenched crystals maintained their shapes. In the present case the rate of quenching varied from $1.6^{\circ}\text{C}/\text{sec}$ to $11.6^{\circ}\text{C}/\text{sec}$. These experiments were conducted upto a temperature of 260°C because beyond this temperature sodium nitrate begins to decompose.

5.3 OBSERVATIONS

The diagonals of the indentation marks produced by various load were measured. Several sets consisting of a large number of observations on freshly cleaved surfaces of virgin or thermally treated sodium nitrate crystals indented by various loads at room temperature were taken and a typical set of observations, recorded in Table 5.1 and 5.2 was studied graphically by plotting $\log d$ versus $\log P$. 'd' is the average value of the diagonal length of the indentation mark in microns and P is the load in grams (Figs. 5.1a, b to 5.8a, b). It should be noted that irrespective of the magnitude of the load the impressions of the indentation marks on cleavage surface of NaNO_3 are geometrically similar (Fig. 5.9 (and 5.9b)).

5.4 RESULTS AND DISCUSSIONS

There are two ways of studying the relationship between microhardness and applied loads. One way of studying this relationship was given by Hanemann⁵ in the form of an empirical rule that was believed to permit the intercomparison of microhardness values. This rule states that the load P is related to diagonal length of an indentation mark by the expression

$$P = a d^n \quad \dots (5.1)$$

Table 5.1 (KNOOP INDENTER:)

QUENCHING TEMPERATURE T _Q °K	303	373	398	423	448	473	498	533
Log P	Log dk							
0.0969	1.6899	1.6675	1.6637	1.6595	1.6575	1.6520	1.6441	1.6359
0.3979	1.7690	1.7246	1.7338	1.7312	1.7178	1.7110	1.7178	1.7178
0.6990	1.8461	1.8441	1.8201	1.8359	1.8307	1.8255	1.8201	1.8147
0.8751	1.8848	1.8931	1.8894	1.8707	1.8707	1.8752	1.8894	1.8754
1.0000	1.9116	1.9180	1.9116	1.9100	1.9086	1.9151	1.9202	1.8939
1.1761	1.9908	2.0115	2.0051	2.0000	1.9908	1.9900	1.9872	1.9835
1.3010	2.0790	2.0720	2.0670	2.0625	2.0600	2.0610	2.0578	2.0515
1.4771	2.1781	2.1700	2.1788	2.1693	2.1645	2.1625	2.1650	2.1507
1.6021	2.2197	2.2380	2.2318	2.2276	2.2234	2.2202	2.2170	2.2148
1.6990	2.2809	2.2790	2.2827	2.2809	2.2790	2.2700	2.2668	2.2639
1.7782	2.3263	2.3217	2.3240	2.3183	2.3183	2.3103	2.3148	2.3182
1.8451	2.3598	2.3604	2.3634	2.3650	2.3588	2.3546	2.3541	2.3462
1.9031	2.3944	2.3947	2.3902	2.3931	2.3916	2.3899	2.3878	2.3815
1.9542	2.4262	2.4248	2.4262	2.4181	2.4113	2.4033	2.4030	2.3988
2.0000	2.4495	2.4453	2.4372	2.4316	2.4380	2.4291	2.4275	2.4168

Table 5.2 (VICKERS INDENTER)

QUENCHING TEMPERATURE T _Q °K	303	373	398	423	448	473	498	533
Log P	log dv							
0.0969	1.2339	1.2297	1.2266	1.2245	1.2191	1.2127	1.2094	1.2017
0.3979	1.2919	1.2827	1.2827	1.2885	1.2780	1.2818	1.2734	1.2686
0.6990	1.3740	1.3665	1.3665	1.3642	1.3603	1.3580	1.3568	1.3510
0.8751	1.4538	1.4431	1.4412	1.4380	1.4334	1.4302	1.4269	1.4235
1.0000	1.4932	1.4914	1.4903	1.4874	1.4851	1.4822	1.4798	1.4763
1.1761	1.5687	1.5600	1.5536	1.5466	1.5451	1.5426	1.5395	1.5349
1.3010	1.6277	1.6276	1.6243	1.6234	1.6213	1.6192	1.6175	1.6149
1.4771	1.7279	1.7178	1.7144	1.7075	1.7047	1.7032	1.7005	1.6970
1.6021	1.7867	1.7845	1.7832	1.7815	1.7782	1.7700	1.7753	1.7732
1.6990	1.8492	1.8385	1.8300	1.8330	1.8286	1.8255	1.8233	1.8223
1.7782	1.8952	1.8871	1.8848	1.8801	1.8754	1.8719	1.8700	1.8671
1.8451	1.9165	1.9163	1.9068	1.9073	1.9064	1.9051	1.9040	1.9029
1.9031	1.9451	1.9491	1.9455	1.9481	1.9471	1.9461	1.9437	1.9410
1.9542	1.9780	1.9742	1.9742	1.9733	1.9723	1.9723	1.9706	1.9666
2.0000	1.9962	1.9944	1.9935	1.9926	1.9908	1.9890	1.9890	1.9824
2.0792	2.0420	2.0387	2.0339	2.0330	2.0256	2.0242	2.0086	2.0331

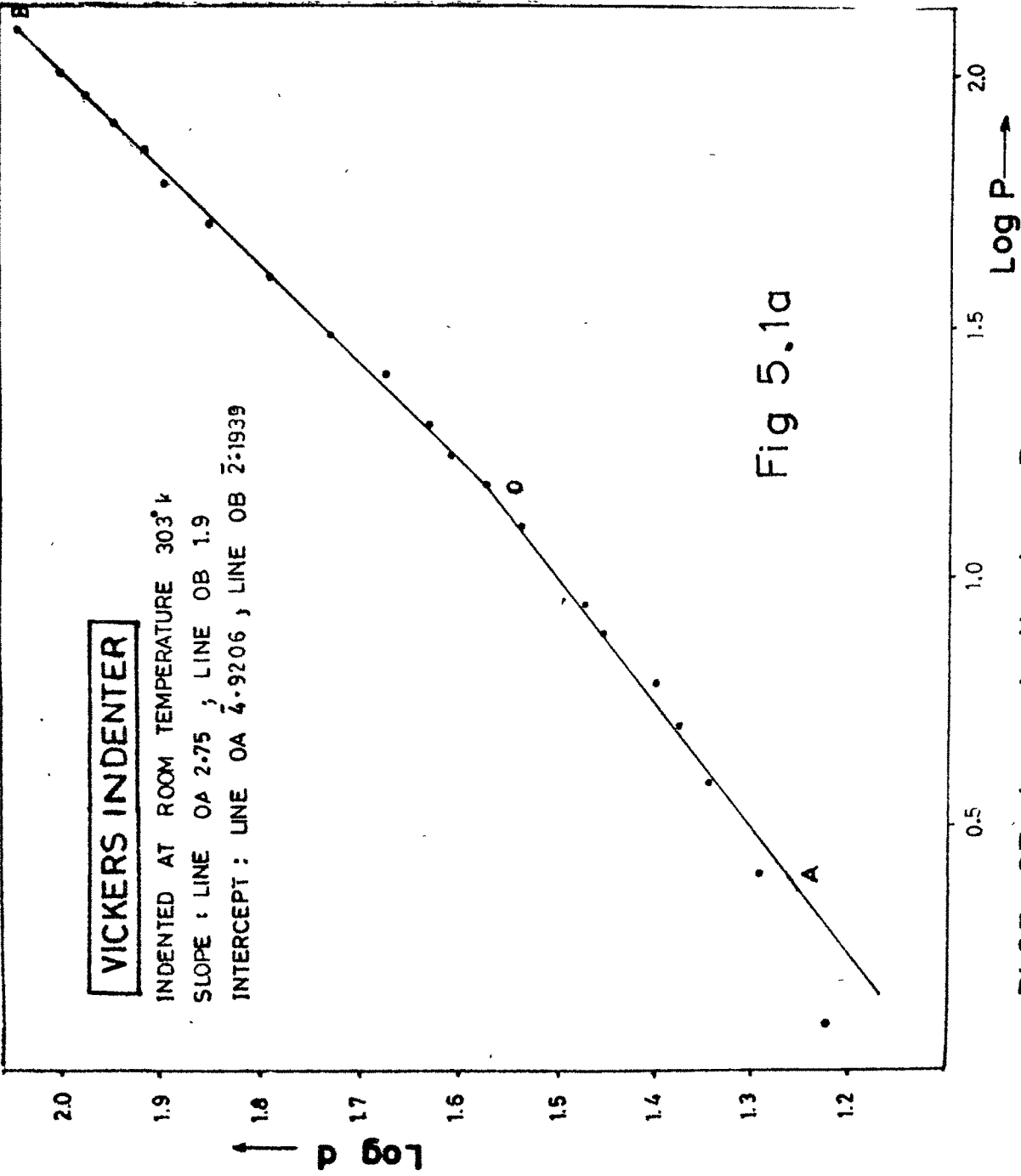
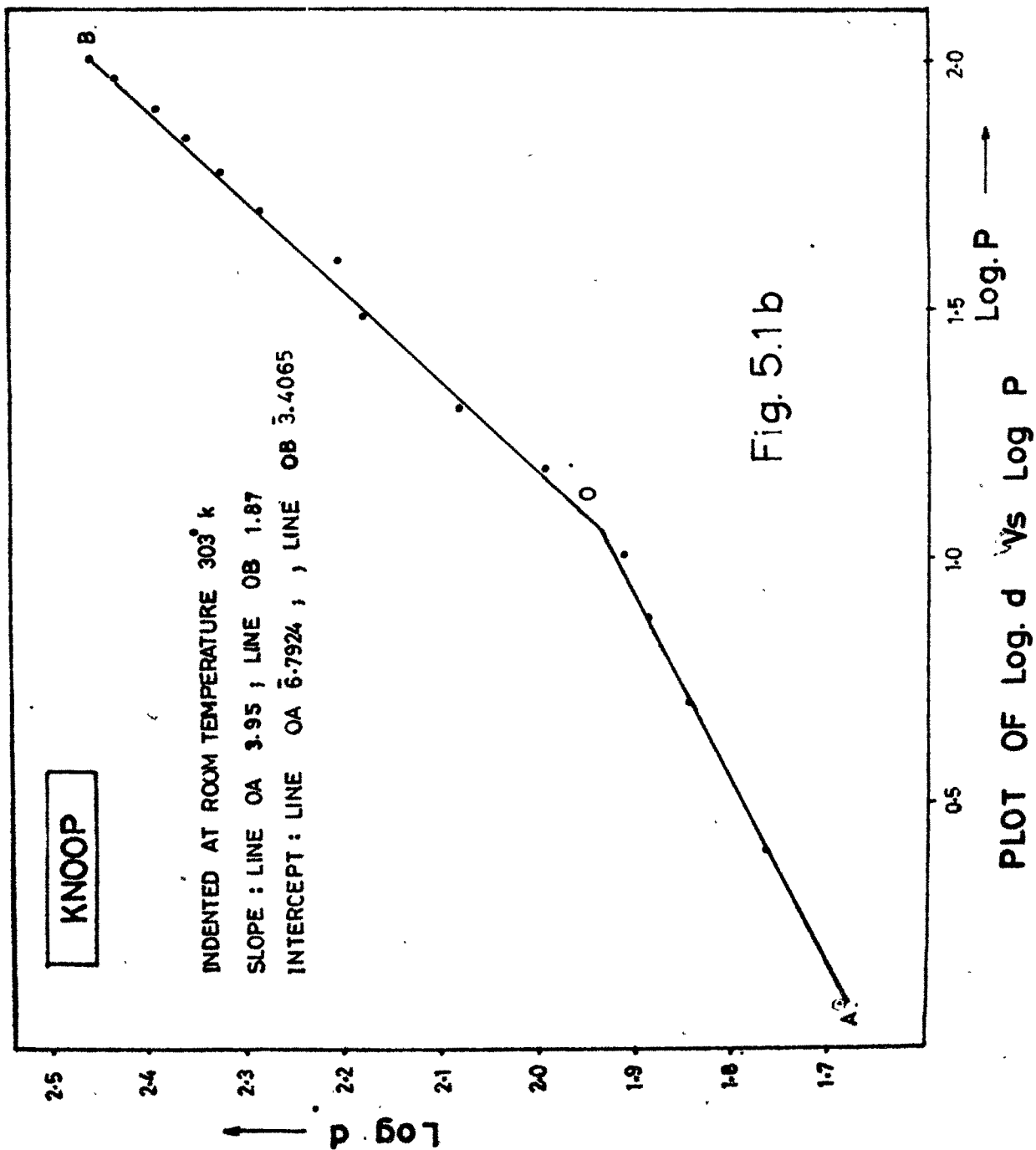
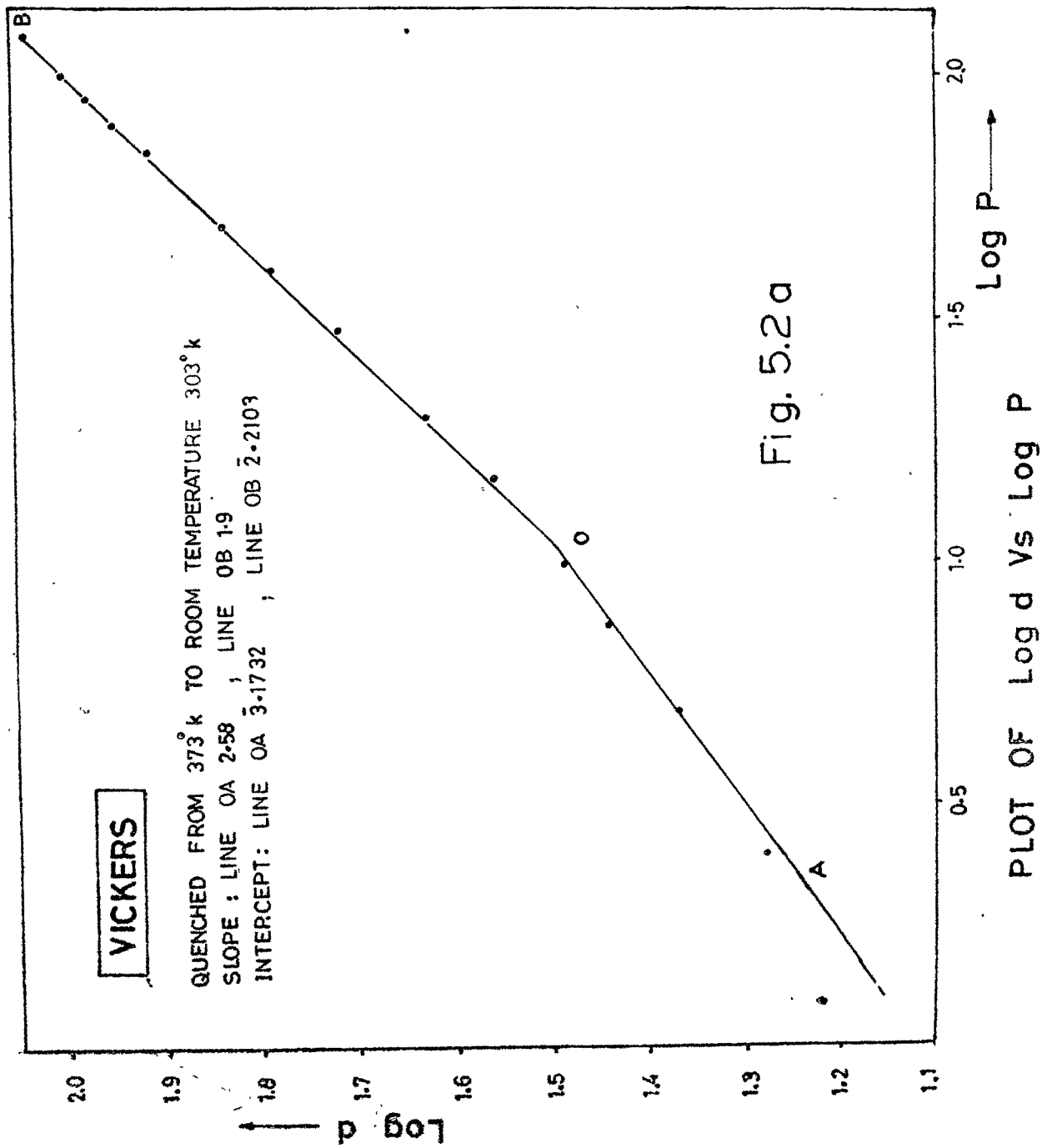
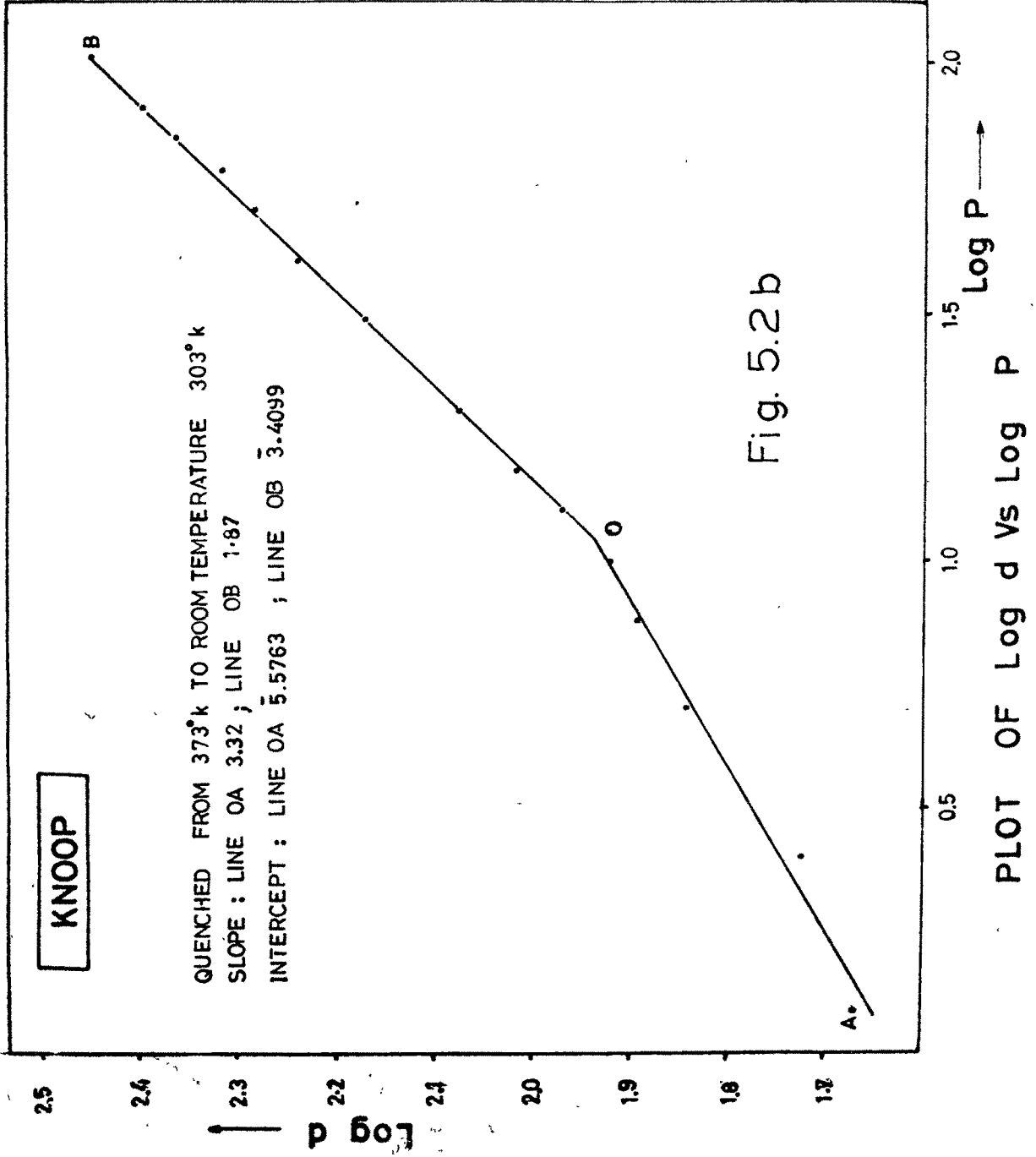


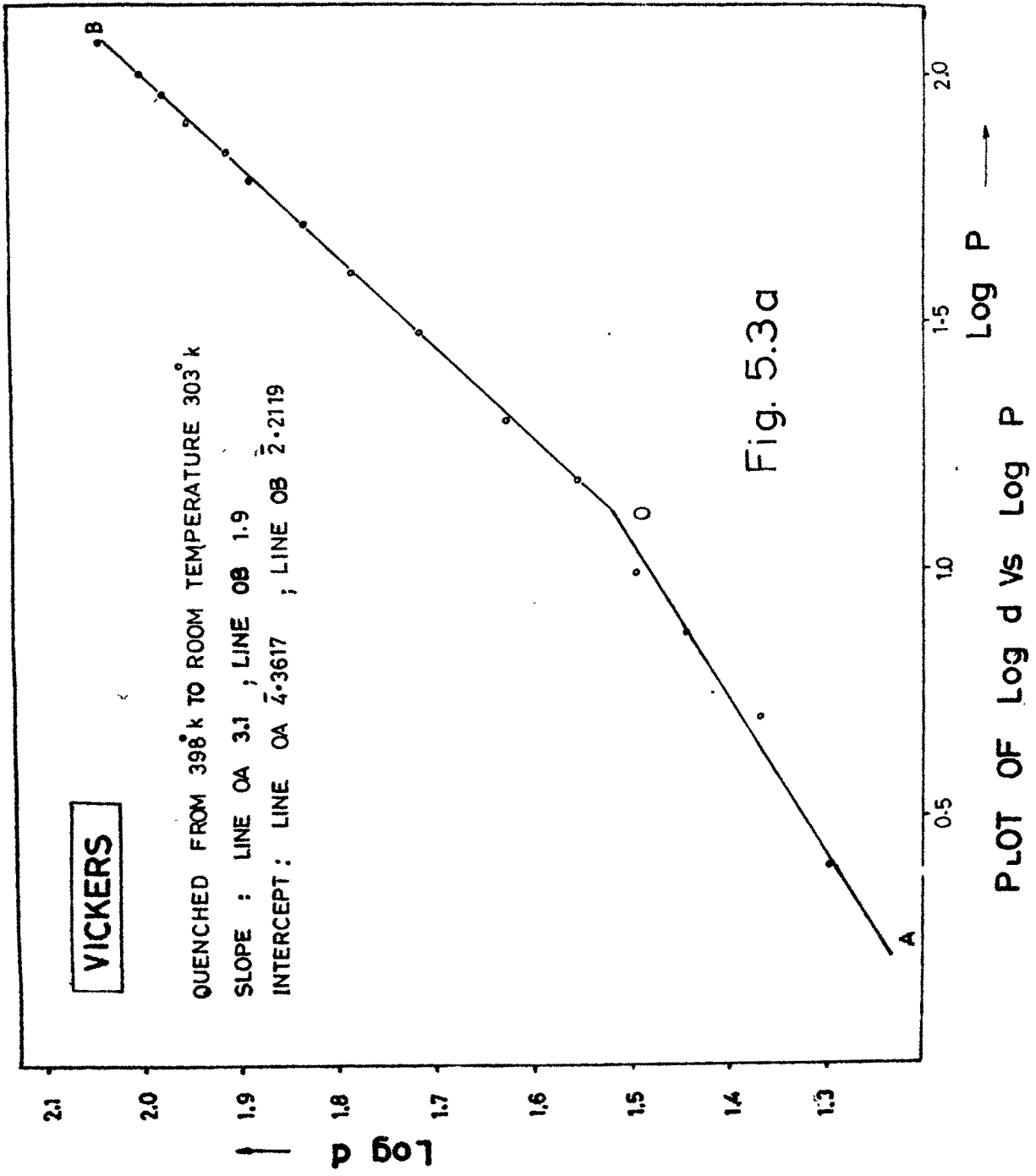
Fig 5.1a

PLOT OF Log d Vs Log P









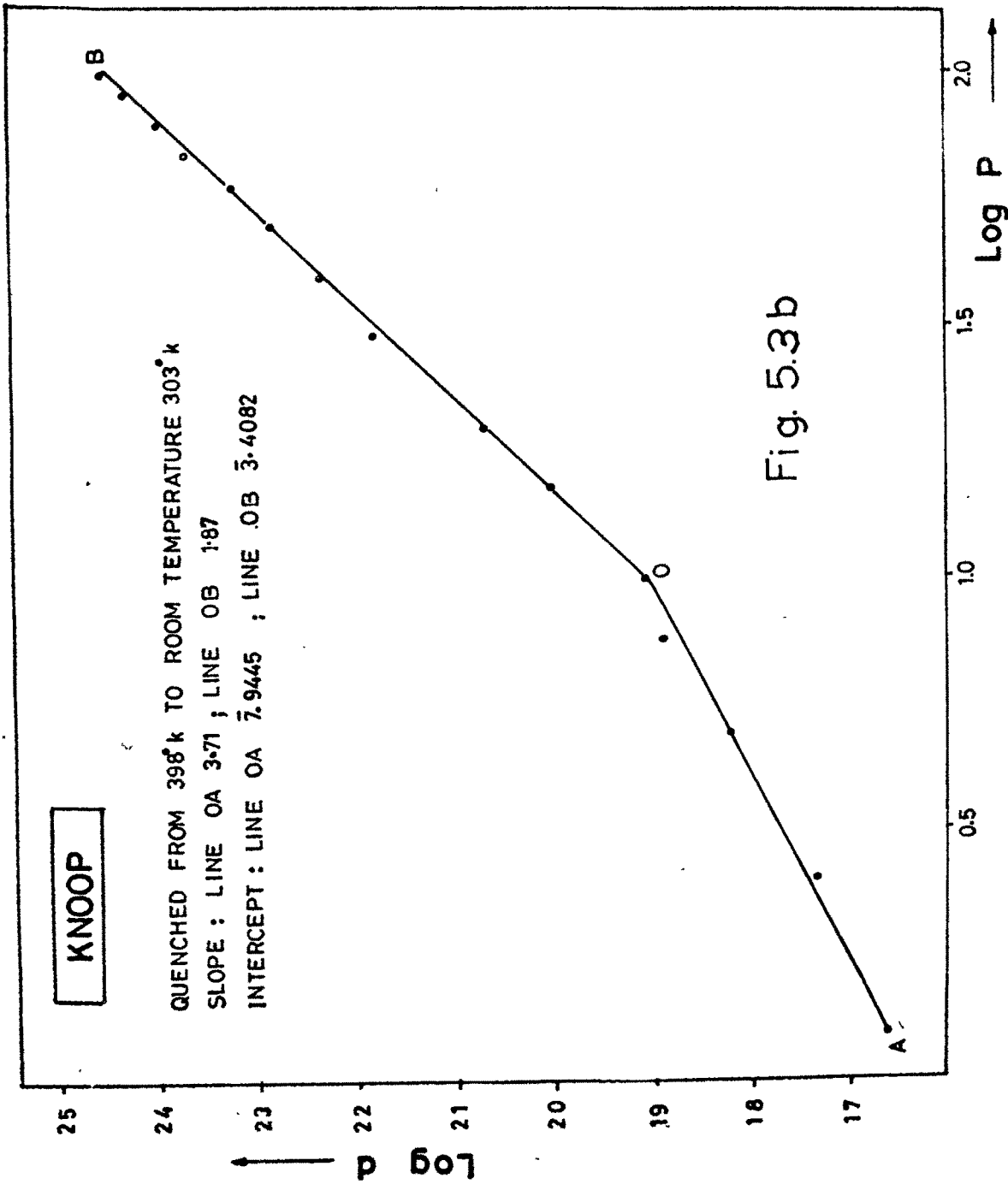
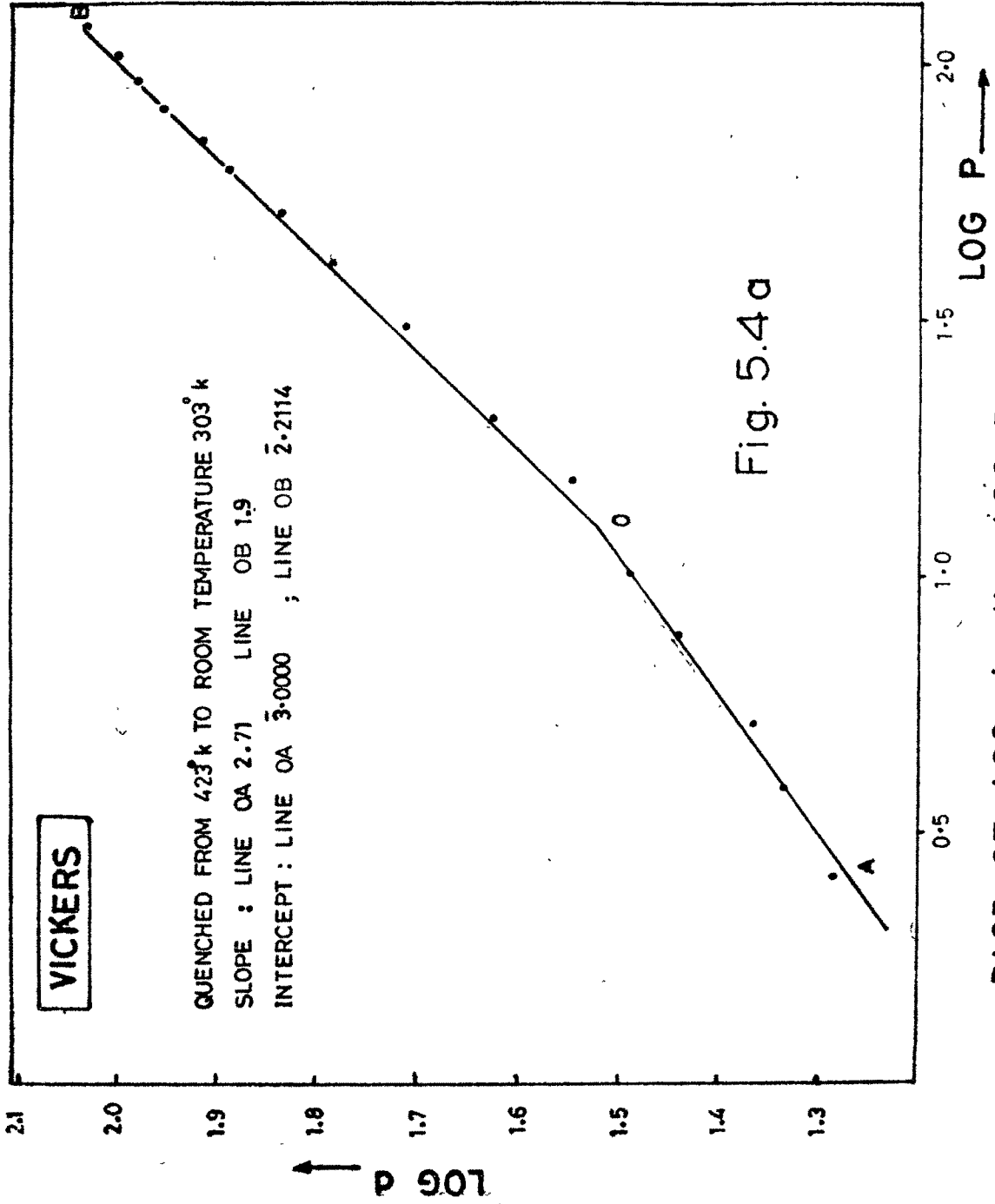
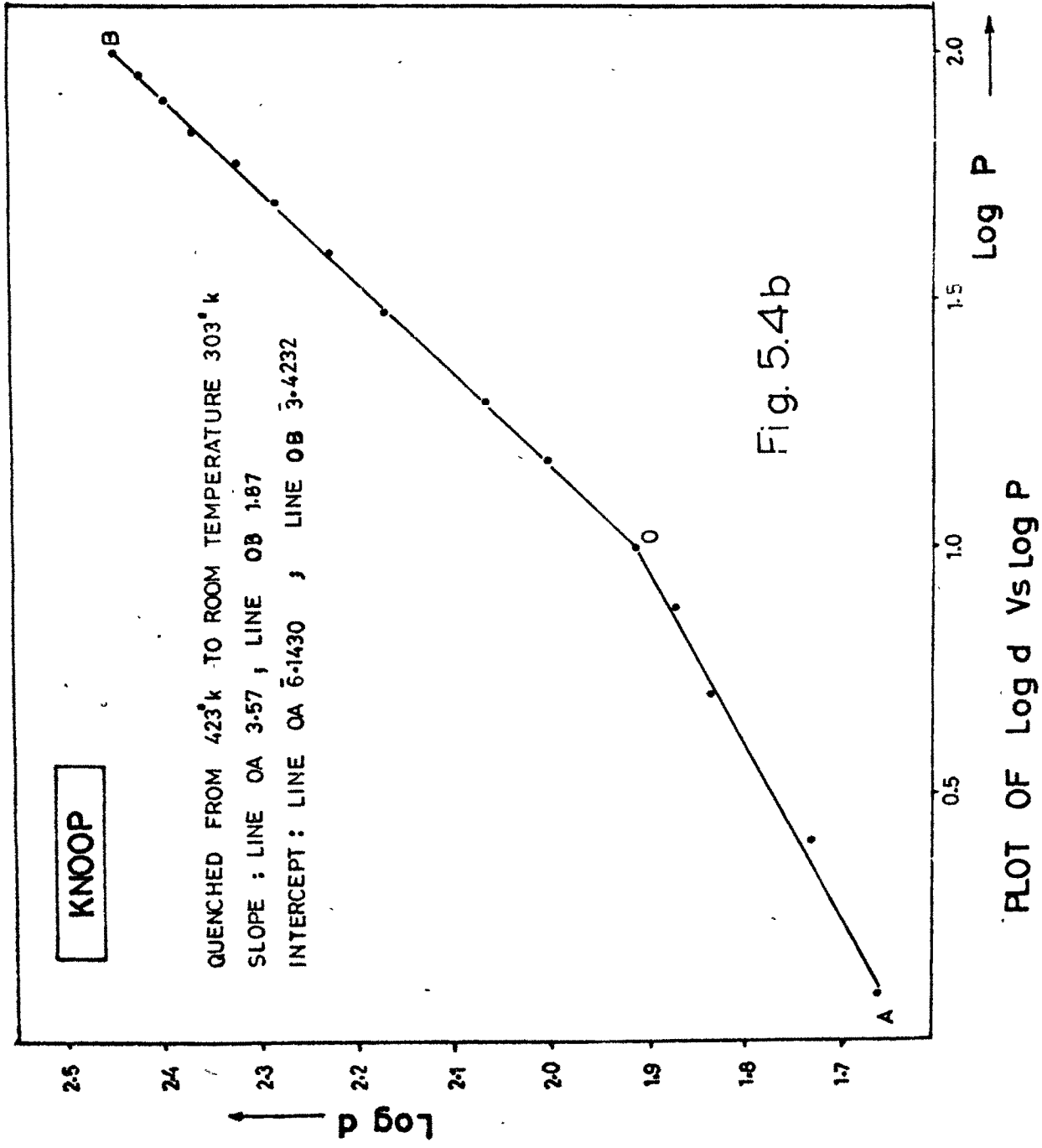


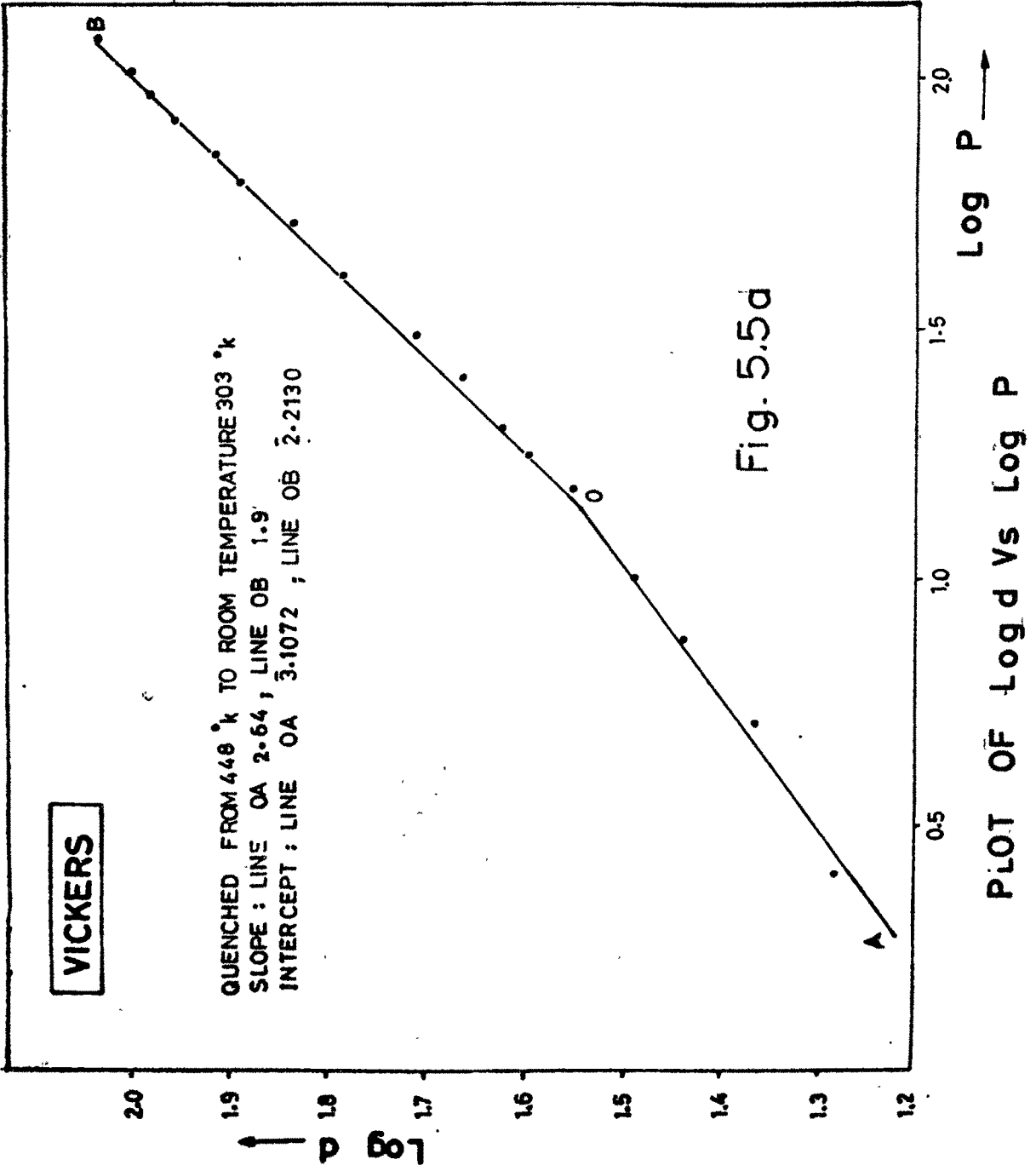
Fig. 5.3b

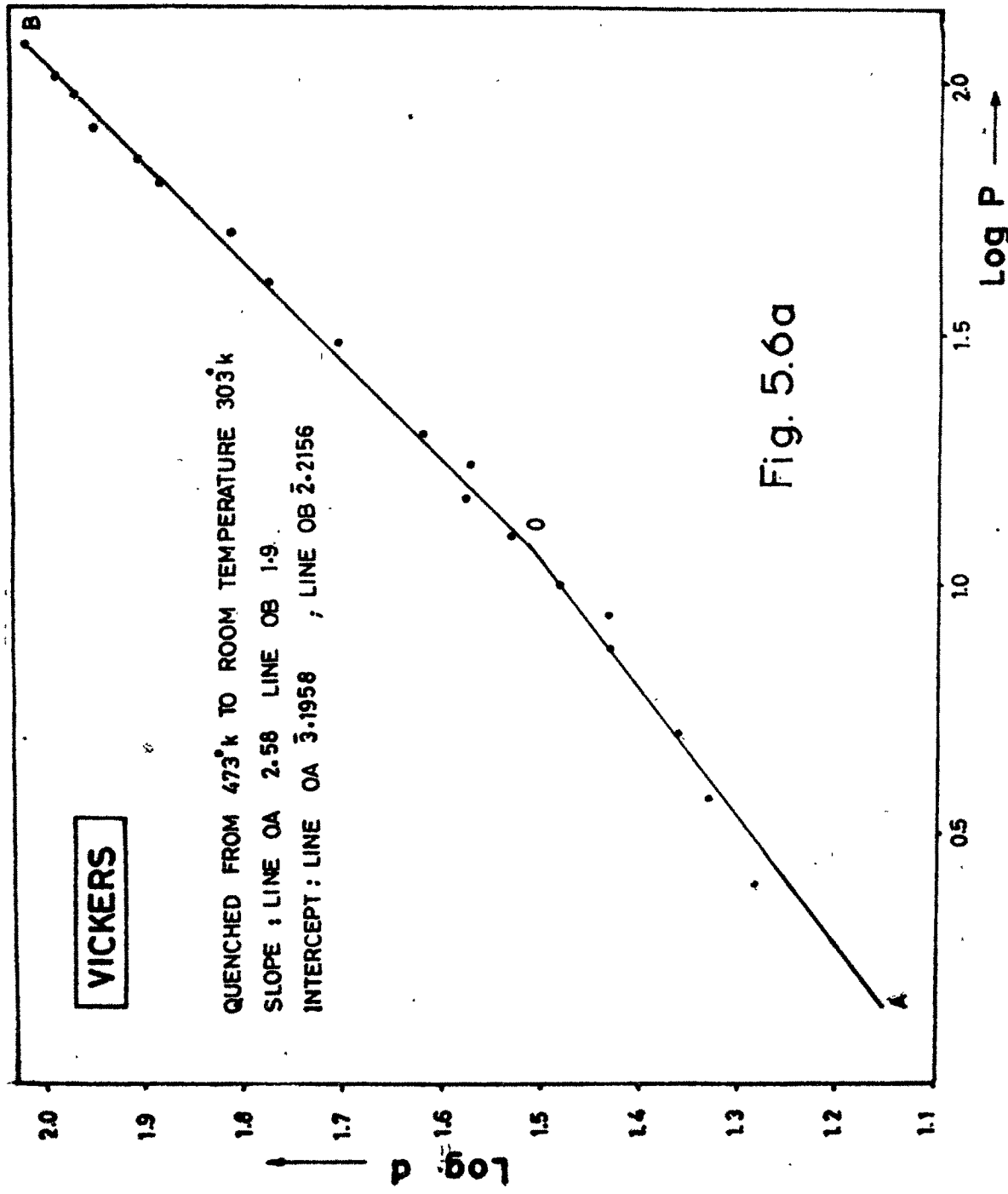
PLOT OF Log d Vs Log P

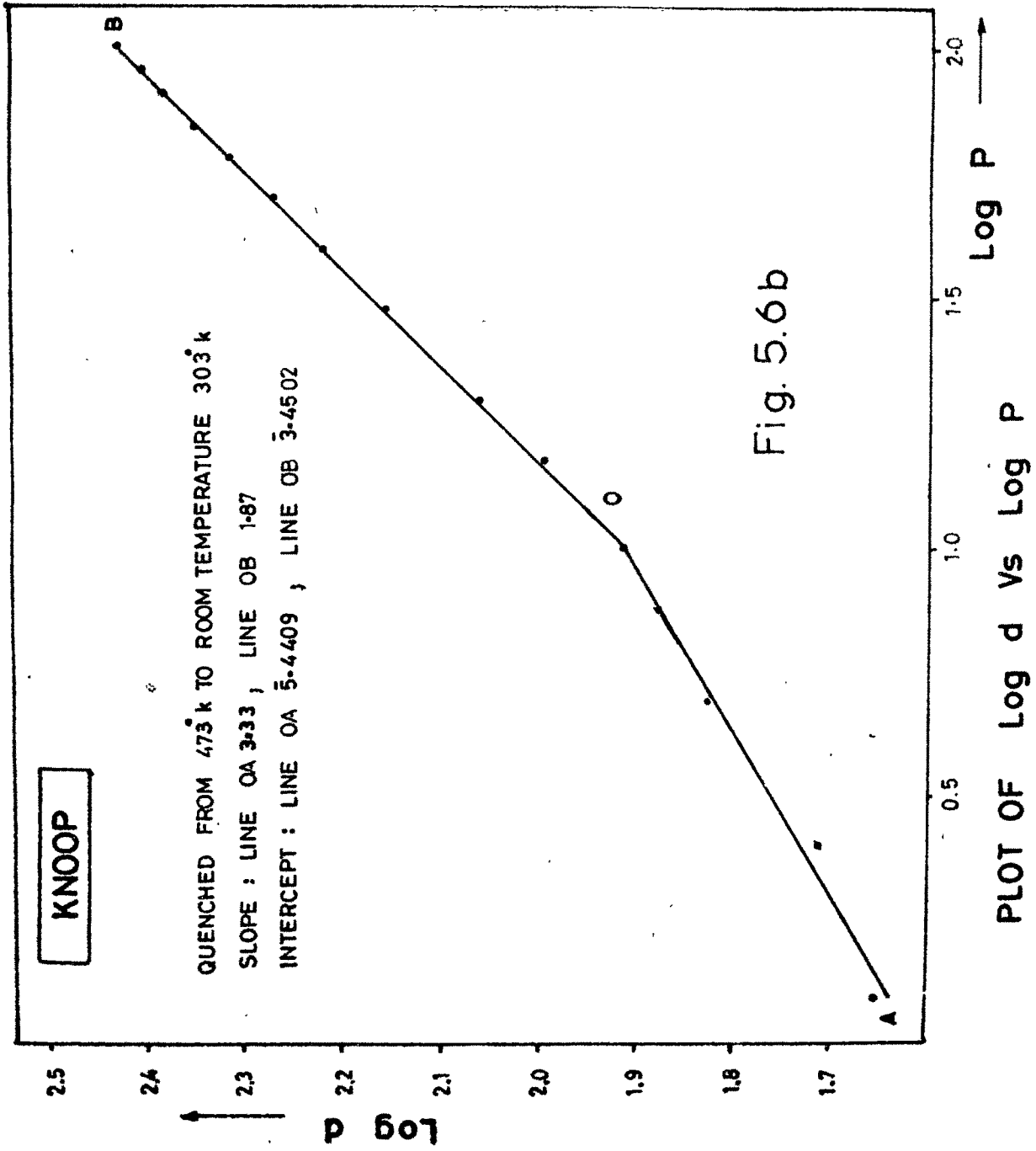


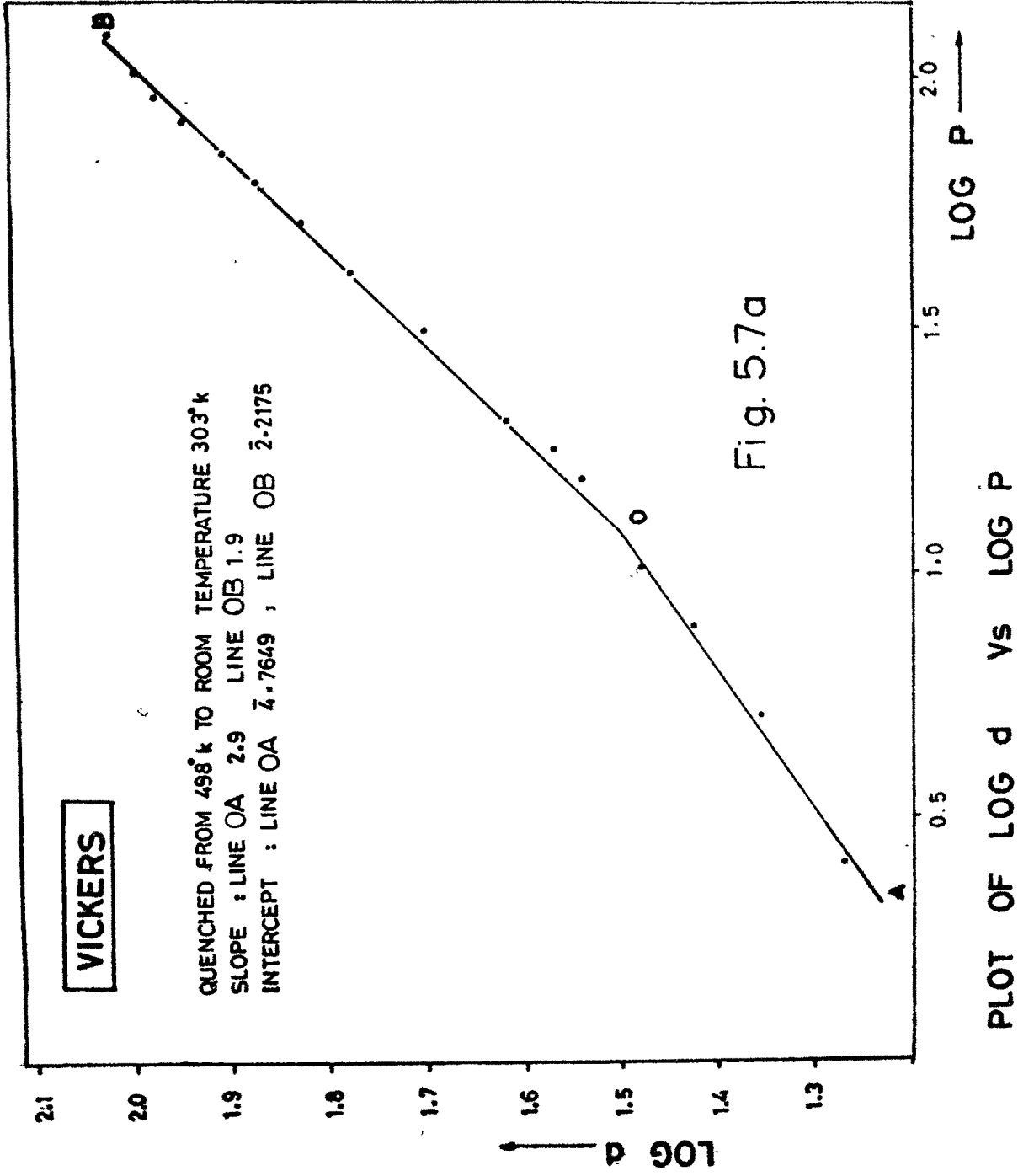
PLOT OF LOG d Vs LOG P

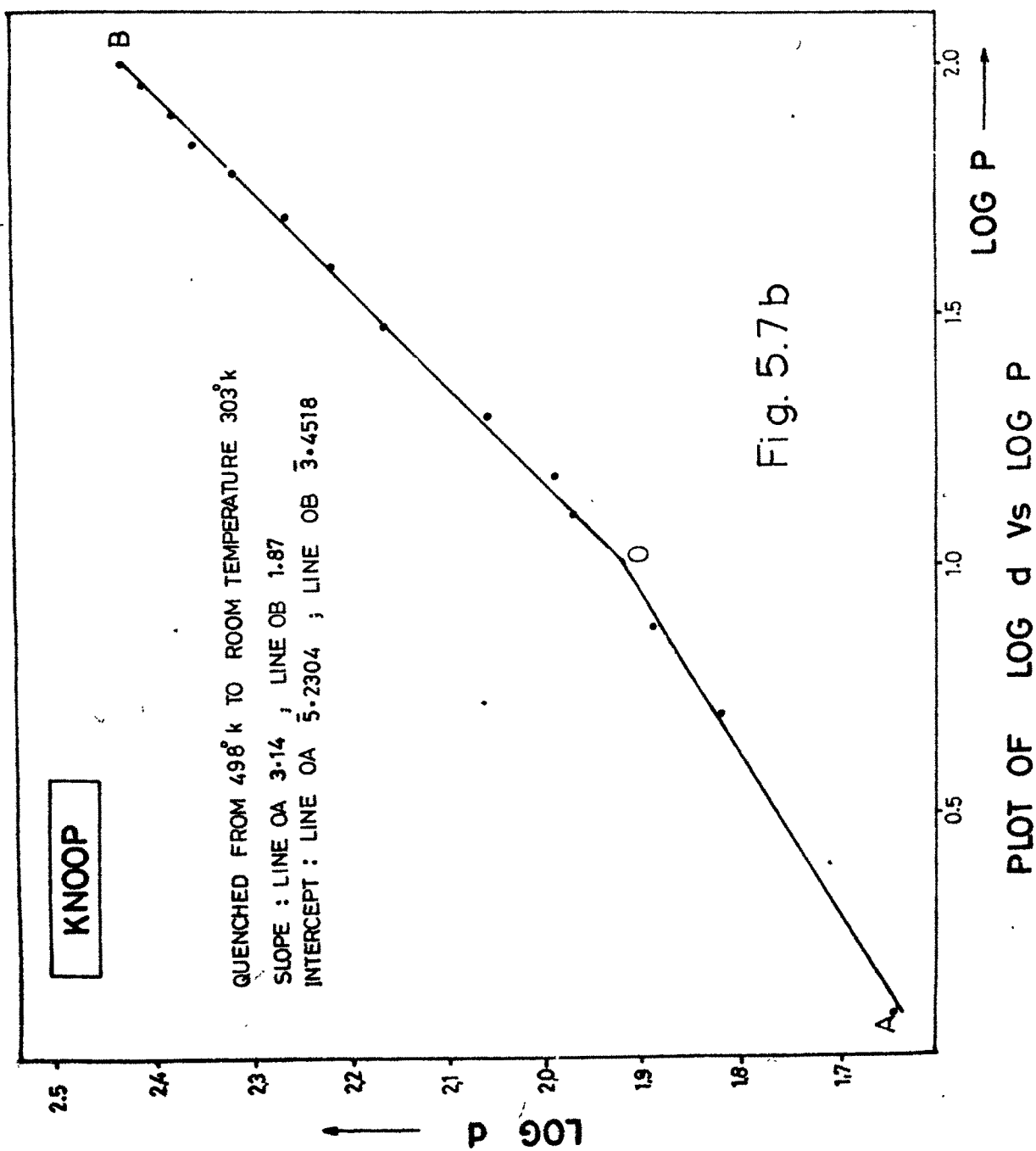


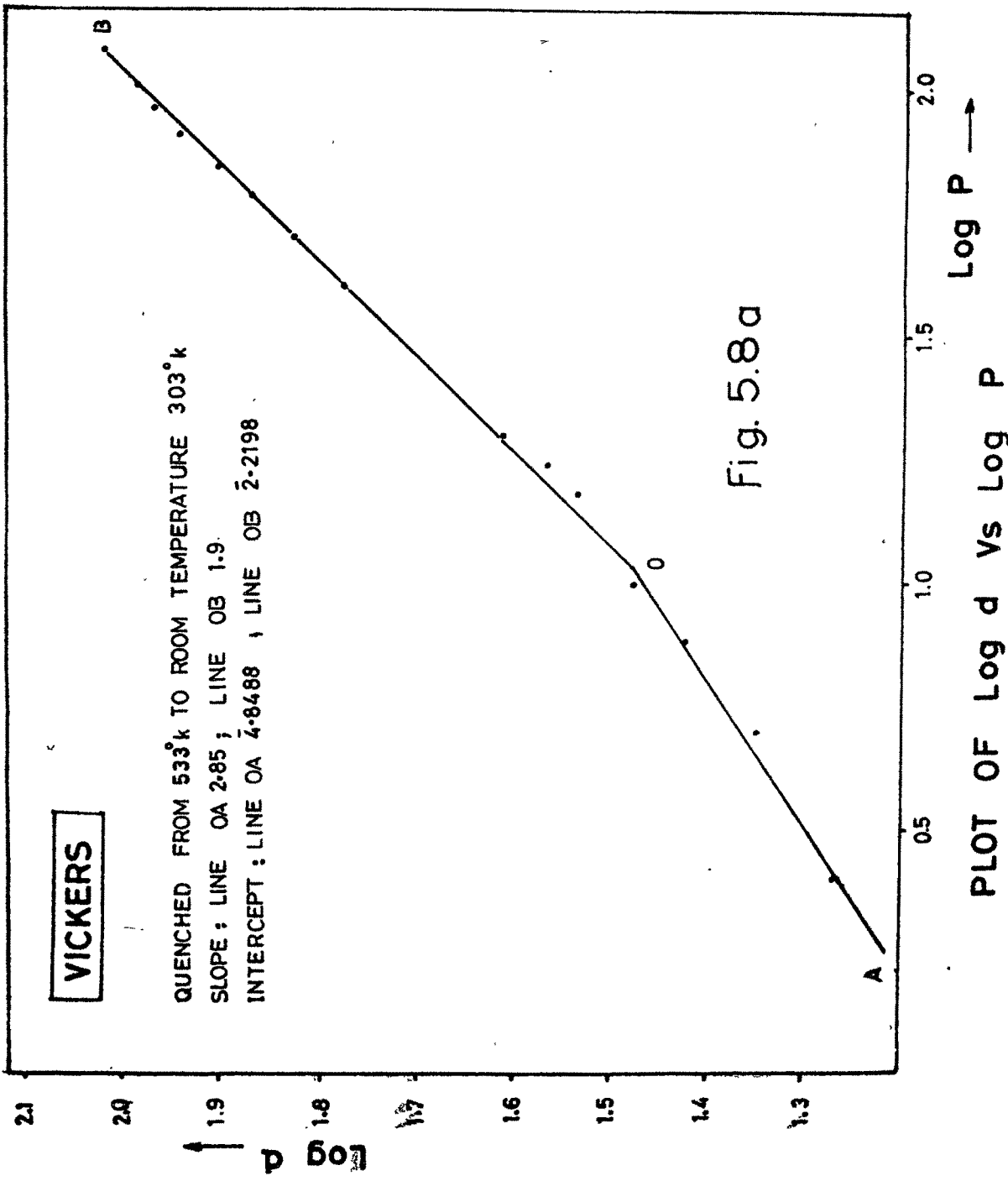


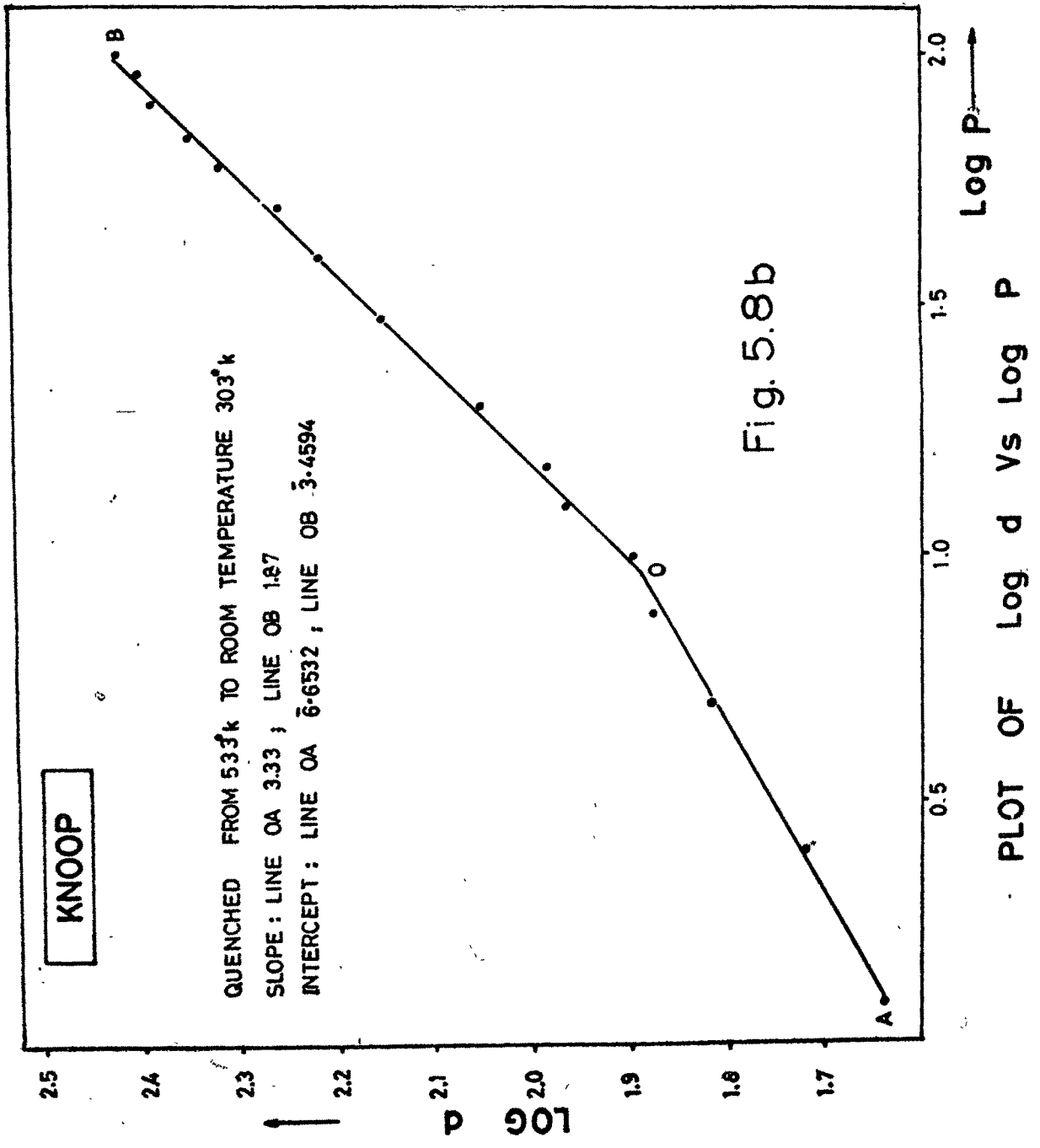












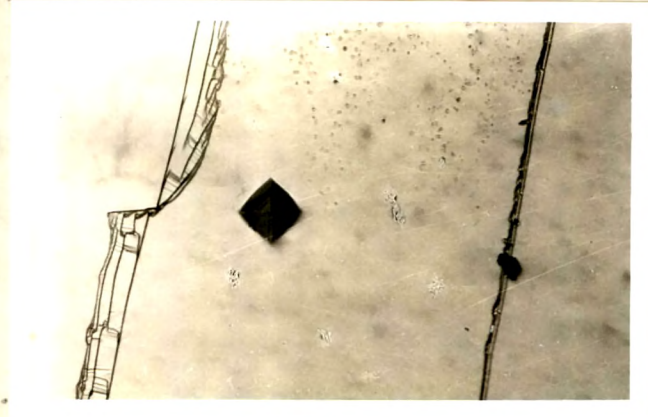


Fig. 5.9 (a,b) show the photomicrographs of indentation marks produced by Vickers and Knoop indenters on cleavage counterparts of melt grown sodium nitrate crystal.

where 'a' and 'n' are constants of the material under test ; 'a' represents the 'standard hardness' for an indenter of fixed diameter and 'n' giving a measure of the variation in hardness as a function of 'P' or 'd'. The other way is to study the variation of hardness (Knoop and Vickers hardness numbers) directly with load.

The equation (5.1) is also known as Meyer's⁶ law. Taking logarithms of both sides yields

$$\log P = \log a + n \log d \quad \dots (5.2)$$

The values of constants 'a' and 'n' can thus be determined from a graph of log d versus log P. Since the relation between log P and log d is linear, the graph is a straight line, the slope of this line gives the value of 'n' and the intercept on log P axis gives the value of log a and hence 'a'. For all indenters that give geometrically similar shapes (impressions), Meyer's law postulates a constant value of 'n' viz. $n = 2$. This implies a constant hardness value for all loads according to the definition of Knoop and Vickers hardness numbers (KHN and VHN).

A careful study of the graphs (log d vs log P) shows that there are two clearly recognisable straight lines of different slopes meeting at a kink which is obtained at a

load of 15 gms. for Knoop and about 20 gms. for Vickers indenters at room temperature. These loads will henceforth be referred to as transition loads P_k . As quenching temperature increases, the kink is found towards lower loads. Further the first part of the straight line corresponding to observations taken at low loads upto P_k at room temperature has slope (n_1) of higher value whereas for the second part of straight line for higher loads, the slope (n_2) has values less than 2. Since n values are different in different regions of the graphs of $\log d$ versus $\log P$, being greater in first region, the 'a' values also vary in two regions being less in first region of low loads and more in second region of high loads. The values of n_1 , n_2 and corresponding intercepts a_1 and a_2 for Knoop and Vickers indentations are recorded in Tables 5.3 and 5.4 respectively. Tables 5.3 and 5.4 also show the load at kink for various quenching temperatures.

It may be remarked in passing that several workers have reported visible scattering in 'n' values. e.g. see Hanemann and Schultz⁵, Onitsch⁷, Grodzinski⁸. However, none has reported the splitting of graphs into two straight lines and their characteristics. The study of variation of load with diagonal length of Vickers indentation mark on faces of different types (c-, m-, d- and o- faces) of natural and synthetic barite crystals (Saraf⁹) has shown

Table 5.3 (KNOOP INDENTER)

QUENCHING TEMPERATURE $T_Q^{\circ}K$	LOW LOAD REGION		HIGH LOAD REGION		$\text{Log } T_Q$	$\text{Log}(a_2 T_Q)$	LOAD AT KINK P gm
	n_1	$a_1 \times 10^{-6}$	n_2	$a_2 \times 10^{-3}$			
303	3.20	6.18	1.87	2.56	2.4814	1.8898	15
373	3.32	3.77	1.87	2.57	2.5717	1.9825	15
398	3.71	0.88	1.87	2.56	2.5999	0.0081	10
423	3.57	1.39	1.87	2.65	2.6263	0.0499	10
448	3.38	3.24	1.87	2.73	2.6513	0.0874	15
473	2.86	27.6	1.87	2.82	2.6749	0.1260	15
498	3.00	17.2	1.87	2.83	2.6972	0.1491	15
533	3.33	4.53	1.87	2.88	2.7267	0.1862	10

Table 5.4 (VICKERS INDENTER)

QUENCHING TEMPERATURE T_q^{OK}	LOW LOAD REGION		HIGH LOAD REGION		Log T_Q	Log ($a_2^T Q$)	LOAD AT KINK Pkgm
	n_1	$a_1 \times 10^{-4}$	n_2	$a_2 \times 10^{-3}$			
303	2.75	8.33	1.9	15.63	2.4814	0.6754	20
373	2.58	14.9	1.9	16.23	2.5717	0.7820	15
398	3.10	2.30	1.9	16.29	2.5999	0.8118	15
423	2.71	10.00	1.9	16.27	2.6263	0.8377	15
448	2.64	12.80	1.9	16.33	2.6513	0.8642	15
473	2.58	15.7	1.9	16.43	2.6749	0.8905	15
498	2.90	5.82	1.9	16.50	2.6972	0.9147	15
533	2.85	7.06	1.9	16.59	2.7267	0.9465	15

very clearly the existence of two clearly recognisable straight lines of the graph of $\log d$ versus $\log P$. Later, Mehta¹⁰, Shah² and Acharya³ verified the splitting of graph of $\log d$ versus $\log P$ on calcite, zinc, TGS and KBr crystals. In the present investigation, the author has verified the splitting of the graph into two regions using Knoop pyramidal indenter also. It is thus certain that the splitting of the graph into two straight lines is natural and is due to varied reactions of the crystal surfaces to different applied loads used for producing indentations.

5.4.1 Characteristics of two straight line regions in the graph

The separation of the straight graph into two regions with different slopes indicates that in the first region of low loads, the value of hardness is strictly dependent on load and in the second region of high loads this dependence on applied loads is relatively reduced. It appears that besides this dependence on load, there could also be other factors contributing to this behaviour.

In order to determine the relative importance of these factors affecting the values of 'a' and 'n', the study was carried out on crystal surfaces which were quenched

from high temperatures to room temperature. It is obvious from Tables 5.3 and 5.4 that the values of a_1 and n_1 for low load region show comparatively large differences at all quenching temperatures whereas for the second part of the graph there are less difference in ' a_2 ' and ' n_2 ' values. This clearly indicates that ' n_1 ' and ' a_1 ' values are dependent on the previous history of the sample, whereas the second part of the graph giving ' n_2 ' and ' a_2 ' values remain comparatively less affected by the previous history of the sample. It should be remarked here that n_1 values in case of Vickers indenter (Table 5.4) show less variation with quenching temperature whereas for Knoop indenter, marked variation of n_1 values with quenching temperatures are noticeable (Table 5.3). Hence the two regions correspond in general with the structure sensitive and structure insensitive properties of the crystal. They can roughly correspond with extrinsic and intrinsic properties of the crystals. Further, the initial indentation under low loads i.e. initial plastic deformation produces cold working of the crystal. There will also be certain amount of recovery from this deformation. As a result the degree of hardening of crystal surface should increase. This is more true for low loads near kink. Hence with an increase in applied load the surfaces should offer high resistance to the indentation. The hardness in this region will therefore be lower than

that in first region, mostly near kink. The surface is likely to follow *Peyel*'s law and the value of ' n_2 ' will be nearly equal to 2. In addition to the cold working and recovery of strained crystals, several factors such as surface energy, concentration of different types of imperfections and their interactions, effect of penetration of indenter etc. are also operating in a way unpredictable at present. The experimentally observed deviations from the above remarks are therefore likely to be due to these factors which are not yet clearly understood. It is therefore difficult to conjecture conclusively from ' n_1 ' and ' a_1 ' values only, the behaviour of crystal surface. The marked variation of n_1 with the temperature of quenching in case of Knoop indenter indicates that surface layers of the specimen are more susceptible to change in quenching temperature because the Knoop pyramidal indenter, in general, measures the hardness of surface layers. It should be mentioned here that although the indentation work was carried out on freshly cleaved surfaces of quenched crystals with the intention of removing surface hardening of quenched specimens, the hardness study of the cleaved surfaces which were once the inner parts or interiors of quenched crystal has shown a noticeable change with quenching temperature i.e. 'body' hardness is affected by heat treatment, of course this change is obviously smaller than that of surface hardening of the quenched specimens.

5.5 CONCLUSIONS

The following conclusions are drawn from the above discussion :

- (i) The graph of $\log d$ versus $\log P$ consists of two clearly recognisable straight lines having different slopes and intercepts on the axes.
- (ii) The indenter load P_k corresponding to kink representing a transition from one straight line to another depends upon quenching temperature.
- (iii) The slope of first part corresponding to low load region of the graph is greater than that of the second part. The intercept made by the first line has less value than that made by second line.
- (iv) The slopes ' n_1 ' corresponding to low loads are more susceptible to quenching temperature. In particular for Knoop diamond pyramidal indenter ' n_1 ' is more susceptible to quenching temperature than for Vickers pyramidal indenter.
- (v) The defect structures operate differently in low and high load regions corresponding to two parts of the graph of $\log d$ vs. $\log P$.

REFERENCES

1. Mott, B.W. 'Microindentation hardness testing', Butterworths Scientific Publications, London, Ch.1, 1956.
2. Shah, R.T. Ph.D. Thesis, M.S. University of Baroda, Baroda, 1976.
3. Acharya, C.T. Ph.D. Thesis, M.S. University of Baroda, Baroda, 1978.
4. Bhagia, L.J. Ph.D. Thesis, M.S. University of Baroda, Baroda, 1982.
5. Hanemann, H. and Schultz, F. Z. Metalkunde, 33, 122-34, 1941.
6. Mejerzyl. Quoted in 'The Science of hardness Testing and Its Research Applications'. American Soc. for Metals, Ohio, 1973.
7. Onitsch, E.M. Microscopie, 2, 131-4, 1947.
8. Grodzinski, P. Schwaiz, arch. angew wiss, 18, 282-92, 1952.
9. Saraf, C.L. Ph.D. Thesis, M.S. University of Baroda, Baroda, 1971.
10. Mehta, B.J. Ph.D. Thesis, M.S. University of Baroda, Baroda, 1972.

CHAPTER - VI

VARIATION OF HARDNESS WITH LOAD

CHAPTER - VI

VARIATION OF HARDNESS WITH LOAD

	<u>PAGE</u>
6.1 Introduction	111
6.2 Observations	115
6.3 Results and Discussion	116
6.3.1 Relation between hardness and quenching temperature	117
6.3.2 Relation between microhardness and electrical conductivity	131
6.4 Conclusions	142

REFERENCES

6.1 INTRODUCTION

It is clear from the discussion of the previous chapter that 'Standard' hardness 'a' is a function of quenching temperature ; 'a₁' and 'a₂' in general vary with quenching temperature (T_Q). However, the variation of a₁ with quenching temperature is more noticeable than that of a₂. In particular, a₁ in case of Knoop indentation is more susceptible to quenching temperature than that obtained by Vickers indentation. The present Chapter reports detailed study of changes in hardness number with quenching temperature.

The Knoop and Vickers hardness numbers (H_K and H_V) are defined by equations,¹

$$\text{KHN, } H_K = 14230 P/d^2 \quad \dots (6.1)$$

$$\text{VHN, } H_V = 1854.4 P/d^2 \quad \dots (6.2)$$

where load P is measured in grams and the diagonal length d, of the indentation mark in microns. The hardness number is not an ordinary number, but a constant having dimensions and has a deep, but less understood, physical meaning. The combination of these equations with

$$P = a d^n \quad \dots (6.3)$$

yield,

$$H = a d^{n-2} \quad \dots (6.4)$$

or

$$H = a P^{(n-2)/2} \dots\dots (6.5)$$

In case of Vickers microhardness, the value of exponent n equals 2 for all indenters that give impressions geometrically similar to one another. Thus, $n = 2$ implies that hardness for a given shape of pyramidal indenter is constant and independent of load. For a solid subjected to uniaxial compression, the modulus of elasticity (young's modulus) is given by

$$E = \sigma/\epsilon \dots\dots (6.6)$$

where σ is the compressive stress defined as load per unit area

$$\sigma = P/A \dots\dots (6.7)$$

and the compressive strain ϵ is defined as the decrease in length per unit length. Now the area of cross-section, A , increases with compression. Hence for a constant volume of a solid, length is inversely proportional to the area of cross-section. If A_0 represents initial area of cross-section with a normal length l_0 , and A the final area with normal length l after small compression, one obtains

$$l A = l_0 A_0$$

or,

$$l/l_0 = A_0/A \dots\dots (6.8)$$

Therefore,

$$\epsilon = (l - l_0) / l = (A_0 - A) / A \quad \dots (6.9)$$

substitution of σ and ϵ from equations (6.7) and (6.9) gives,

$$E = \sigma / \epsilon = P / (A_0 - A) \quad \dots (6.10)$$

Hence for a simple uniaxial compressive stress when the area is a geometrical function of the deformation, determined here by constant volume, the resistance to permanent deformation can be expressed simply in terms of load and corresponding area. In indentation hardness work the volume change is very very small. Hence the indentation hardness can be measured by using the above formula (6.10). Indenters are made in various geometrical shapes such as spheres, pyramids etc. The area over which the force due to load on indenter acts increases with the depth of penetration. The resistance to permanent deformation or hardness can be expressed in terms of force or load and area alone (and/or depth of penetration). These remarks are true for solids which are amorphous or highly homogeneous and isotropic.

The above analysis presents a highly simplified picture of the process involved because there is a great difference between deforming a solid in a simple uniaxial

compression and deforming a surface of a solid by pressing a small indenter into it. Around the indentation mark, the stress distribution is exceedingly complex and the stressed material is under the influence of multi-axial stresses. The sharp corners of a pyramidal indenter produces a sizable amount of plastic deformation which may reach 30% or more at the top of the indenter. Further the surface of contact is inclined by varying amounts to the directions of applied force. In view of these complications a simple expression corresponding to that for the modulus of elasticity cannot be derived for hardness. In the absence of any formula based on sound theory, an arbitrary expression is used which includes both known variables - load and area - in the present case. Hence the hardness number, H , is defined as the ratio of the load to the area of impression,

$$H = P/A \quad \dots\dots (6.11)$$

For pyramidal indenters the load (P) varies as the square of the diagonal (d). Thus for a given shape of pyramid,

$$P = bd^2 \quad \dots\dots (6.12)$$

where b is a constant which depends on the material and shape of pyramid. The area of the impression, A , is also proportional to the square of the diagonal,

$$A = Cd^2 \quad \dots\dots (6.13)$$

where C depends upon the shape of the pyramid. Combination of equations 6.5, 6.6 and 6.7 gives,

$$H = bd^2/Cd^2 = b/c = \text{constant} \dots (6.14)$$

Hence for a given shape of pyramidal indenter hardness is independent of load and size of indentation. This statement represents *Meyer's* law. In view of defining equation (6.5) for hardness, hardness number can also be considered as hardening modulus.

Due to complicated behaviour of indented anisotropic single crystals of various materials and as a result of the development of arbitrary expression for hardness, it is clear that the theoretical treatment of the problem is extremely difficult. Hence it is desirable to approach this problem via experimental observations, interpretations and with a probable development of empirical relation(s). The present work is taken up from this phenomenological point of view and is an extension of the work carried out by Saraf², Mehta³, Shah⁴, Acharya⁵ and Bhagia⁶ in this laboratory.

6.2 OBSERVATIONS

The observations which were recorded for studying the equation $P = a d^n$ are used in the present

Table 6.1 (KNOOP INDENTER)

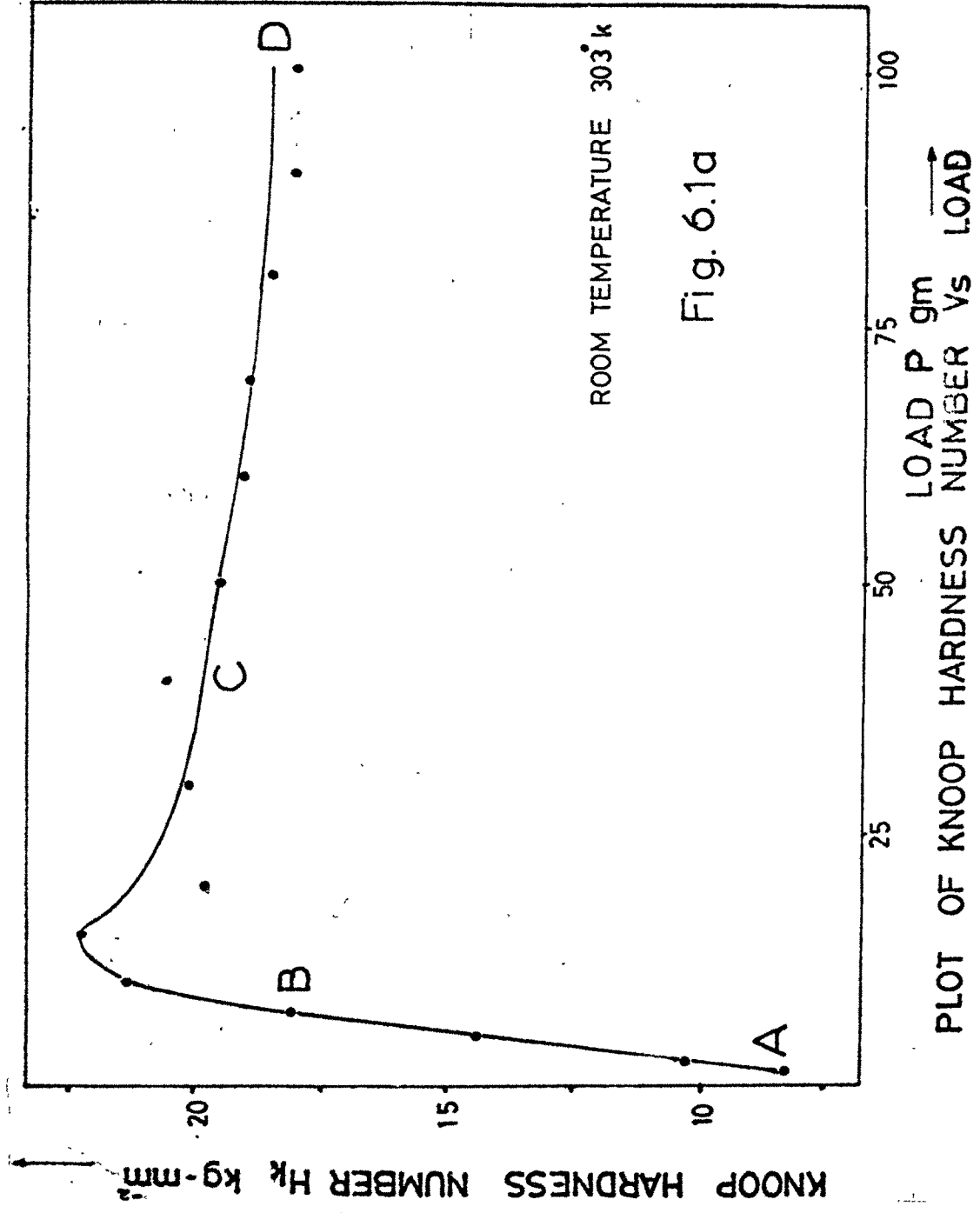
CRYSTAL : MELT GROWN NaNO_3

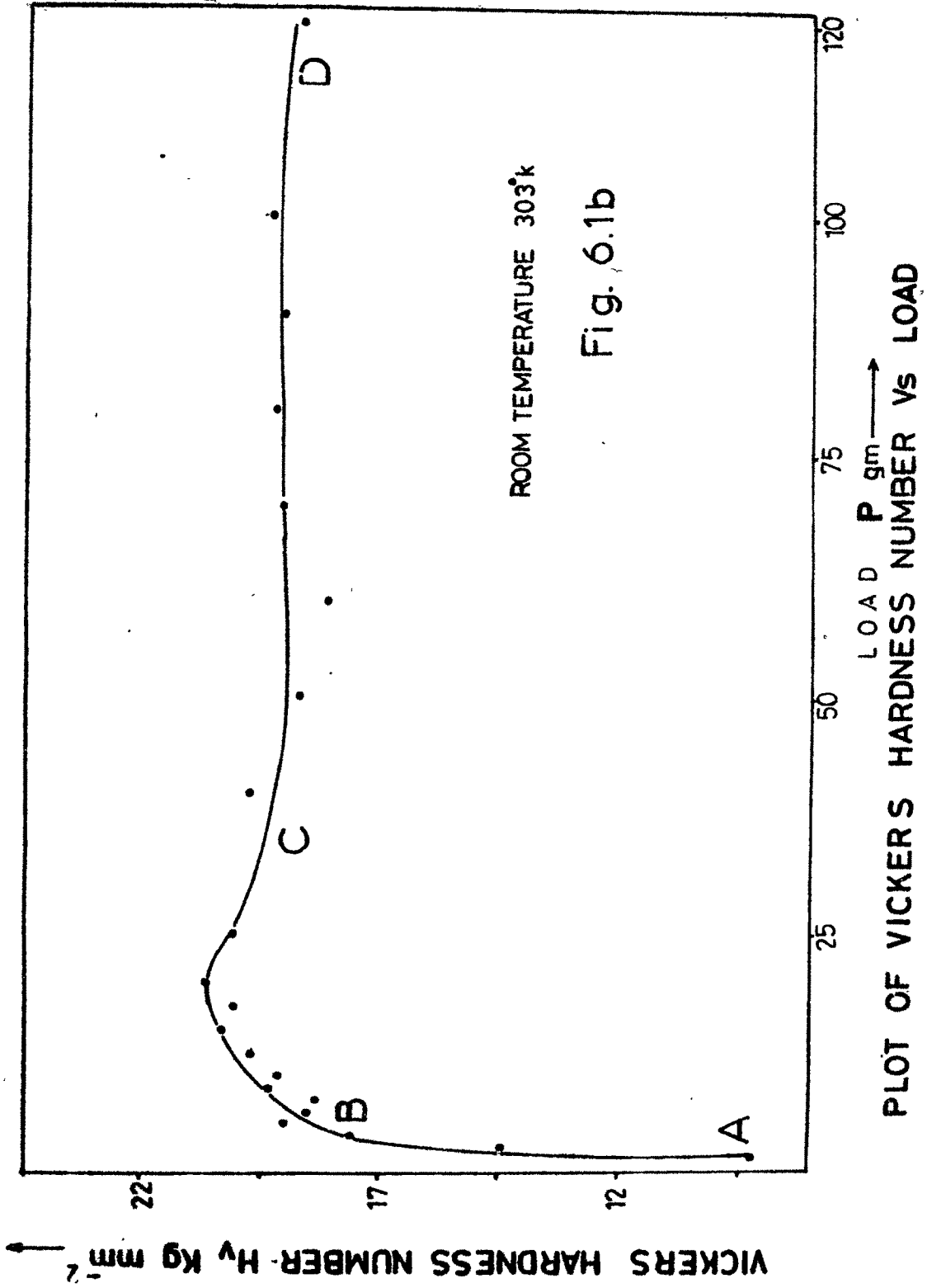
QUENCHING TEMPERATURE T_q °K	303	373	398	423	448	473	498	533
LOAD P gm	KNOOP HARDNESS NUMBER $H_K = 14230 P \cdot d^{-2}$ kg - mm ⁻²							
1.25	7.42	8.22	8.37	8.52	8.61	8.83	9.16	9.73
2.5	10.31	12.64	12.12	12.26	13.04	13.46	13.04	13.04
5.0	14.45	14.58	16.30	15.14	15.51	15.89	16.28	16.69
7.5	18.14	17.39	17.76	18.98	19.35	18.96	17.75	18.93
10	21.37	20.76	21.37	21.53	21.67	21.04	20.54	23.19
15	22.26	21.01	20.71	21.34	22.26	22.35	22.64	23.02
20	19.78	20.42	20.90	21.34	21.59	21.59	21.80	22.44
30	20.03	19.50	18.73	19.57	20.00	20.20	19.96	21.39
40	20.40	19.02	19.57	19.95	20.34	20.64	20.95	21.16
50	19.51	19.68	19.34	19.51	19.68	20.52	20.82	21.10
60	18.99	19.40	19.20	19.71	20.03	20.46	20.03	19.71
70	19.00	18.94	18.67	18.54	19.08	19.45	19.49	20.22
80	18.42	18.50	18.87	18.62	18.74	18.89	19.02	19.64
90	17.99	18.09	17.98	18.66	19.26	19.98	20.01	20.40
100	17.95	18.17	18.30	19.00	19.50	19.72	19.81	20.87

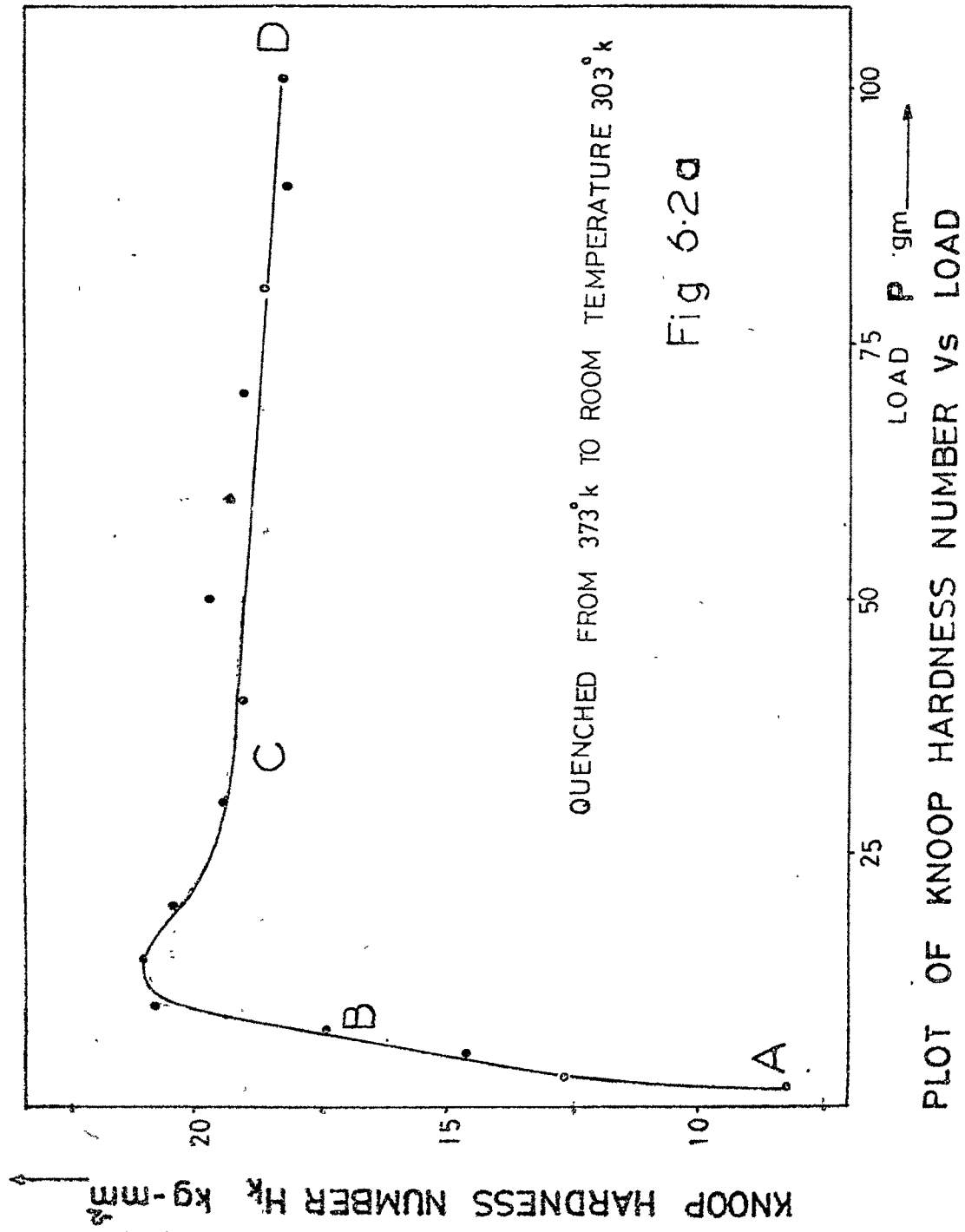
Table 6.2 (VICKERS INDENTER)

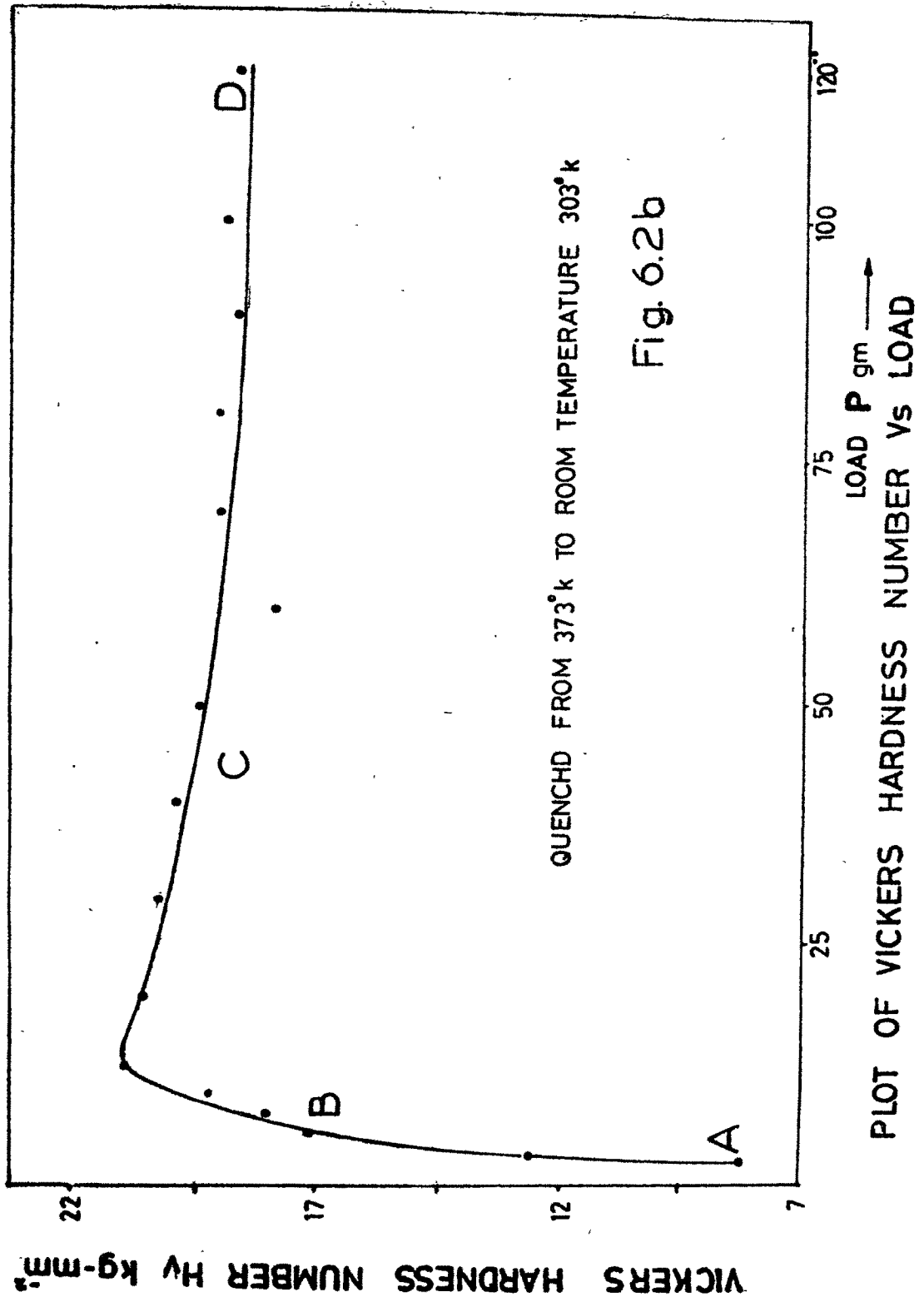
CRYSTAL : MELT GROWN NaNO_3

QUENCHING TEMPERATURE T_c °K	303	373	398	423	448	473	498	533
	VICKERS HARDNESS NUMBER $H_V = 18.54.4 \text{ P.d}^{-2} \text{ kg - mm}^{-2}$							
LOAD P gm	7.89	8.05	8.16	8.23	8.45	8.72	8.84	9.15
	12.08	12.60	12.60	12.44	12.88	12.66	13.16	13.45
	16.56	17.15	17.15	17.33	17.65	17.76	17.96	18.41
	17.20	18.07	18.23	18.49	18.89	19.18	19.47	19.77
	19.13	19.28	19.39	19.65	19.85	20.13	20.34	20.68
	20.27	21.09	21.72	22.43	22.59	22.86	23.18	23.68
	20.60	20.59	20.92	21.00	21.20	21.42	21.50	21.84
	19.47	20.39	20.72	21.39	21.66	21.82	22.08	22.45
	19.67	20.00	20.12	20.28	20.59	20.73	20.89	21.08
	18.57	19.50	19.73	20.00	20.41	20.71	20.91	21.01
	18.02	17.86	18.91	19.32	19.74	20.06	20.24	20.51
	19.06	19.18	19.93	19.89	19.97	20.09	20.19	20.29
	19.10	18.75	18.80	18.83	18.92	19.01	19.22	19.46
	18.46	18.78	18.78	18.87	18.95	18.95	19.10	19.45
	18.86	19.02	19.10	19.10	19.34	19.5	19.66	19.83
	18.33	18.64	19.03	19.10	19.77	19.90	19.50	19.10









VICKERS HARDNESS NUMBER HV kg-mm²

A

B

C

D

7

22

17

12

25

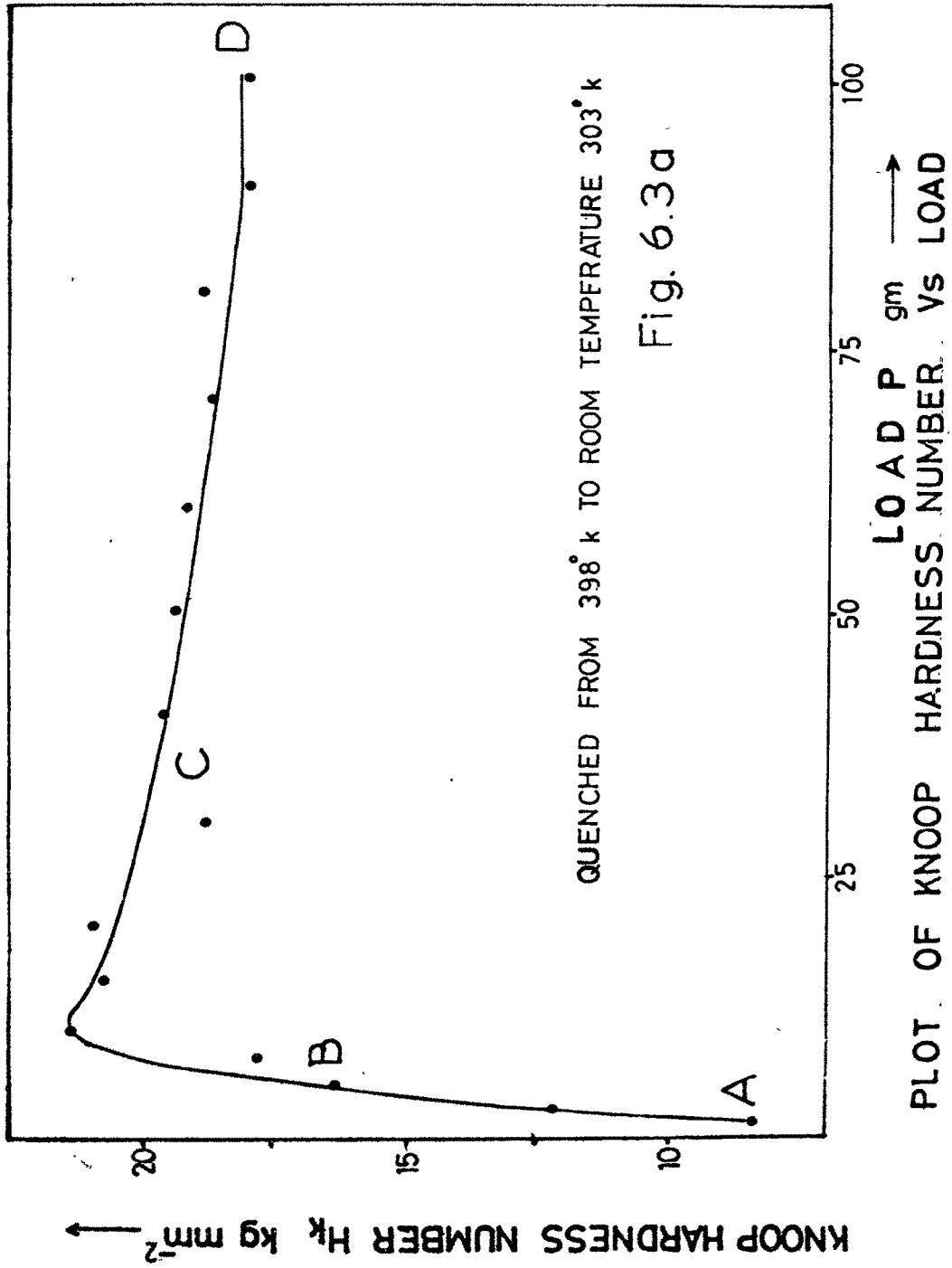
50

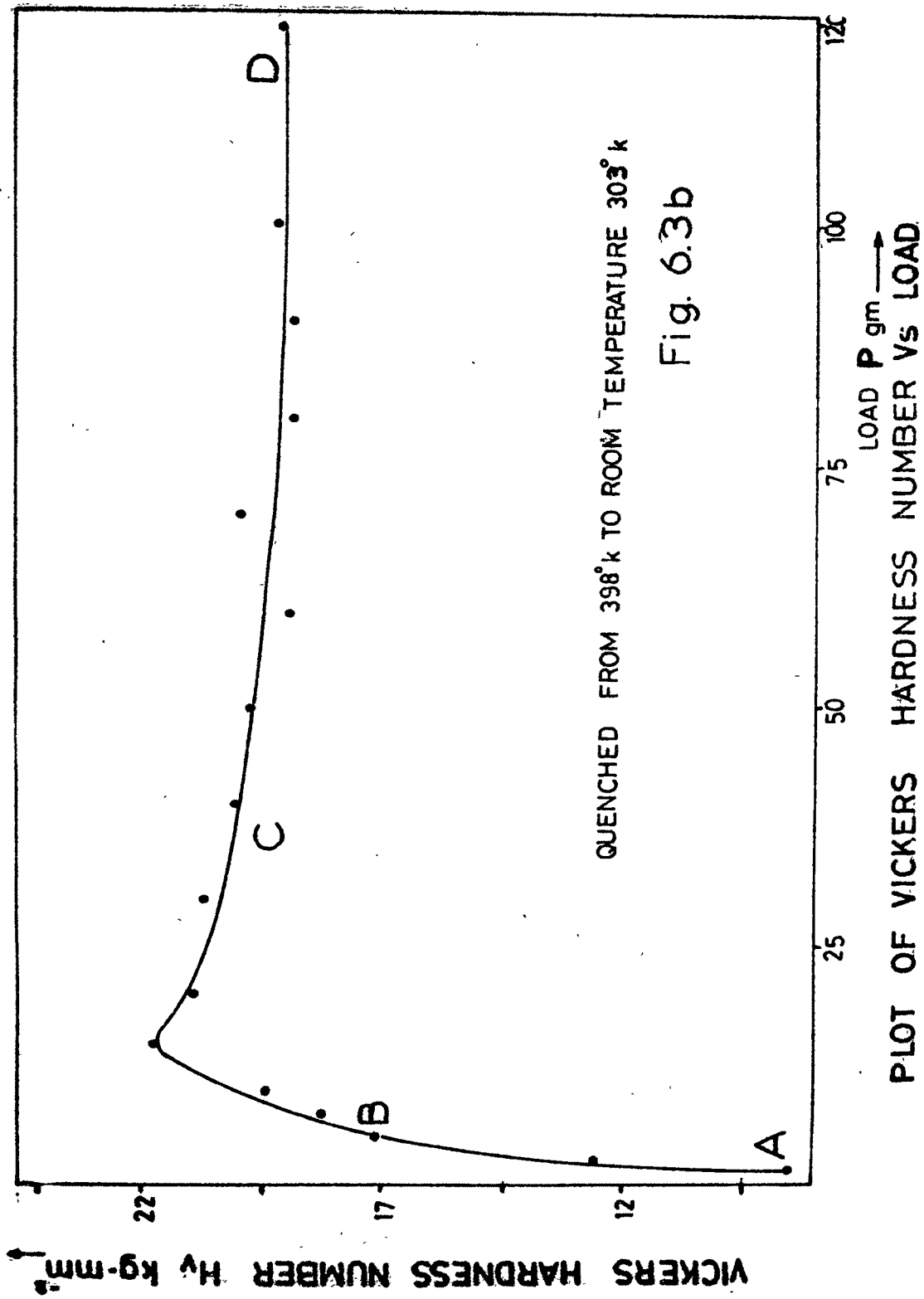
75

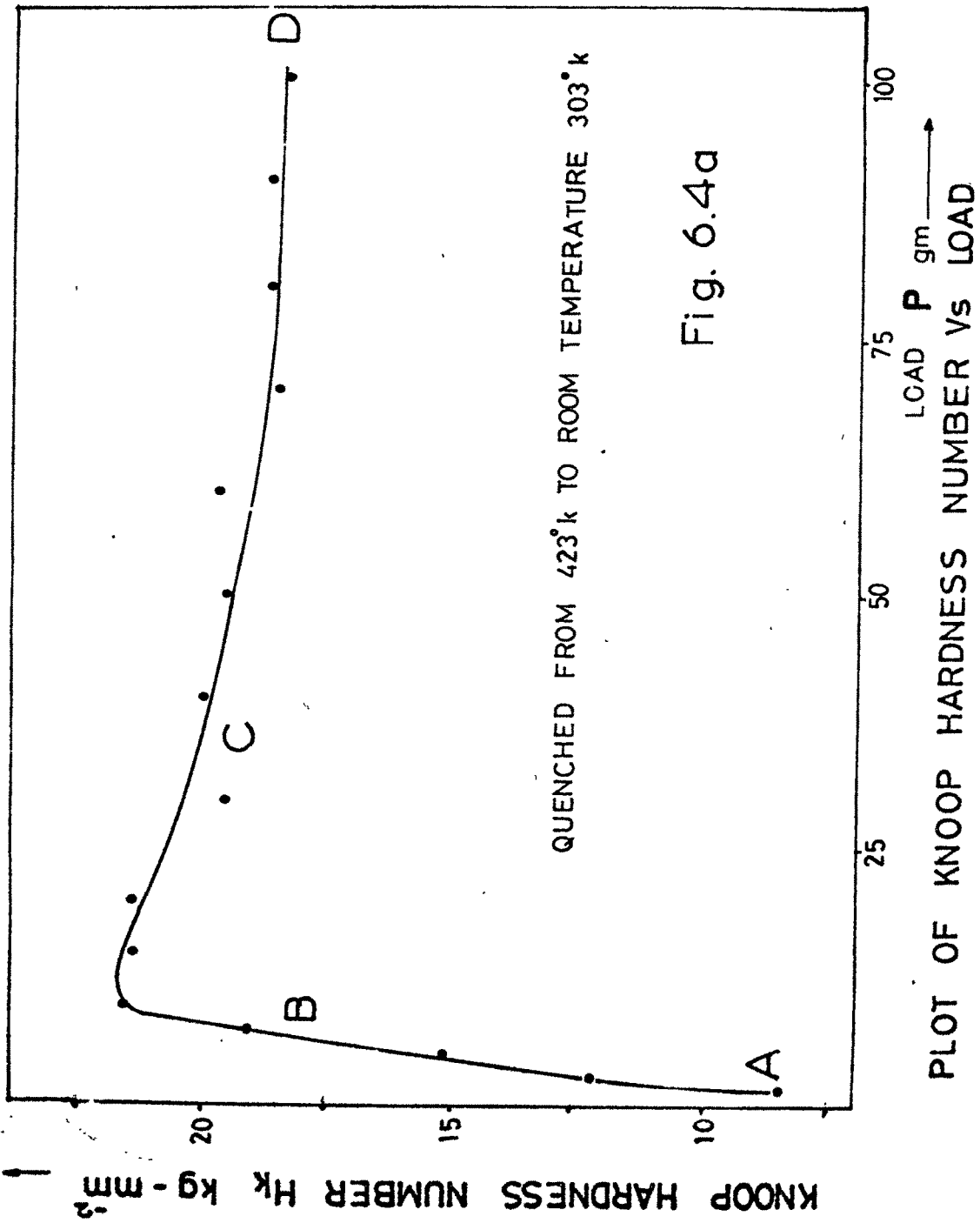
100

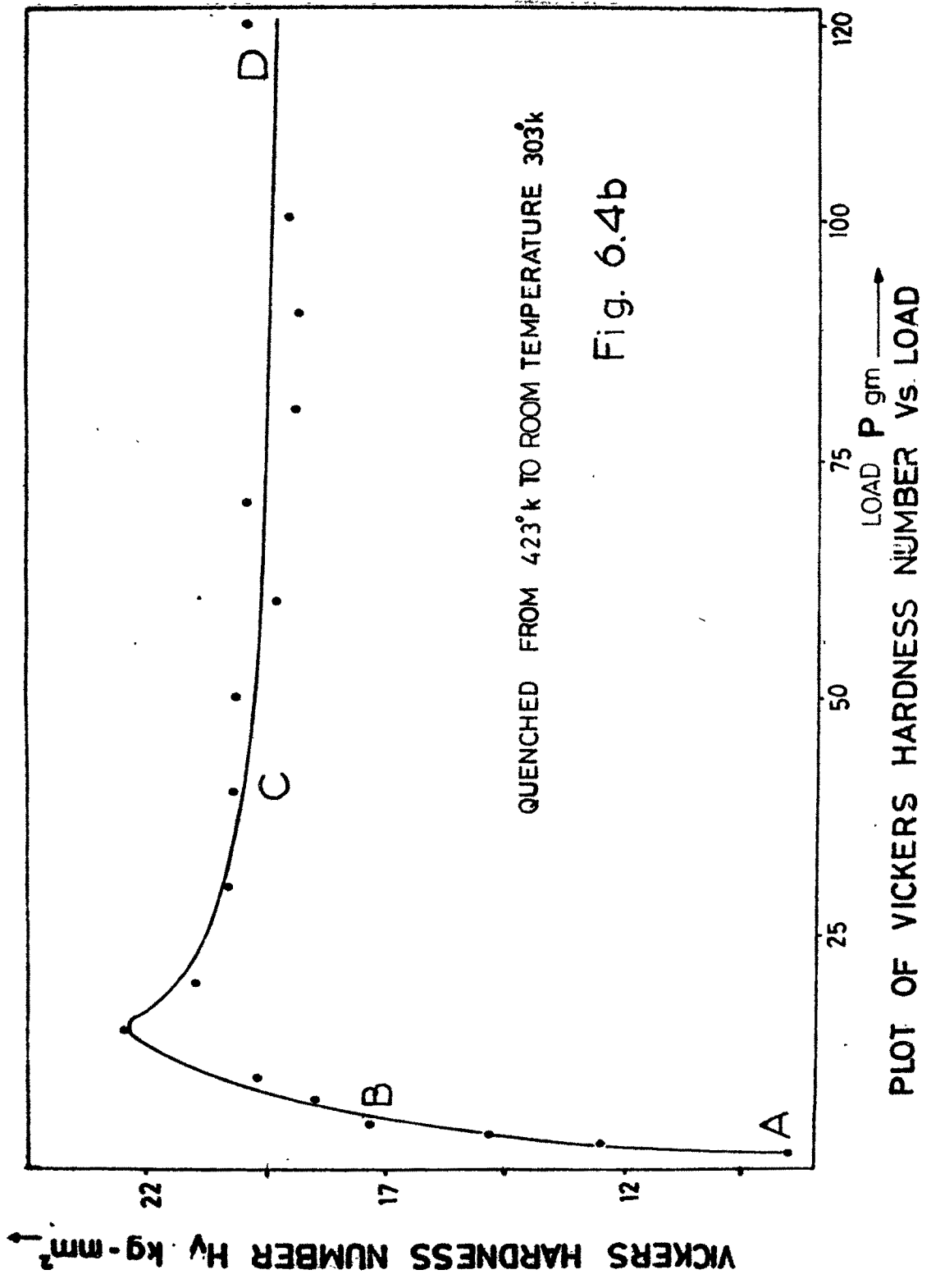
120

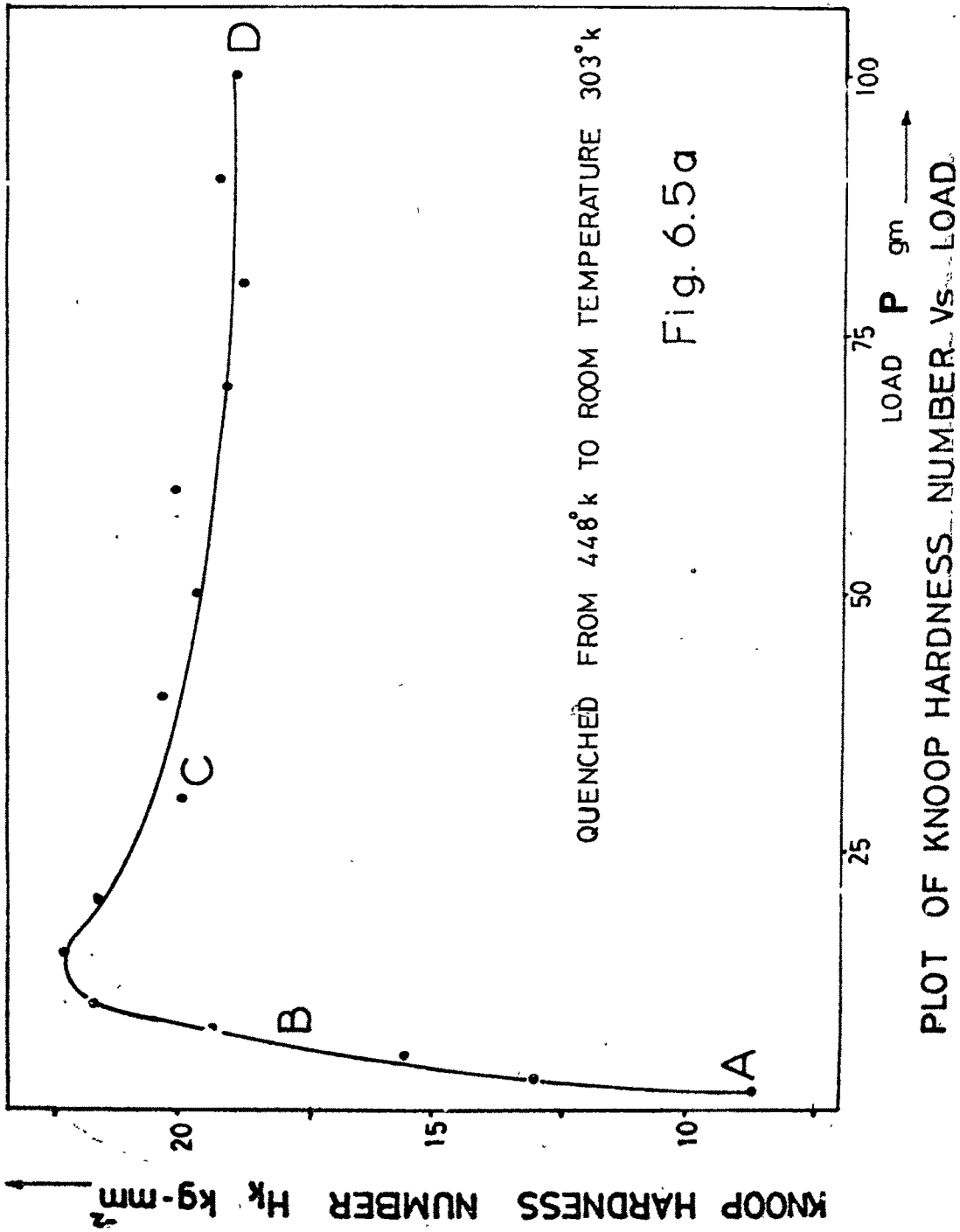
LOAD P gm →

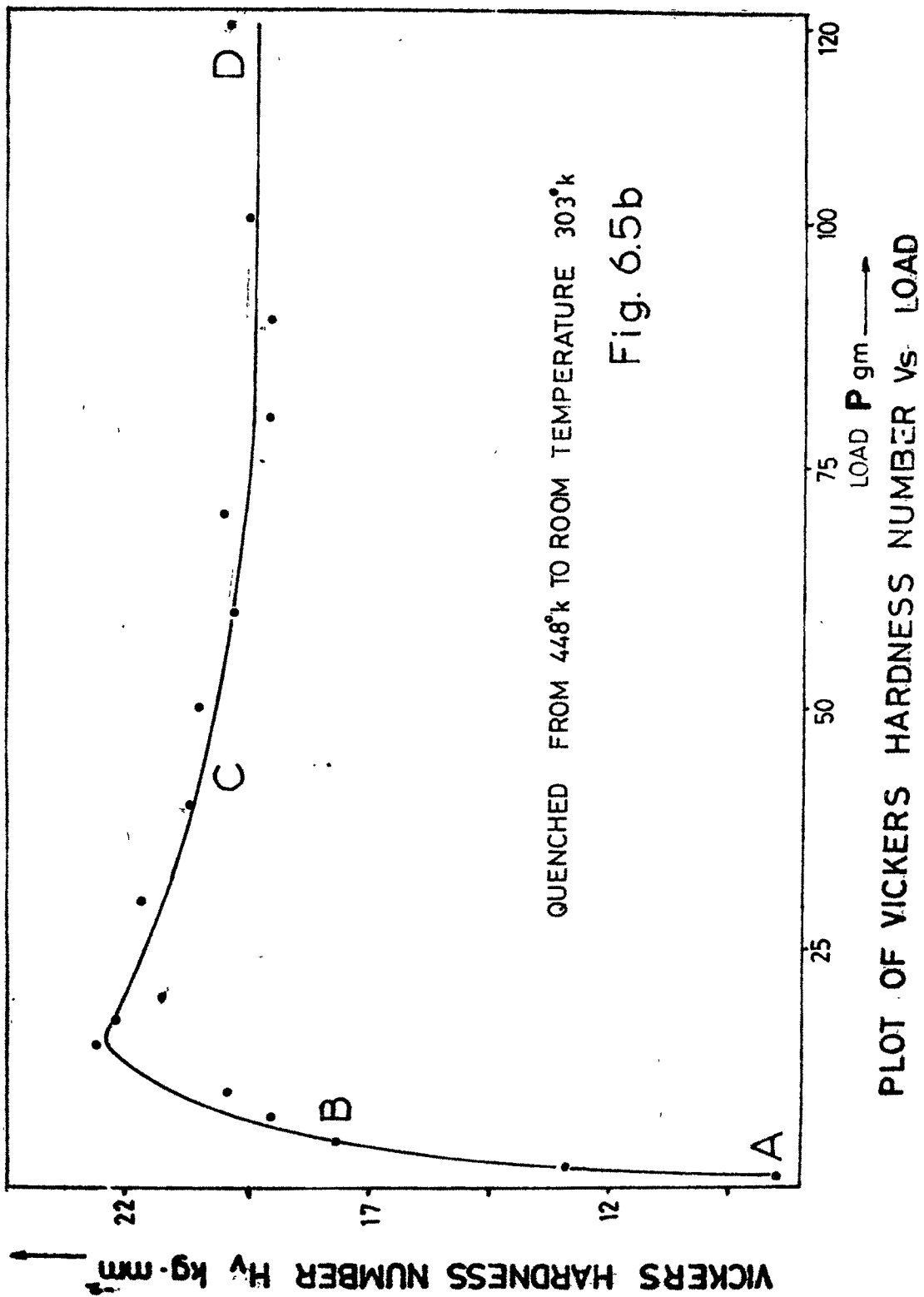


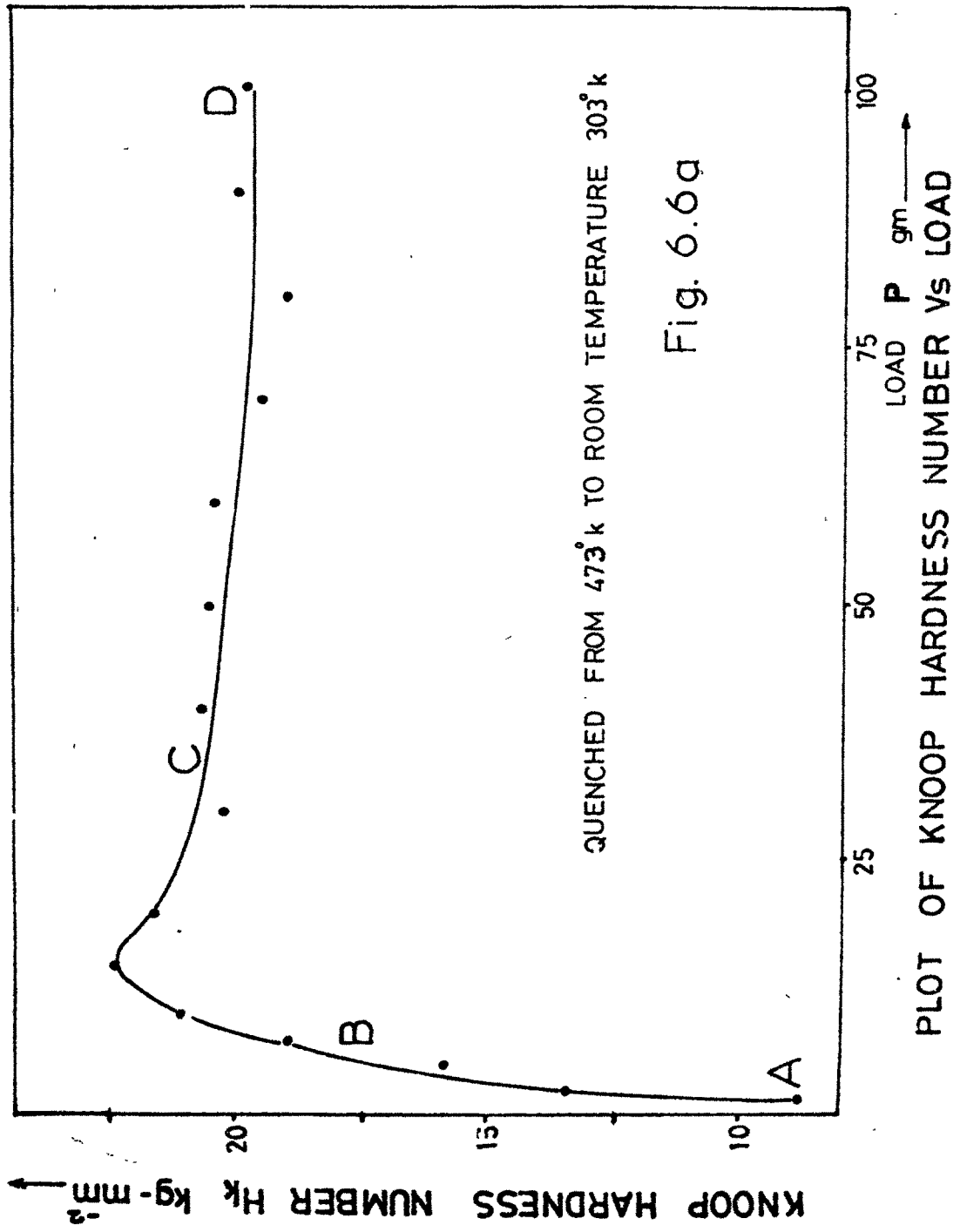


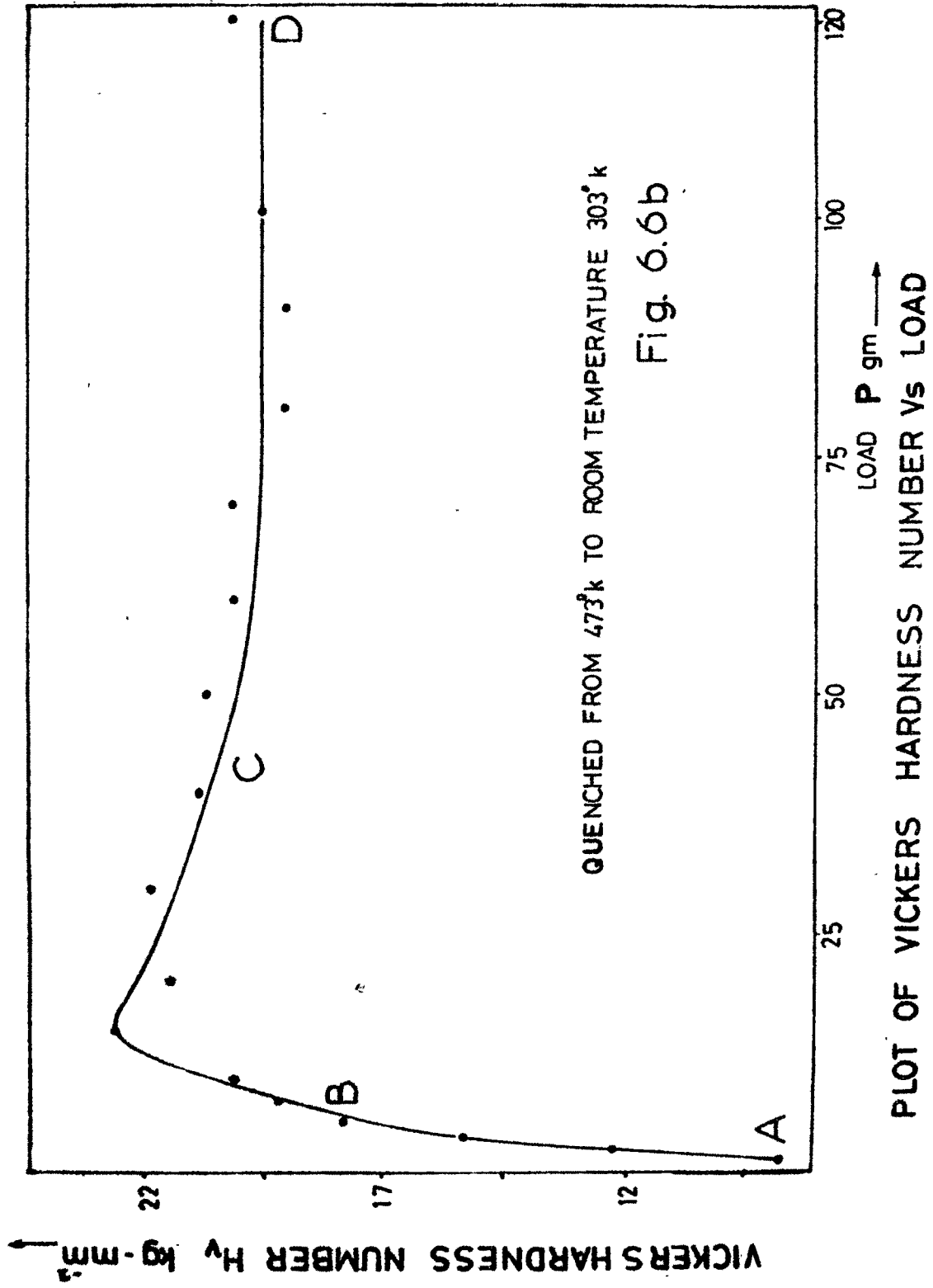


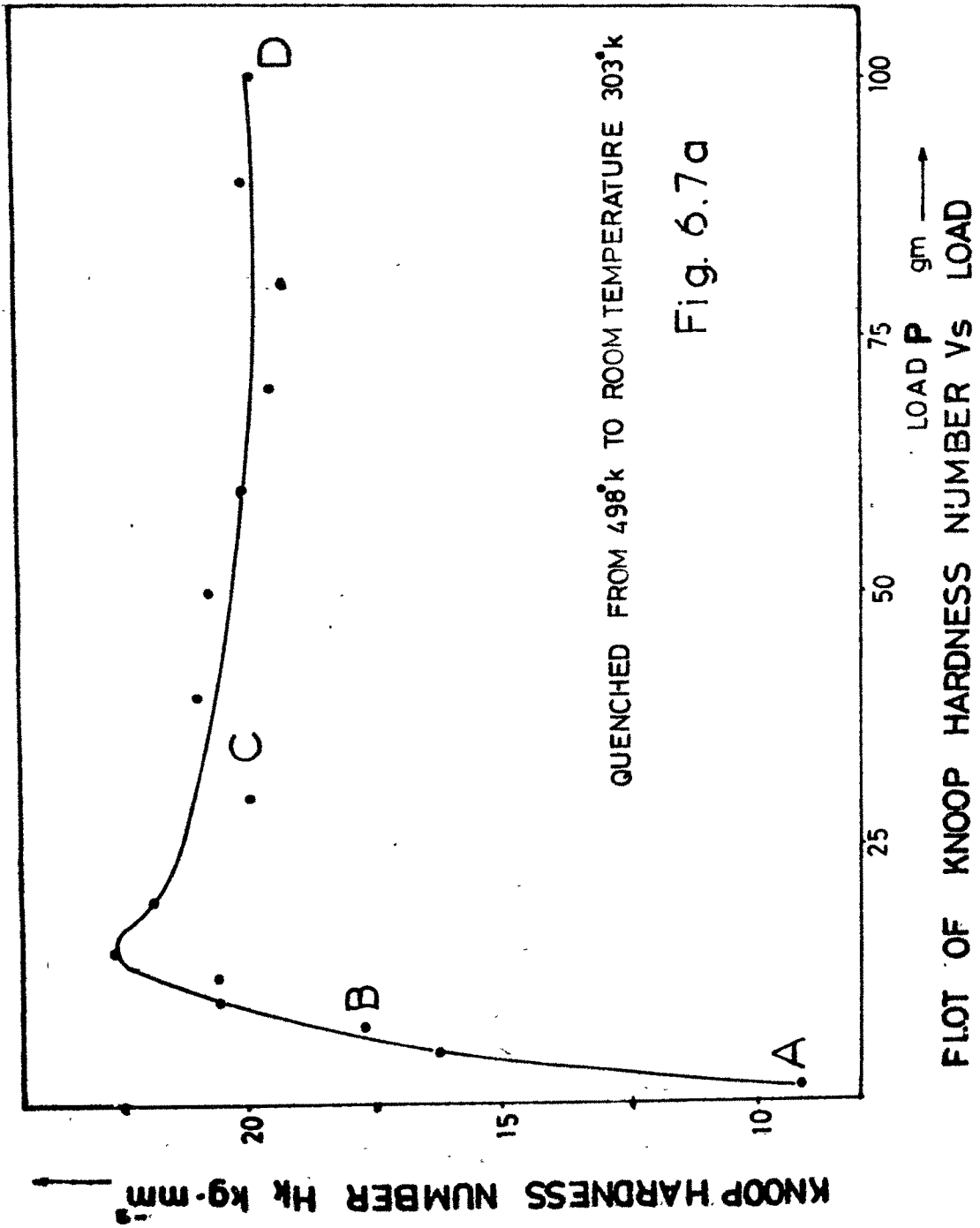


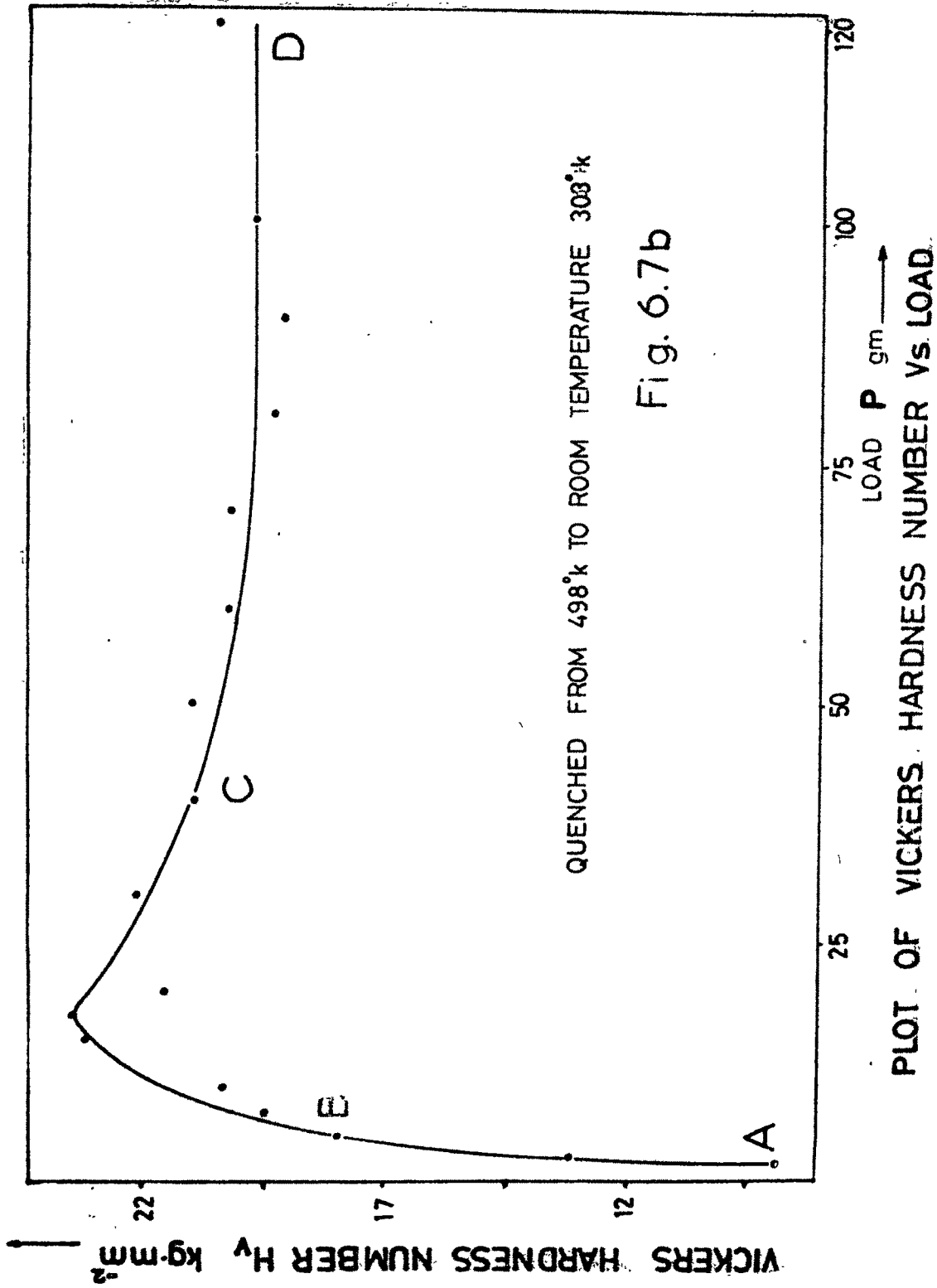












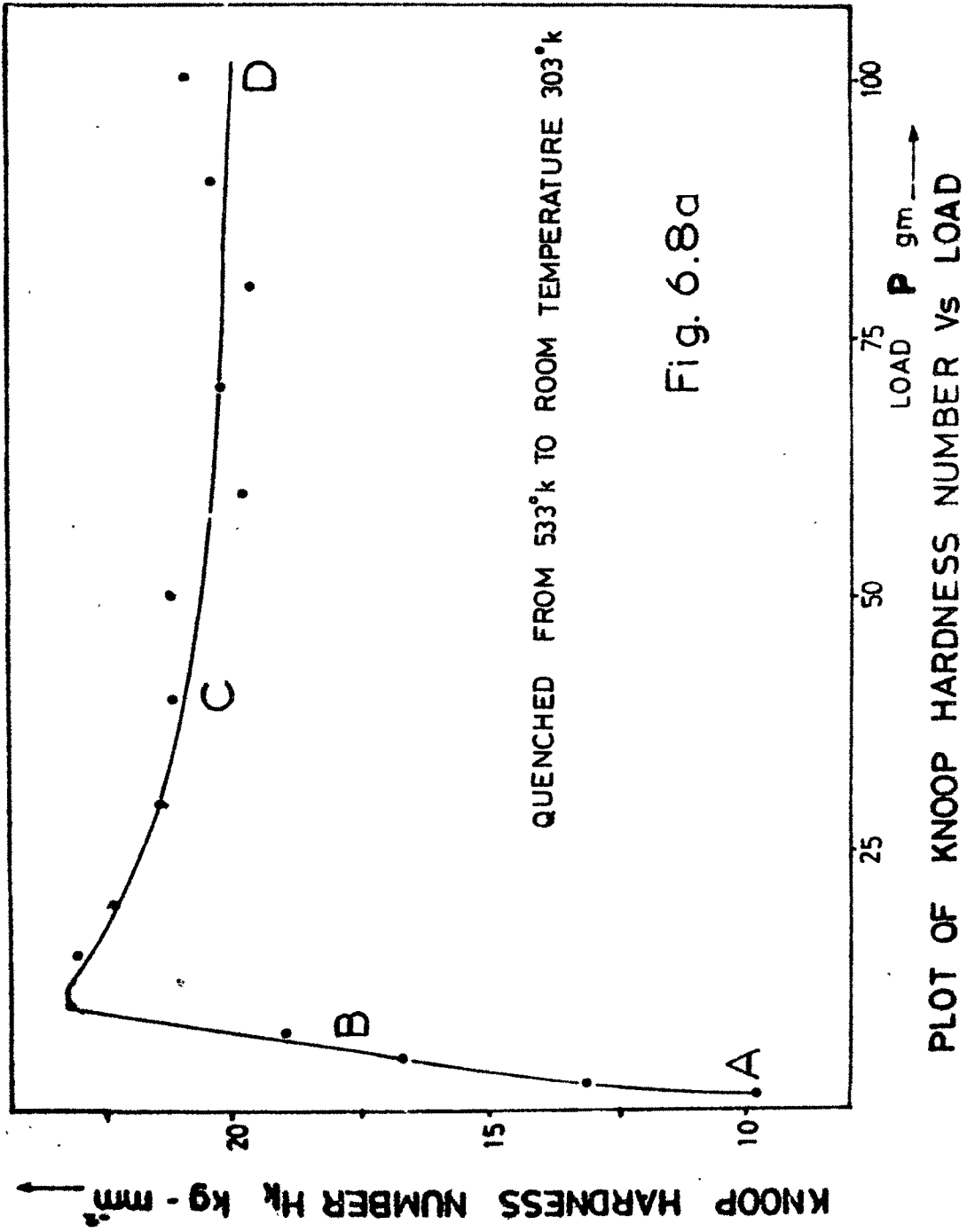
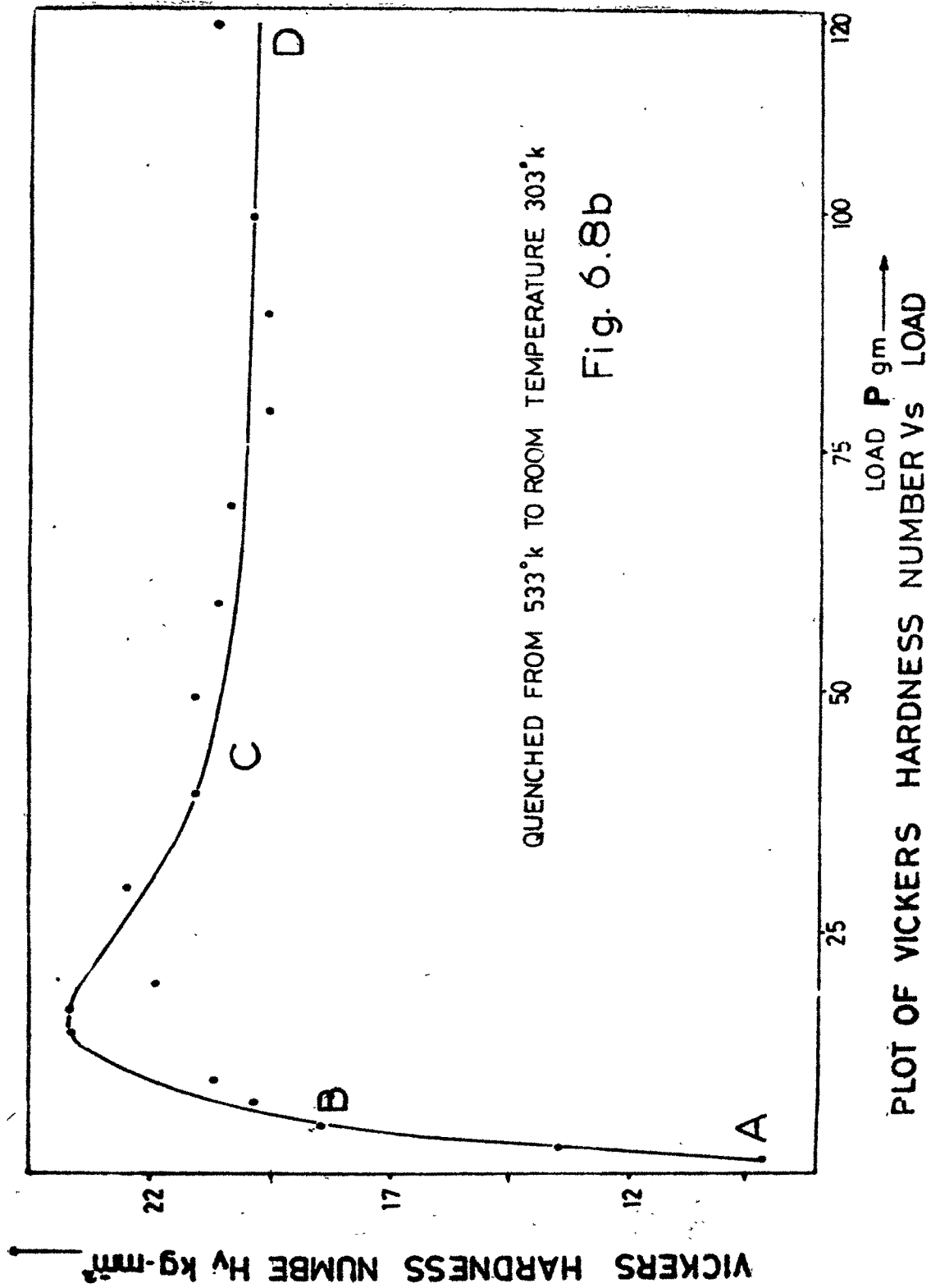


Fig. 6.8a



investigation (Table 6.1 and 6.2). The Knoop and Vickers hardness numbers are calculated using equation (6.1) and (6.2) for thermally treated and untreated samples. The observations are graphically studied by plotting the graphs of hardness number (H_V or H_K) versus load (P). (cf. Fig. 6.1a,b to Fig. 6.8a,b). In what follows the hardness and hardness number will be used to indicate the same meaning.

6.3 RESULTS AND DISCUSSION

It is clear from the graphs of hardness number (H) versus load (P) that contrary to theoretical expectations the hardness varies with load. The hardness at first increases with load, reaches a maximum value then gradually decreases, and attains a constant value for all loads. This behaviour is found for both types of hardness numbers viz. Knoop hardness number (H_K) and Vickers hardness number (H_V). The theoretical conclusion that hardness is independent of load thus appears to be true only at higher loads. The maximum value of hardness corresponds with a load which is nearer the value of the load at which kink in the graph of $\log d$ versus $\log P$ is observed (cf. Chapter V). The graph of H versus P can be conveniently divided into three parts AB, BC and CD where the first part represents linear relation between hardness and load, the second part, the

non-linear relation and the third part the linear one. It should be noted that there is a fundamental difference between linear portions AB and CD of the graph ABCD. This possibly reflects varied reactions of the cleavage surface to loads belonging to different regions. Besides it supports, to a certain extent, the earlier view about the splitting of the graph of $\log d$ versus $\log P$ into two recognizable lines (cf, Chapter V).

The complex behaviour of microhardness with load can be explained qualitatively on the basis of the depth of penetration of the indenter. At small loads the indenter penetrates only surface layers, hence the effect is shown more sharply at these loads. However as the depth of the impression increases, the effect of surface layers becomes less dominant and after a certain depth of penetration, the effect of inner layers becomes more and more prominent than those of surface layers and ultimately there is practically no change in value of hardness with load. This is clear from graphs of Knoop hardness number and Vickers ^{hardness} number versus load for different quenching temperatures.

6.3.1 Relation between hardness and quenching temperature

It is clear from the observations of hardness of quenched and unquenched samples (Tables 6.1 and 6.2) that

hardness depends upon the quenching temperature (T_Q). Hardness in high load region (HLR) is independent of load. Hence average values of hardness (\bar{H}) in high load region are computed and are recorded in Table 6.3. Fig. 6.9 shows the plot of $\log (\bar{H} T_Q)$ versus $\log T_Q$. The plot is a straight line for Knoop as well as Vickers hardness number. Further both the lines are falling on one another having constant slope and constant intercepts on $\log \bar{H} T_Q$ axis. The straight line graph follows the equation,

$$\log \bar{H} T_Q = m \log T_Q + \log C \quad \dots\dots (6.15)$$

where m is the slope and C is an intercept. Therefore,

$$\bar{H} T_Q^{1-m} = C \quad \dots\dots (6.16)$$

or

$$\bar{H} T_Q^k = C \quad \dots\dots (6.17)$$

where $k = 1 - m$. The value of k is -0.17 for sodium nitrate crystals.

It is clear from table 6.4 that Knoop hardness number is almost same as the Vickers hardness number of freshly cleaved faces of sodium nitrate in HLR region. Further for both indenters, the hardness number increases

Table 6.3

QUENCHING TEMPERATURE T_Q OK	Log T_Q	Constant Average Knoop Hardness In H.L.R.	Constant Average Vickers Hardness in H.L.R.	$\overline{H_K}$ kg - mm ⁻²	$\overline{H_V}$ kg - mm ⁻²	Log ($\overline{H_K T_Q}$)	Log ($\overline{H_V T_Q}$)	$\overline{H_K/H_V}$	Mean $\overline{H_K/H_V}$
303	2.4814	18.89	18.75	18.89	18.75	3.7576	3.7544	1.0074	
373	2.5717	18.82	18.95	18.82	18.95	3.8463	3.8497	0.9931	
398	2.5999	18.89	19.30	18.89	19.30	3.8761	3.8854	0.9787	
423	2.6263	19.14	19.42	19.14	19.42	3.9082	3.9146	0.9855	1.0
448	2.6513	19.51	19.71	19.51	19.71	3.9415	3.9459	0.9898	
473	2.6749	19.95	19.71	19.95	19.71	3.9748	3.9695	1.0121	
498	2.6972	20.01	19.96	20.01	19.96	3.9984	3.9973	1.0025	
533	2.7267	20.44	20.09	20.44	20.09	4.0372	4.0297	1.0174	

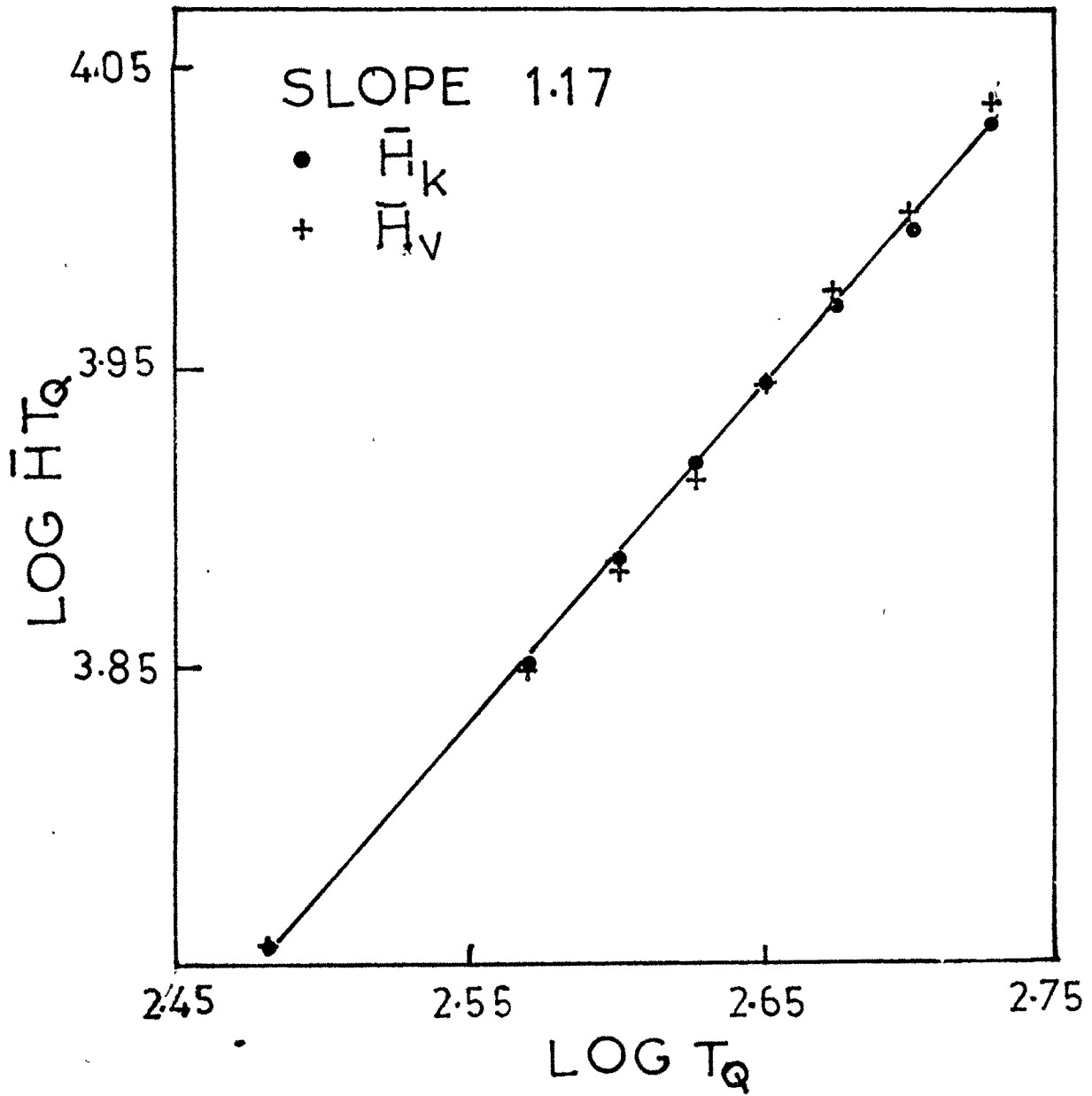


FIG. 69 PLOT OF LOG $\bar{H} T_Q$ vs LOG T_Q

Table 6.4

QUENCHING TEMPERATURE T_Q °K	C_k	C_v	Of C_k (graph)		Of C_v (graph)	
			% Deviation From Mean C_k	% Deviation from value	% Deviation From Mean C_v	% Deviation From Value
303	7.15	7.09	2.91	2.76	1.89	1.89
373	6.87	6.92	- 1.12	- 1.26	- 0.55	- 0.55
398	6.83	6.97	- 1.70	- 1.84	0.17	0.17
423	6.85	6.95	- 1.41	- 1.55	- 0.11	- 0.11
448	6.91	6.98	- 0.55	- 0.69	0.32	0.32
473	7.00	6.91	0.75	0.60	- 0.69	- 0.69
498	6.96	6.94	0.17	0.03	- 0.26	- 0.26
533	7.03	6.91	1.18	1.03	- 0.69	- 0.69
MEAN	6.948	6.958				
VALUES FROM GRAPH	6.958	6.958				

with quenching temperature. However the percentage increase in hardness at 533°K with respect to hardness at room temperature (303°K) is quite small. This percentage change for Knoop hardness and Vickers hardness are 8.2% and 7.14% respectively. The mean ratio of \bar{H}_K/\bar{H}_V is 1.0 at different quenching temperature (Table 6.3).

It is desirable to ascertain how far the relation,

$$\bar{H} T_Q^k = \text{Constant},$$

is true for individual observations on quench hardness. This constant is designated by C and the subscripts k and v indicate respectively use of Knoop and Vickers indenters for obtaining the hardness values (Table 6.4). The percentage changes in hardness from its mean value are small. Further the comparison indicates that the percentage changes for Knoop hardness number are almost the same as those of Vickers hardness number. Since the Knoop indenter is normally used for studying crystalline anisotropy, the large deviations are found for Knoop hardness number compared to those for Vickers hardness number. The author had consistently tried to find the reason for these small deviations by repeating the work several times. However, the results were not significantly different from the present ones. At present there is no theoretical explanation for small deviations.

From the empirical formulae for Knoop and Vickers hardness numbers it is obvious that hardness number is inversely proportional to square of the diagonal of the indentation mark for a constant load. Since hardness depends upon temperature of quenching, the diagonal length of the indentation mark would also depend on the quenching temperature. Thus for both the indenters.

$$H = R P/d^2 \quad \dots (6.18)$$

where R is a constant depending upon the geometry of the indenter. Further,

$$H T_Q^k = C \quad \dots (6.19)$$

Combination of above equations gives,

$$P T_Q^k / d^2 = C/R = \text{Constant} = S \dots (6.20)$$

or,

$$T_Q/d^2 \times P T_Q^k - 1 = S \quad \dots (6.20)$$

$$T_Q/d^2 = (S/P) T_Q^{1-k} \quad \dots (6.21)$$

$$\text{or } \log T_Q/d^2 = \log (S/P) + (1-k) \log T_Q$$

$$\text{or } \log T_Q/d^2 = (1-k) \log T_Q + \log S - \log P \dots (6.22)$$

$$\text{or } \log T_Q/d^2 = m_1 \log T_Q + \log A \quad \dots (6.23)$$

on simplifying it one gets (using equation 6.20).

$$\frac{T_Q^{1 - m_1}}{d^2} = A = \frac{S}{P} = \frac{C}{RP} \dots\dots(6.24a)$$

OR,

$$T_Q^k / d^2 = C/RP = A \dots\dots(6.24b)$$

It is obvious from the above equation that for a given applied load if a graph of $\log (T_Q/d^2)$ is plotted against $\log T_Q$, the slope of the graph will be $(1 - k)$. However if this is repeated for several applied loads, it is evident from above equation that graph of $\log (T_Q/d^2)$ versus $\log T_Q$ should consist of straight lines parallel to one another having slope $(1 - k)$ and different intercepts. Further, the slope of any one plot (Fig. 6.10 and 6.11) is 1.17

$$\text{i.e. } 1 - k = m_1 = 1.17$$

Hence the value of k is $- 0.17$ which is identical with the value of the exponent k in the equation (6.19) connecting hardness number and quenching temperature.

In Chapter V the variation of applied load with diagonal of an indentation mark was studied by critically examining empirical formula, known as Meyer's law.⁷

$$P = a d^n \dots\dots(6.25)$$

Table 6.5 (KNOOP INDENTER)

QUENCHING TEMPERATURE T _Q °K	303	373	398	423	448	473	498	533
LOAD P gm	Log (T _Q /d _k ²)							
40	2.0414	2.0955	2.1360	2.1709	2.2044	2.2343	2.2630	2.2986
50	3.9196	2.0133	2.0342	2.0645	2.0931	2.1348	2.1634	2.1987
60	3.8288	3.9282	3.9518	3.9898	2.0216	2.0543	2.0675	2.0902
70	3.7613	3.8508	3.8729	3.8963	3.9336	3.9655	3.9889	2.0342
80	3.6921	3.7826	3.8194	3.8401	3.8678	3.8927	3.9216	3.9637
90	3.6290	3.7136	3.7701	3.7900	3.8255	3.8612	3.8911	3.9291
100	3.5824	3.6778	3.7091	3.7519	3.7880	3.8165	3.8421	3.8931

Table 6.6 (VICKERS INDENTER)

QUENCHING TEMPERATURE T_Q °K	303	373	398	423	448	473	498	533
LOAD P gm	$\bar{\log} (T_Q/a_V^2)$							
40	2.9079	1.0026	1.0330	1.0633	1.0934	1.1212	1.1464	1.1801
50	2.7831	2.8949	2.9279	2.9609	2.9939	1.0236	1.0505	1.0819
60	2.6910	2.7973	2.8299	2.8661	2.8998	2.9309	2.9571	2.9925
70	2.6483	2.7363	2.7860	2.8116	2.8382	2.8643	2.8887	2.9206
80	2.5912	2.6730	2.7024	2.7300	2.7566	2.7825	2.8096	2.8414
90	2.5254	2.6231	2.6513	2.6794	2.7059	2.7300	2.7745	2.7931
100	2.4891	2.5827	2.6117	2.6413	2.6693	2.6968	2.7226	2.7559
120	2.3973	2.4940	2.5315	2.5603	2.5999	2.6262	2.6407	2.6604

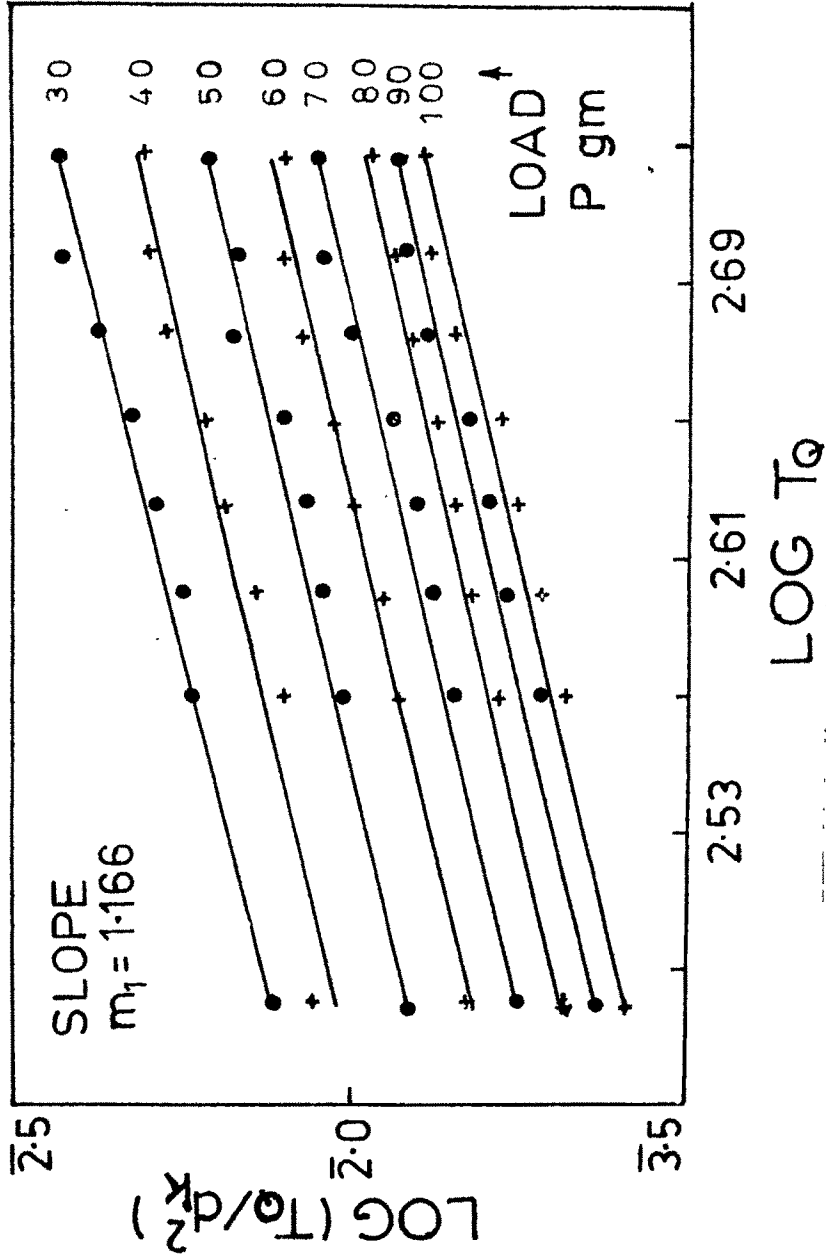


FIG. 6.10 PLOT OF LOG T_g/dk^2 vs LOG T_g

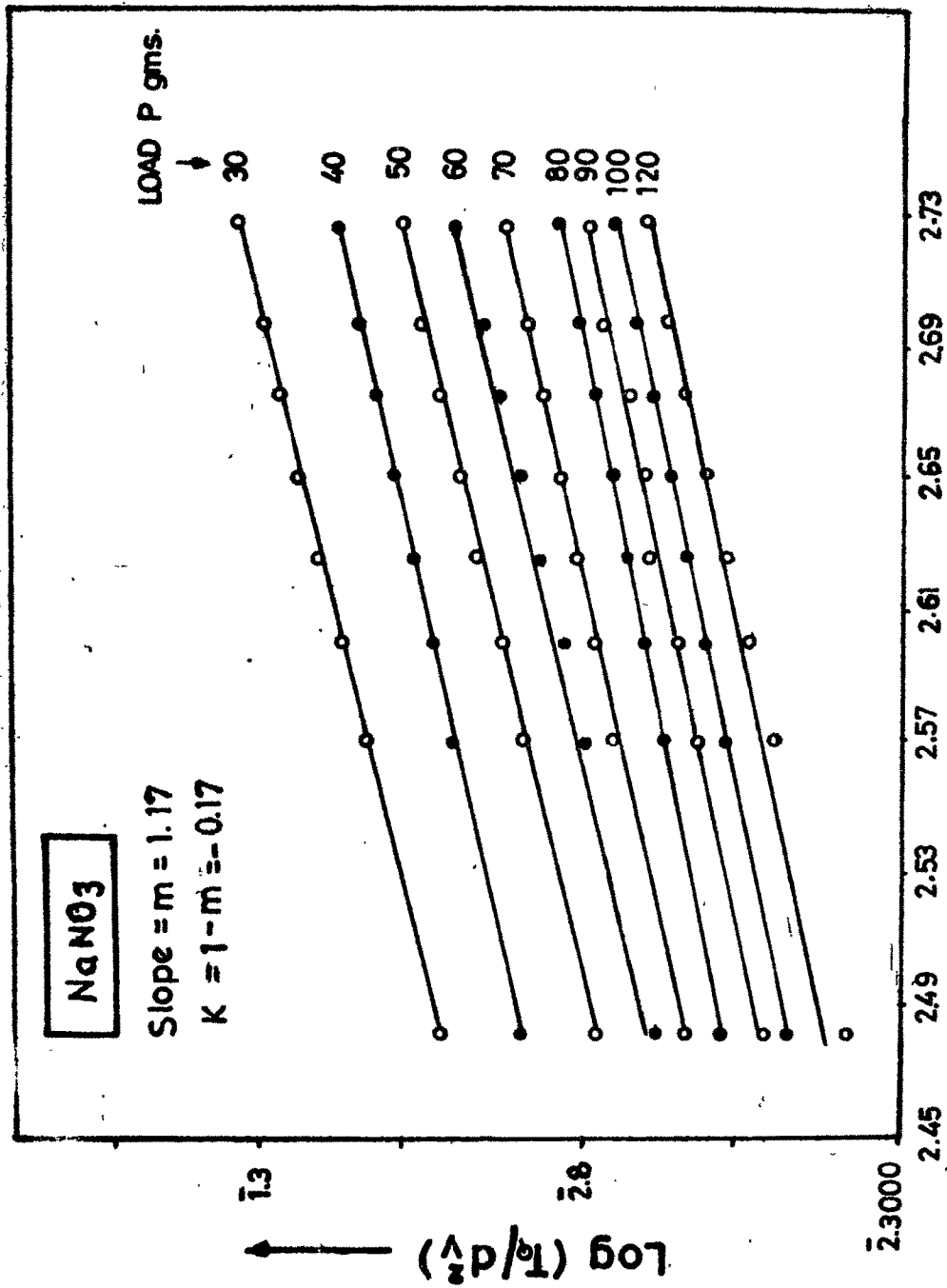


FIG. 5.11 PLOT OF $\log (T_p/d^2)$ Vs $\log T_a$

It was shown that 'a' and 'n' are constants and the straight line represented by the plot of $\log d$ versus $\log P$ consists of two straight lines with slopes n_1 and n_2 and intercepts a_1 and a_2 respectively. The slope n_2 and intercept a_2 approximately correspond to HLR region of the graph of hardness versus load. (Fig. 6.1a,b to 6.8a,b). The combination of equations 6.20 and 6.25 yields,

$$\frac{a_2 d^{n_2} T_Q^k}{d^2} = S \quad \dots (6.26)$$

substituting $d^2 = P/a_2 \cdot d^{n_2 - 2}$ in equation 6.24(a), one gets

$$(T_Q^{1 - m_1/P}) \times a_2 d^{n_2 - 2} = A \quad \dots (6.27)$$

Since n_2 is not having an integral value, it is necessary to have a different approach. If graph of $\log (a_2 d^2 k/T_Q)$ versus $\log T_Q$ are plotted, they consist of a series of parallel lines corresponding to different intercepts (Fig. 6.12 and 6.13 ; Table 6.7 and 6.8). Thus each straight line follows the general equation,

$$\log \frac{a_2 d^2}{T_Q} = m_2 \log T_Q + \log B \quad \dots (6.28)$$

Table 6.7 (KNOOP INDENTER)

QUENCHING TEMPERATURE T _Q °K	303	373	398	423	448	473	498	533
LOAD P gm								
				Log (a ₂ d _K ² /E ₀)				
30	1.2889	1.1791	1.1662	1.1359	1.1139	1.1012	1.0846	1.0327
40	1.3663	1.3151	1.2721	1.2525	1.2317	1.2167	1.1887	1.1625
50	1.4887	1.3971	1.3740	1.3590	1.3429	1.3162	1.2824	1.2449
60	1.5796	1.4826	1.4565	1.4336	1.4144	1.3968	1.3843	1.3692
70	1.6466	1.5598	1.5354	1.5272	1.5025	1.4856	1.4630	1.4253
80	1.7177	1.6281	1.5890	1.5834	1.5682	1.5562	1.5303	1.4958
90	1.7793	1.6888	1.6609	1.6336	1.6076	1.5899	1.5608	1.5304
100	1.8259	1.7330	1.6990	1.6717	1.6482	1.6345	1.6098	1.5664

Table 6.8 (VICKERS INDENTER)

QUENCHING TEMPERATURE T _Q °K	303	373	398	423	448	473	498	533
LOAD P gm	Log (a ₂ d _V ² /T _Q)							
30	1.1684	1.0753	1.0408	1.0002	2.9712	2.9471	2.9813	2.8870
40	1.2860	1.2087	1.1085	1.1479	1.1183	1.0943	1.0708	1.0395
50	1.4108	1.3167	1.2839	1.2504	1.2190	1.1917	1.1669	1.1377
60	1.5029	1.4139	1.3816	1.3452	1.3126	1.2846	1.2602	1.2273
70	1.5456	1.4740	1.4257	1.3996	1.3746	1.3509	1.3282	1.2988
80	1.6027	1.5378	1.5090	1.4813	1.4558	1.4341	1.4076	1.3782
90	1.6685	1.5882	1.5606	1.5316	1.5065	1.4855	1.4428	1.4283
100	1.7050	1.6286	1.5991	1.5704	1.5434	1.5188	1.4946	1.4638
120	1.7965	1.7172	1.6798	1.6511	1.6129	1.5894	1.5766	1.5275

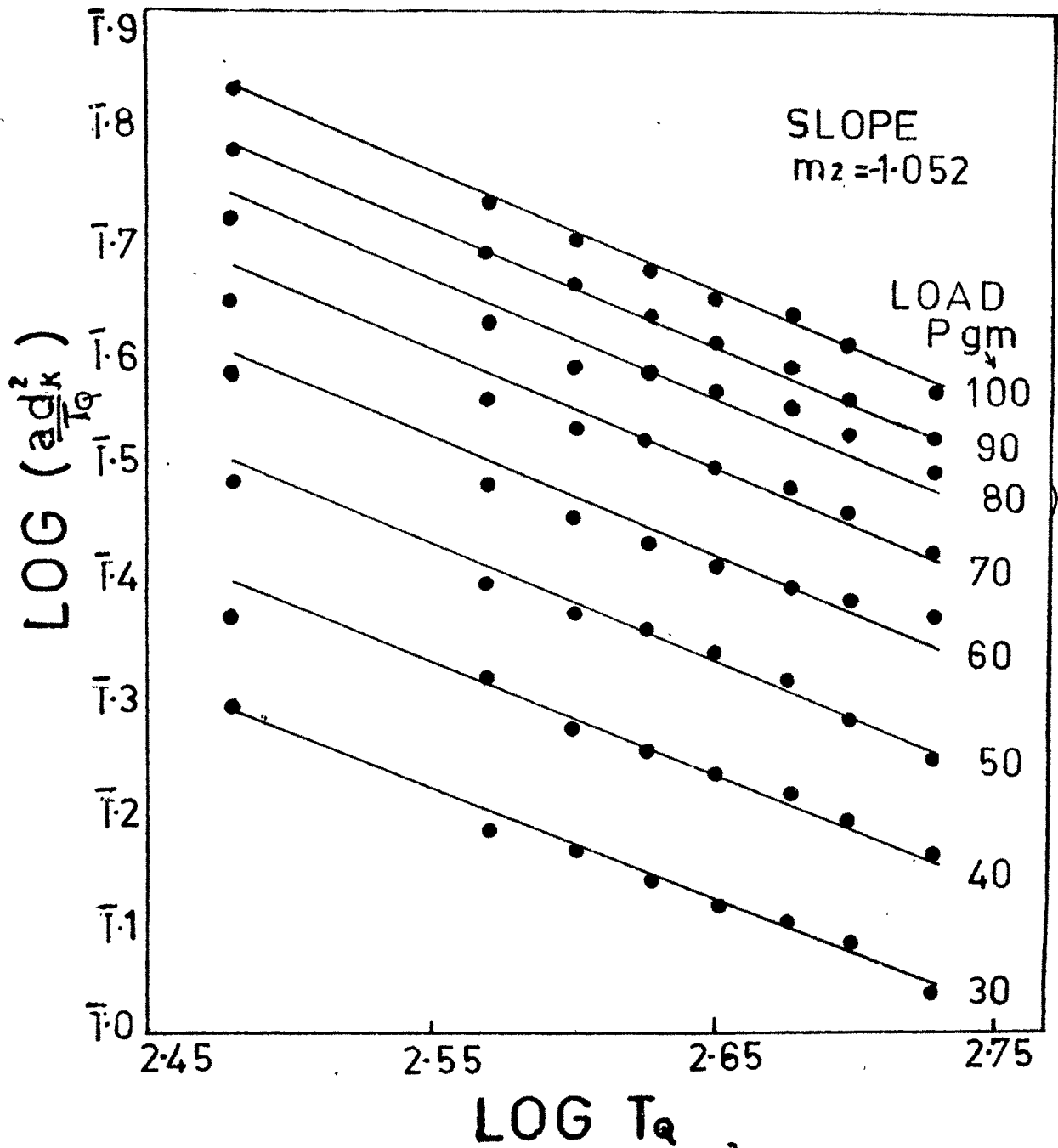


FIG. 6-12 PLOT OF $\text{LOG } adk^2/T_q$ vs $\text{LOG } T_q$

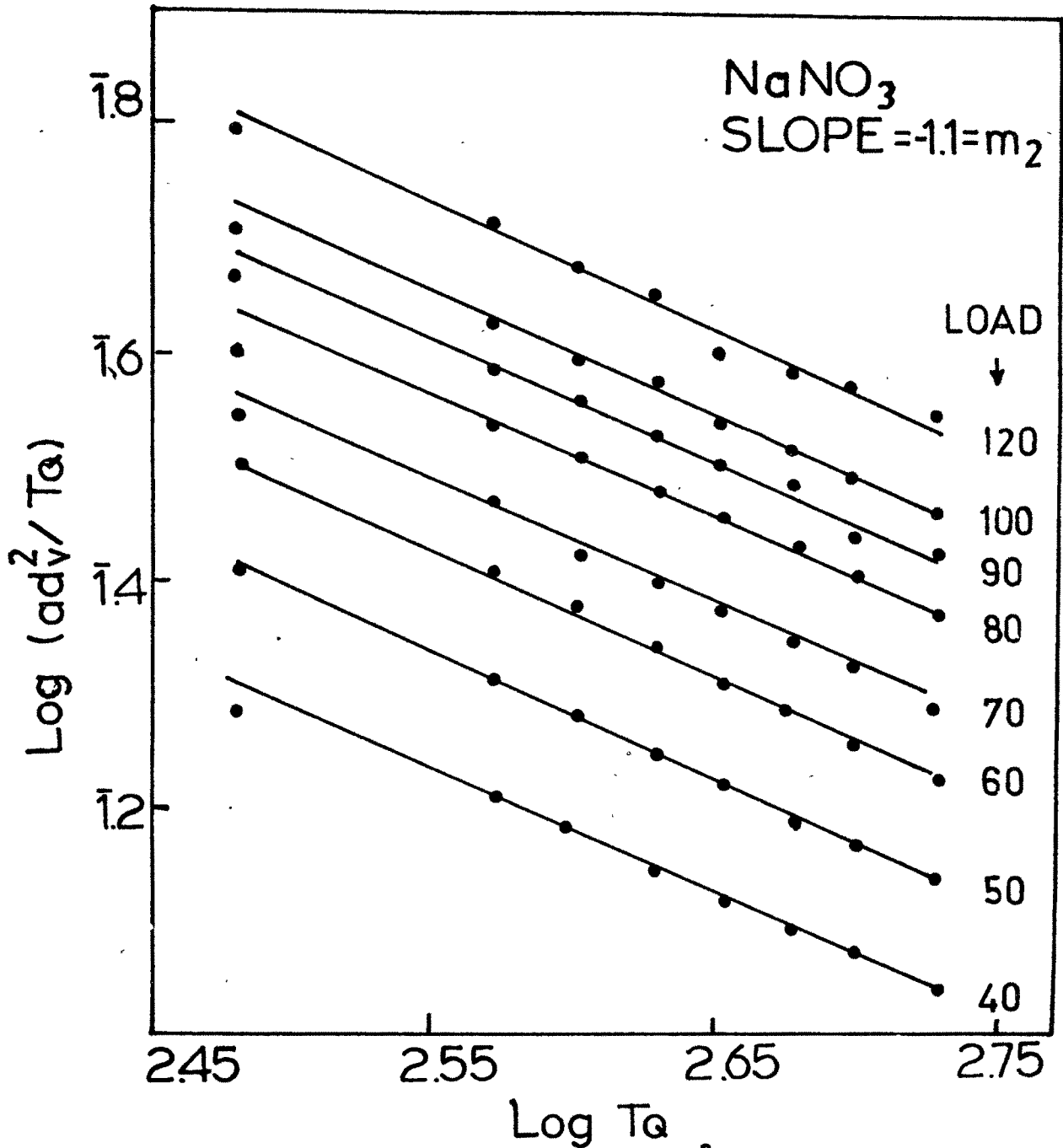


FIG. 6-13 PLOT OF LOG adv^2/T_g vs LOG T_g

Slope of straight lines are $m_2 = -1.1$. Simplification of the above equation yields,

$$a_2 d^2 T_Q^{-(m_2 + 1)} = B \quad \dots\dots (6.29)$$

Combining above equation with Eqn. (6.25) one obtains

$$P d^{2-n} T_Q^{-(m_2 + 1)} = B \quad \dots\dots (6.30)$$

Comparison of Meyer's law (Eqn. 6.25) with formulae for hardness number (Eqn. 6.1 and 6.2) clearly suggests that the constant a and hardness numbers are related. Inspection of the variation of various functions involving H , a_2 and T_Q has disclosed that the graph of $\log (\bar{H} T_Q/a_2)$ versus $\log T_Q$ would be a straight line, following the equation,

$$\log \frac{\bar{H} T_Q}{a_2} = m_3 \log T_Q + \log E \quad \dots\dots (6.31)$$

where m_3 is slope and E is constant. These plots for Knoop and Vickers hardness numbers are presented in Fig. 6.14 (Table 6.9).

The values of slope m_3 are 1.1 for Knoop and Vickers indenters.

Substitution of equations $a_2 = (P/d^2) \times d^{2-n_2}$ and

$$H = R(P/d^2) \text{ in equation (6.31)}$$

Table 6.9

QUENCHING TEMPERATURE T_Q °K	$\text{Log } T_Q$	$\text{Log } \bar{H}_k$	$\text{Log } \bar{H}_v$	$\text{Log } a_2 \bar{H}_k$	$\text{Log } a_2 \bar{H}_v$	$\text{Log } \frac{\bar{H}_k^{T_Q}}{a_2}$	$\text{Log } \frac{\bar{H}_v^{T_Q}}{a_2}$
303	2.4814	1.2762	1.2730	2.6844	1.4669	6.3494	5.5605
373	2.5717	1.2746	1.2776	2.6845	1.4879	6.4364	5.6394
398	2.5999	1.2762	1.2885	2.6844	1.4974	6.4679	5.6735
423	2.6263	1.2819	1.2882	2.7051	1.4996	6.4850	5.7032
448	2.6513	1.2902	1.2947	2.7264	1.5076	6.5054	5.7330
473	2.6749	1.2999	1.2947	2.7502	1.5103	6.5246	5.7539
498	2.6972	1.3012	1.3000	2.7530	1.5176	6.5466	5.7798
533	2.7267	1.3105	1.3029	2.7698	1.5228	6.5778	5.8099

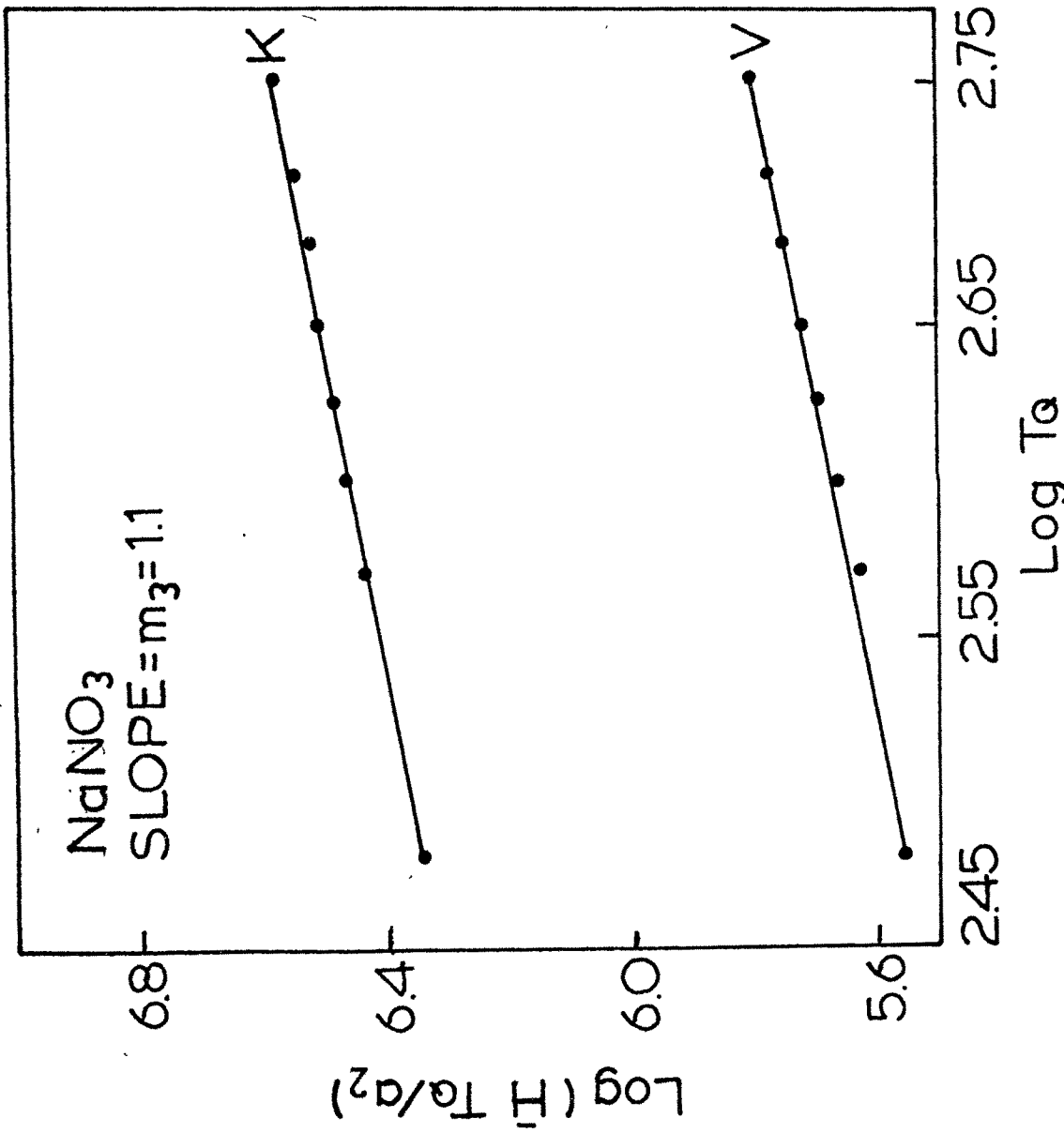


FIG. 6.14 PLOT OF LOG $\bar{H} T_a/a_2$ VS LOG T_a

yields,

$$E = (R T_Q^{1 - m_3}) \times d^{n_2 - 2} \quad \dots (6.32)$$

Combination of the above three equation gives

$$\frac{\bar{H} T_Q^{1 - m_3}}{a_2} = E \quad \dots (6.33)$$

i.e.

$$\frac{\bar{H} T_Q^{-0.1}}{a_2} = E \quad \dots (6.34)$$

Multiplication of eqn. (6.27) by eqn. (6.30) gives

$$a_2 T_Q^{-(m_1 + m_2)} = AB = \text{Constant} \dots (6.35)$$

Thus the intercepts a_2 could be associated with the quenching temperature. This can also be understood from a graphical plot of $\log(a_2 T_Q)$ versus $\log T_Q$, which follows the equation,

$$\log(a_2 T_Q) = m_4 \log T_Q + \log D \dots (6.36)$$

The graphs of $\log(a_2 T_Q)$ versus $\log T_Q$ for Knoop and Vickers indenters are shown in fig. 6.15 (Table 6.3 and 6.4).

Thus,

$$a_2 T_Q^{1 - m_4} = D \quad \dots (6.37)$$

where m_4 is slope of line (fig. 6.15).

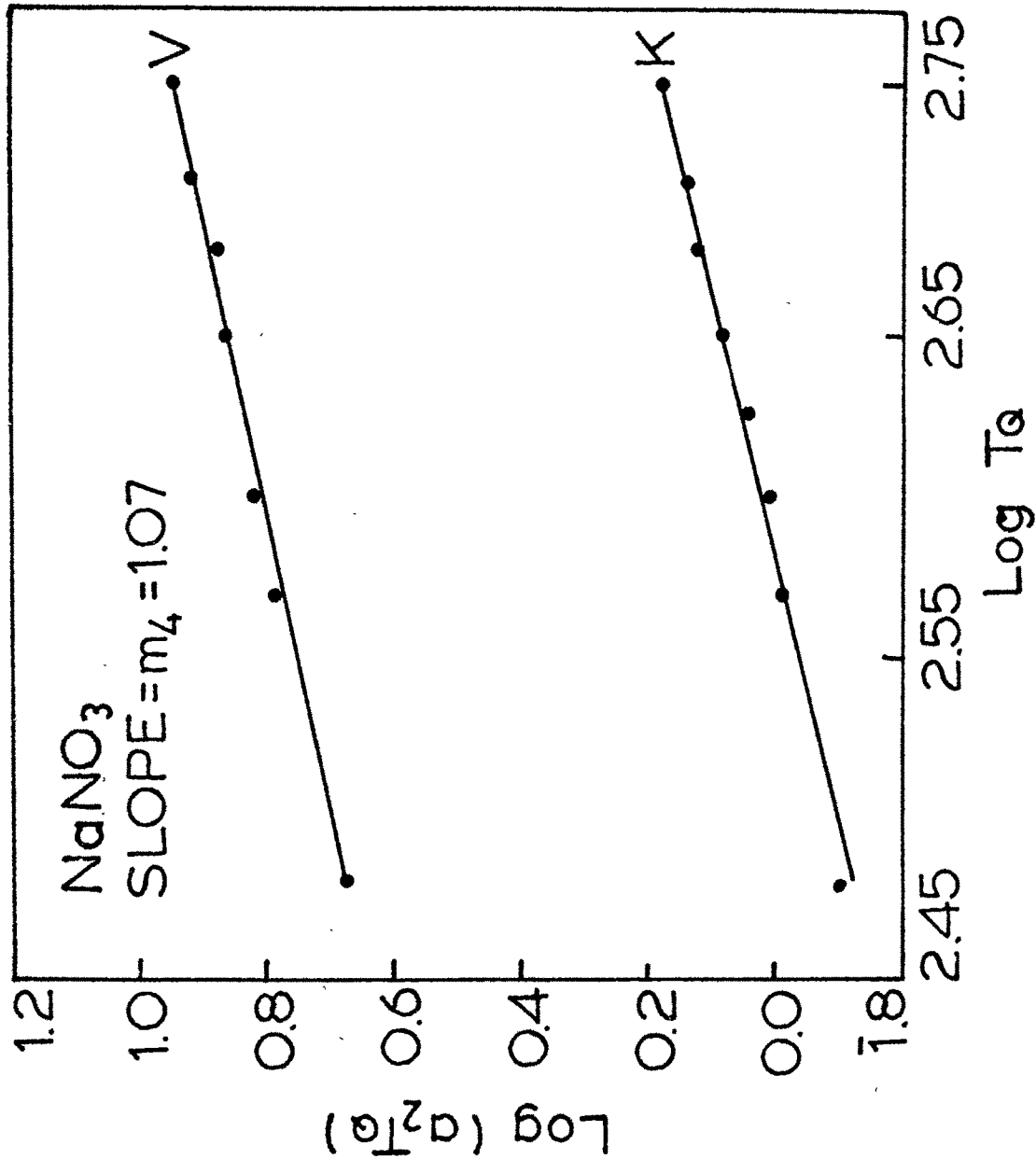


FIG. 6-15 PLOT OF LOG a₂T_q vs LOG T_q

The value of m_4 are 1.07 for Knoop and Vickers indenter. Hence the above equation becomes,

$$a_2 T_Q^{-0.07} = D \quad \dots (6.38)$$

substituting,

$$a_2 = (P/d^2) \times d^{2-n_2} \text{ in eqn. } \dots (6.37)$$

one gets

$$(P/d^2) \times d^{2-n_2} \times T_Q^{1-m_4} = D \quad \dots (6.39)$$

Slight dependence of a_2 on quenching temperature can be expected because value of a_2 is (Table 6.4 and 6.5) quite small. It is suggested from the form of equation (6.25) and (6.18) that there must be some relation between hardness number and a_2 . After considering several functions containing H and a_2 it was found that the plots of $\log (a_2 \bar{H}_K)$ versus $\log \bar{H}_K$ and $\log (a_2 \bar{H}_V)$ versus $\log \bar{H}_V$ give a better straight line, obeying the general equation

$$\log (a_2 \bar{H}) = m_5 \log \bar{H} + \log F \quad \dots (6.40)$$

on simplification one gets

$$a_2 \bar{H}^{1-m_5} = F \quad \dots (6.41)$$

Slopes (m_5) of the above plots (fig. 6.16 ; Table 6.9)

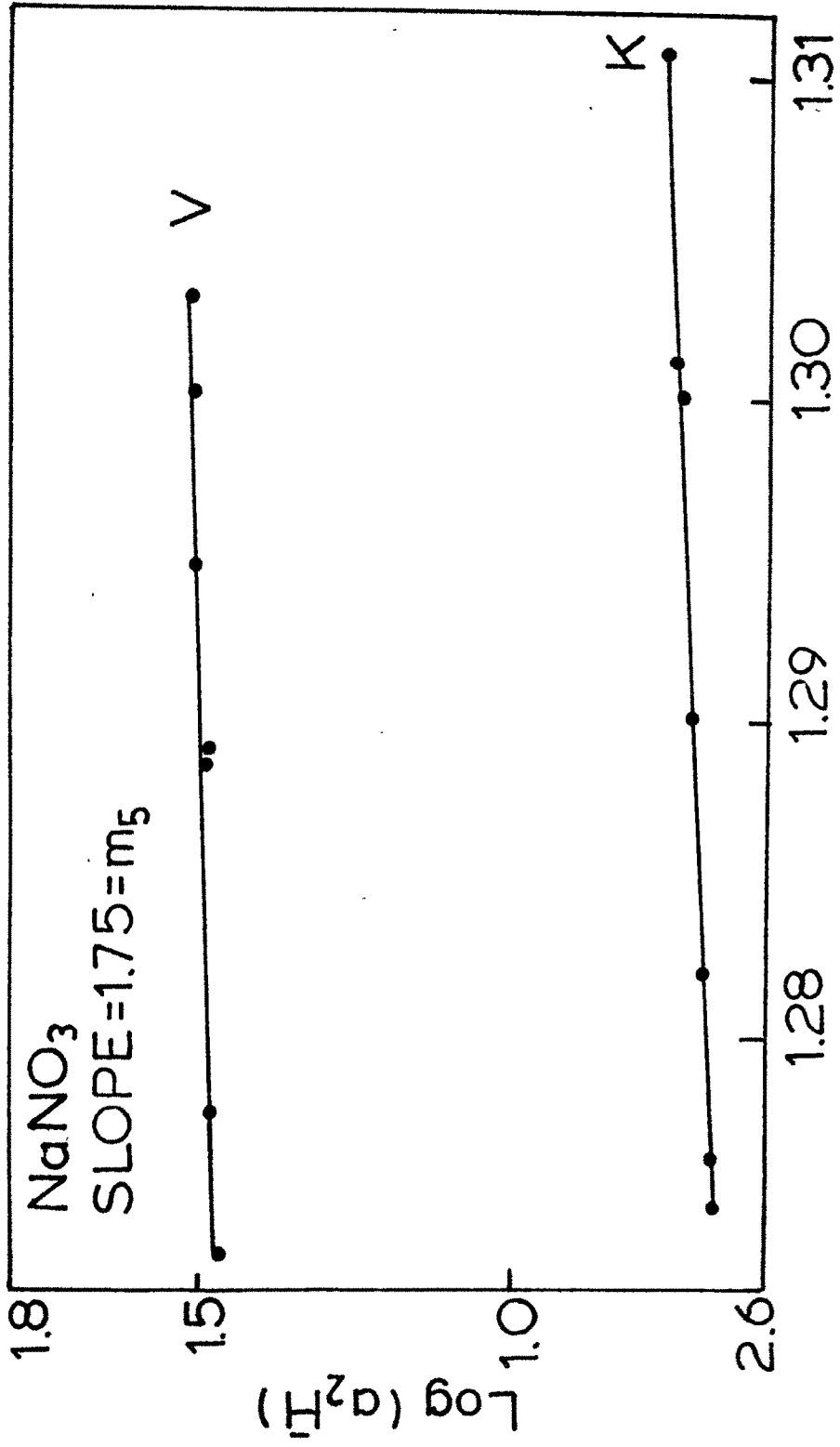


FIG. 6.16 PLOT OF LOG $a_2\bar{H}$ vs LOG \bar{H}

are 1.75. Hence the above equation becomes

$$a_2 \bar{H} - 0.75 = F \quad \dots\dots (6.42)$$

This shows very clearly that hardness number and the intercept of the straight line (cf, fig. 6.16) corresponding to HLR are intimately connected.

It is thus clear from above equations that Meyer's law and formulae for hardness numbers are intimately connected in the HLR region of the graph of hardness number versus applied load.

It is interesting to examine the accuracy of each observation in the above plots by considering the coefficient of variation for different constants associated with different equations above.

The values of A, B, E and D are computed for each observation using equations 6.27, 6.29, 6.32 and 6.39 respectively and are presented in Tables 6.10.1 to 6.10.16. For these tables the above equations are collected here and are given in sequence with new equation numbers.

$$A = \frac{T_Q^{1-m_1}}{P} \times a_2 d^{n_2-2} \quad \dots\dots (6.43)$$

Table 6.10.1 (KNOOP INDENTER)

LOAD P gm	ROOM TEMPERATURE 303°K						
	A x 10 ⁻⁵	B	AB x 10 ⁻³	D x 10 ⁻³	P/B	AP x 10 ⁻⁵	E (DE/14230) x 10 ⁻⁵
40	1.30	137.69	1.789	1.894	0.2905	52.00	4133.8 55.02
50	1.02	175.25	1.787	1.814	0.2853	51.10	4059.8 51.75
60	0.84	213.22	1.791	1.795	0.2814	50.40	4004.3 50.51
70	0.71	251.25	1.783	1.813	0.2786	51.10	3964.4 50.51
80	0.62	290.17	1.799	1.778	0.2757	49.04	3923.2 49.01
90	0.54	329.43	1.778	1.752	0.2732	48.96	3887.6 47.86
100	0.49	368.59	1.806	1.761	0.2713	48.60	3860.6 47.77
MEAN	-	-	1.790	1.801	0.2794	50.17	3976.0 50.34

Table 6.10.2 (KNOOP INDENTER)

LOAD P gm	QUENCHING TEMPERATURE 373°K							
	A x 10 ⁻⁵	B	AB x 10 ⁻³	D x 10 ⁻³	P/B	AP x 10 ⁻⁵	E (DE/14230) x 10 ⁻⁵	
40	1.26	141.29	1.780	1.725	0.2831	50.28	4028.5	48.83
50	0.99	178.82	1.770	1.807	0.2796	49.65	3978.7	50.52
60	0.82	217.39	1.782	1.805	0.2760	49.02	3927.5	49.81
70	0.69	256.5	1.771	1.783	0.2724	48.58	3883.3	48.65
80	0.60	295.2	1.761	1.759	0.2701	48.00	3843.5	47.51
90	0.53	336.32	1.782	1.736	0.2676	47.61	3807.9	46.45
100	0.47	376.08	1.767	1.754	0.2659	47.30	3783.8	46.64
Mean	-	-	1.774	1.767	0.2735	48.63	3893.3	48.34

Table 6.10.3 (KNOOP INDENTER)

LOAD P gm	QUENCHING TEMPERATURE 378°K							
	A x 10 ⁻⁵	B	AB x 10 ⁻³	D x 10 ⁻³	P/B	AP x 10 ⁻⁵	E (DE/14230) x 10 ⁻⁵	
40	1.24	141.99	1.760	1.764	0.2817	49.52	4008.6	49.69
50	0.97	180.18	1.747	1.771	0.2775	48.80	3948.8	49.14
60	0.81	218.89	1.773	1.779	0.2741	48.24	3900.4	48.76
70	0.68	258.49	1.757	1.751	0.2708	47.67	3853.5	47.41
80	0.59	297.73	1.757	1.783	0.2687	47.28	3823.6	47.90
90	0.52	338.6	1.760	1.718	0.2658	46.80	3783.3	45.66
100	0.46	378.35	1.740	1.758	0.2643	46.50	3761.0	46.46
Mean	-	-	1.756	1.760	0.2718	47.83	3868.45	47.86

Table 6.10.4 (KNOOP INDENTER)

LOAD P gm	QUENCHING TEMPERATURE 423°K						
	A x 10 ⁻⁵	B	AB x 10 ⁻³	D x 10 ⁻³	P/B	AP x 10 ⁻⁵	E (DE/14230) x 10 ⁻⁵
40	1.27	142.65	1.811	1.788	0.2804	50.84	3990 50.13
50	1.00	181.22	1.812	1.777	0.2759	50.05	3926 49.02
60	0.83	219.86	1.825	1.816	0.2729	49.50	3883 49.55
70	0.70	260.12	1.821	1.732	0.2691	48.86	3829 46.60
80	0.60	299.85	1.799	1.754	0.2668	48.40	3796 46.78
90	0.53	339.88	1.801	1.771	0.2648	48.06	3768 46.89
100	0.47	379.79	1.785	1.813	0.2643	47.70	3746 47.72
Mean	-	-	1.807	1.778	0.2706	49.06	3848 48.10

Table 6.10.5 (KNOOP INDENTER)

LOAD P gm	QUENCHING TEMPERATURE 448°K							
	A x 10 ⁻⁵	B	AB x 10 ⁻³	D x 10 ⁻³	P/B	AP x 10 ⁻⁵	E (DE/14230) x 10 ⁻⁵	
40	1.29	143.31	1.848	1.814	0.2791	51.88	3971.6	50.62
50	1.02	182.15	1.858	1.784	0.2745	51.05	3906.0	48.96
60	0.84	220.91	1.855	1.836	0.2716	50.52	3865.0	49.86
70	0.71	261.2	1.854	1.772	0.2680	49.91	3813.6	47.49
80	0.62	301.43	1.868	1.758	0.2654	49.44	3776.6	46.65
90	0.55	341.16	1.876	1.817	0.2638	49.14	3753.8	47.93
100	0.49	381.38	1.868	1.850	0.2622	48.70	3731.0	48.50
Mean	-	-	1.861	1.804	0.2692	50.09	3831.0	48.58

Table 6.10.6 (KNOOP INDENTER)

LOAD P gm	QUENCHING TEMPERATURE 473°K							
	A x 10 ⁻⁵	B	AB x 10 ⁻³	D x 10 ⁻³	P/B	AP x 10 ⁻⁵	E (DE/14230) x 10 ⁻⁵	
40	1.33	143.93	1.910	1.832	0.2779	53.28	3954.5	50.91
50	1.05	182.61	1.917	1.848	0.2738	52.55	3896.0	50.59
60	0.86	221.81	1.907	1.865	0.2705	51.90	3849.2	50.45
70	0.73	262.2	1.914	1.797	0.2669	51.24	3798.0	47.96
80	0.63	302.91	1.908	1.764	0.2641	50.72	3758.0	47.08
90	0.56	342.46	1.917	1.846	0.2628	50.49	3739.6	48.51
100	0.50	383.11	1.915	1.863	0.2610	50.10	3714.0	48.62
Mean	-	-	1.912	1.831	0.2681	51.47	3815.0	49.16

Table 6.10.7 (KNOOP INDENTER)

LOAD P gm	QUENCHING TEMPERATURE 498°K							
	A x 10 ⁻⁵	B	AB x 10 ⁻³	D x 10 ⁻³	P/B	AP x 10 ⁻⁵	E (DE/14230) x 10 ⁻⁵	
40	1.32	144.56	1.908	1.851	0.2767	52.96	3937	51.21
50	1.04	183.42	1.907	1.867	0.2726	52.20	3879	50.89
60	0.85	223.29	1.897	1.822	0.2687	51.48	3823	48.94
70	0.73	263.55	1.923	1.794	0.2656	50.89	3779	47.64
80	0.63	304.29	1.917	1.774	0.2629	50.40	3741	46.63
90	0.56	343.9	1.925	1.896	0.2617	50.13	3724	48.91
100	0.50	384.91	1.924	1.869	0.2598	49.80	3697	48.55
Mean	-	-	1.914	1.835	0.2668	51.12	3797	48.97

Table 6.10.8 (KNOOP INDENTER)

LOAD P gm	QUENCHING TEMPERATURE 533°K							
	A x 10 ⁻⁵	B	AB x 10 ⁻³	D x 10 ⁻³	P/B	AP x 10 ⁻⁵	E (DE/14230) x 10 ⁻⁵	
40	1.33	145.45	1.934	1.859	0.2750	53.32	3913.0	51.11
50	1.05	184.5	1.937	1.881	0.2710	52.60	3856.0	50.97
60	0.86	225.05	1.935	1.787	0.2660	51.78	3796.7	47.67
70	0.73	264.75	1.932	1.848	0.2644	51.31	3762.0	48.85
80	0.63	305.81	1.926	1.814	0.2616	50.80	3723.0	47.40
90	0.56	345.75	1.936	1.894	0.2603	50.58	3704.0	49.29
100	0.50	386.25	1.931	1.948	0.2589	50.30	3684.0	50.43
Mean	-	-	1.933	1.861	0.2653	51.52	3777.0	49.40

Table 6.10.9 (VICKERS INDENTER)

LOAD P gm	ROOM TEMPERATURE 303°K							
	A x 10 ⁻⁵	B	AB x 10 ⁻³	D x 10 ⁻³	P/B	AP x 10 ⁻⁴	E	(DE/1854.4) x 10 ⁻⁴
40	10.01	104.57	10.47	10.56	0.3825	40.04	714.96	40.71
50	7.90	132.50	10.47	10.03	0.3773	39.52	704.76	38.12
60	6.52	160.61	10.47	9.84	0.3735	39.12	697.33	37.00
70	5.56	188.26	10.47	10.47	0.3718	38.94	693.91	39.10
80	4.84	216.50	10.47	10.54	0.3695	38.69	689.76	39.17
90	4.27	245.31	10.47	10.26	0.3668	38.42	684.17	37.85
100	3.83	273.66	10.47	10.53	0.3654	38.27	681.29	38.68
120	3.16	331.69	10.47	10.33	0.3617	37.88	674.15	37.55
MEAN	-	-	10.47	10.317	0.3711	38.86	692.54	38.52

Table 6.10.10 (VICKERS INDENTER)

LOAD P gm	QUENCHING TEMPERATURE 373°K							
	A x 10 ⁻⁵	B	AB x 10 ⁻³	D x 10 ⁻³	P/B	AP x 10 ⁻⁴	E (DE/1854.4) x 10 ⁻⁴	
40	10.06	106.75	10.74	10.50	0.3747	40.24	701.37	39.71
50	7.96	135.02	10.74	10.36	0.3703	39.80	692.71	38.69
60	6.56	163.75	10.74	10.05	0.3664	39.37	685.00	37.12
70	5.59	192.32	10.74	10.73	0.3639	39.11	680.20	39.36
80	4.85	221.31	10.74	10.21	0.3615	38.84	675.29	37.18
90	4.29	250.35	10.74	10.28	0.3594	38.63	671.39	37.22
100	3.88	279.40	10.74	10.45	0.3579	38.46	668.27	37.66
120	3.17	338.43	10.74	10.33	0.3545	38.10	661.49	36.85
MEAN	-	-	10.74	10.36	0.3636	39.06	679.46	37.97

Table 6.10.11 (VICKERS INDENTER)

LOAD: P gm	QUENCHING TEMPERATURE 398°K							
	A x 10 ⁻⁵	B	AB x 10 ⁻³	D x 10 ⁻³	P/B	AP x 10 ⁻⁴	E (DE/1854.4) x 10 ⁻⁴	
40	9.97	107.42	10.71	10.67	0.3723	39.89	697.28	40.12
50	7.89	135.82	10.71	10.52	0.3681	39.43	688.87	39.08
60	6.50	164.74	10.71	10.43	0.3642	39.02	681.17	38.31
70	5.54	193.13	10.71	10.10	0.3624	38.83	677.71	36.91
80	4.81	222.73	10.71	10.70	0.3592	38.48	671.25	38.73
90	4.25	251.98	10.71	10.24	0.3571	38.26	667.27	36.85
100	3.81	281.16	10.71	10.45	0.3556	38.10	664.32	37.44
120	3.15	340.38	10.71	10.51	0.3525	37.76	658.17	37.30
MEAN	-	-	10.71	10.45	0.3614	38.72	675.75	38.09

Table 6.10.12 (VICKERS INDENTER)

LOAD P gm	QUENCHING TEMPERATURE 423°K							
	A x 10 ⁻⁵	B	AB x 10 ⁻³	D x 10 ⁻³	P/B	AP x 10 ⁻⁴	E	(DE/1854.4) x 10 ⁻⁴
40	9.86	108.03	10.65	10.55	0.3702	39.45	693.55	39.46
50	7.80	136.56	10.65	10.62	0.3661	39.01	685.42	39.25
60	6.43	165.57	10.65	10.27	0.3624	38.61	677.97	37.55
70	5.48	194.32	10.65	10.64	0.3602	38.38	673.74	38.66
80	4.75	224.07	10.65	10.10	0.3570	38.04	667.44	36.57
90	4.20	253.47	10.65	10.24	0.3550	37.83	663.58	36.64
100	3.77	282.82	10.65	10.45	0.3535	37.67	660.62	37.23
120	3.12	342.40	10.65	10.69	0.3505	37.38	654.52	37.73
MEAN	-	-	10.65	10.44	0.3594	38.29	672.10	37.88

Table 6.10.13 (VICKERS INDENTER)

LOAD P gm	QUENCHING TEMPERATURE 448 °K							
	A x 10 ⁻⁵	B	AB x 10 ⁻³	D x 10 ⁻³	P/B	AP x 10 ⁻⁴	E.	(DE/1854.4) x 10 ⁻⁴
40	9.81	108.58	10.65	10.70	0.3684	39.23	690.29	39.83
50	7.76	137.23	10.65	10.68	0.3643	38.82	682.33	39.29
60	6.40	166.36	10.65	10.44	0.3606	38.41	675.02	38.00
70	5.45	195.41	10.65	10.63	0.3582	38.15	670.22	38.42
80	4.73	225.32	10.65	10.17	0.3550	37.82	663.97	36.41
90	4.18	254.88	10.65	10.23	0.3531	37.60	660.12	36.42
100	3.74	284.35	10.65	10.49	0.3516	37.45	657.32	37.18
120	3.09	343.82	10.65	10.80	0.3490	37.16	652.06	37.98
MEAN	-	-	10.65	10.52	0.3775	38.08	668.91	37.94

Table 6.10.14 (VICKERS INDENTER)

LOAD P gm	QUENCHING TEMPERATURE 473°K							
	A x 10 ⁻⁵	B	AB x 10 ⁻³	D x 10 ⁻³	P/B	AP x 10 ⁻⁴	E (DE/1854.4) x 10 ⁻⁴	
40	9.78	109.13	10.67	10.69	0.3665	39.12	686.98	39.60
50	7.74	137.88	10.67	10.79	0.3626	38.71	679.32	39.53
60	6.39	167.14	10.67	10.56	0.3589	38.32	672.10	38.27
70	5.43	196.41	10.67	10.65	0.3564	38.04	666.98	38.31
80	4.71	226.49	10.67	10.17	0.3532	37.69	660.72	36.23
90	4.16	256.27	10.67	10.20	0.3512	37.48	656.73	36.12
100	3.74	285.78	10.67	10.53	0.3499	37.35	654.21	37.15
120	3.08	345.59	10.67	11.00	0.3472	36.99	648.93	38.49
MEAN	-	-	10.67	10.57	0.3557	37.96	665.74	37.96

Table 6.10.15 (VICKERS INDENTER)

LOAD P gm	QUENCHING TEMPERATURE 498 °K						
	A x 10 ⁻⁵	B	AB x 10 ⁻³	D x 10 ⁻³	P/B	AP x 10 ⁻⁴	E (DE/1854.4) x 10 ⁻⁴
40	9.74	109.66	10.68	10.72	0.3647	38.96	683.88
50	7.71	138.53	10.68	10.85	0.3609	38.55	676.35
60	6.36	167.93	10.68	10.61	0.3573	38.16	669.12
70	5.41	197.38	10.68	10.67	0.3546	37.88	663.90
80	4.69	227.54	10.68	10.24	0.3516	37.55	657.86
90	4.15	257.50	10.68	10.24	0.3495	37.33	653.79
100	3.72	287.35	10.68	10.58	0.3480	37.20	651.30
120	3.07	347.66	10.68	10.50	0.3452	36.86	645.18
MEAN	-	-	10.68	10.55	0.3539	37.81	662.67

Table 6.10.16 (VICKERS INDENTER)

LOAD P gm	QUENCHING TEMPERATURE 533°K							
	A x 10 ⁻⁵	B	AB x 10 ⁻³	D x 10 ⁻³	P/B	AP x 10 ⁻⁴	E (DE/1854.4) x 10 ⁻⁴	
40	9.69	110.36	10.69	10.60	0.3624	38.74	679.81	38.86
50	7.67	139.44	10.69	10.68	0.3586	38.33	672.17	38.71
60	6.32	168.97	10.69	10.53	0.3551	37.96	665.27	37.77
70	5.38	198.68	10.69	10.59	0.3523	37.66	659.81	37.39
80	4.66	229.04	10.69	10.08	0.3493	37.34	653.81	35.89
90	4.13	259.03	10.69	10.21	0.3474	37.14	650.19	35.79
100	3.69	288.99	10.69	10.45	0.3460	36.99	647.39	36.46
120	3.05	350.41	10.69	10.90	0.3424	36.60	640.32	37.64
MEAN	-	-	10.69	10.50	0.3517	37.59	658.59	37.32

Table 6.11 (KNOOP INDENTER)

QUENCHING TEMPERATURE °K	AB x 10 ⁻³	D x 10 ⁻³	AP x 10 ⁻⁵	(DE/14230) x 10 ⁻⁵	P/B	E	C	C/D
303	1.790	1.801	50.17	50.35	0.2794	3976	7.15	3970
373	1.774	1.767	48.63	48.34	0.2735	38.93	6.87	3888
398	1.756	1.760	47.83	47.86	0.2718	3868	6.83	3881
423	1.807	1.778	49.06	48.10	0.2706	3848	6.85	3861
448	1.861	1.804	50.09	48.58	0.2692	3831	6.91	3830
473	1.912	1.831	51.47	49.16	0.2681	3815	7.00	3823
498	1.914	1.835	51.12	48.97	0.2668	3797	6.96	3793
533	1.933	1.861	51.52	49.40	0.2653	3777	7.03	3777
Mean	1.843	1.804	49.98	48.85	0.2706	3850	6.98 ⁴	3853
Coefficient of variation %	2.97	3.218	2.99	57.46	1.196	2.364	2.42	3.56
Values from graph	1.875	1.77	51.54	48.67	0.2747	3913	6.598	3727

Table 6.12 (VICKERS INDENTER)

QUENCHING TEMPERATURE °K	AB x 10 ⁻³	D x 10 ⁻³	AP x 10 ⁻⁴	(DE/1854.4) x 10 ⁻⁴	P/B	E	C	C/D
303	10.47	10.32	38.86	38.52	0.3711	692.54	7.09	687.0
373	10.74	10.36	39.06	37.92	0.3636	679.46	6.92	667.9
398	10.71	10.45	38.72	38.09	0.3614	675.75	6.97	662.2
423	10.65	10.44	38.29	37.88	0.3594	672.10	6.95	665.7
448	10.65	10.52	38.08	37.94	0.3575	668.91	6.98	663.5
473	10.67	10.57	37.96	37.96	0.3557	665.74	6.91	653.7
498	10.68	10.55	37.81	37.71	0.3539	662.67	6.94	657.8
533	10.69	10.50	37.59	37.32	0.3517	658.59	6.91	658.1
Mean	10.657	10.4637	38.296	37.92	0.3593	671.97	6.9587	664.5
Coefficient of variation %	0.72	0.85	1.347	1.634	1.356	1.49	0.8	1.297
Values from graph	10.66	10.54	37.38	38.506	0.3509	677.48	6.958	660.15

$$A_k = \frac{T_Q^{1-m_1}}{P} \times a_{2k} d_k^{n_2-2} \dots\dots (6.43a)$$

$$A_v = \frac{T_Q^{1-m_1}}{P} \times a_{2v} d_v^{n_2-2} \dots\dots (6.43b)$$

$$B = P d^{2-n_2} T_Q^{0.1} \dots\dots (6.44)$$

$$B_k = P d_k^{2-n_2} T_Q^{0.1} \dots\dots (6.44a)$$

$$B_v = P d_v^{2-n_2} T_Q^{0.1} \dots\dots (6.44b)$$

$$P/B = d^{n_2-2} / T_Q^{0.1} \dots\dots (6.45)$$

$$P/B_k = d_k^{n_2-2} / T_Q^{0.1} \dots\dots (6.45a)$$

$$P/B_v = d_v^{n_2-2} / T_Q^{0.1} \dots\dots (6.45b)$$

$$AB = \frac{P T_Q^{k+0.1}}{d^2} \dots\dots (6.46)$$

$$A_k B_k = \frac{P T_Q^{k+0.1}}{d_k^2} \dots\dots (6.46a)$$

$$A_V B_V = \frac{P T_Q^{k+0.1}}{d_V^2} \dots\dots (6.46b)$$

$$AP = T_Q^{1-m_1} a_2 d^{n_2-2} \dots\dots (6.47)$$

$$A_K P = T_Q^{1-m_1} a_{2k} d_k^{n_2-2} \dots\dots (6.47a)$$

$$A_V P = T_Q^{1-m_1} a_{2v} d_V^{n_2-2} \dots\dots (6.47b)$$

$$D = \frac{P}{d^2} d^2 - n_2 T_Q^{1-m_4} \dots\dots (6.48)$$

$$D_K = \frac{P}{d_K^2} d_K^2 - n_2 T_Q^{1-m_4} \dots\dots (6.48a)$$

$$D_V = \frac{P}{d_V^2} d_V^2 - n_2 T_Q^{1-m_4} \dots\dots (6.48b)$$

$$E = R T_Q^{1-m_3} d^{n_2-2} \dots\dots (6.49)$$

$$E_K = 14230 T_Q^{1-m_3} d_k^{n_2-2} \dots\dots (6.49a)$$

$$E_V = 1854.4 T_Q^{1-m_3} d_V^{n_2-2} \dots\dots (6.49b)$$

$$DE = \frac{R P}{d^2} T_Q^{(2 - m_3 - m_4)} \dots (6.50)$$

$$D_k E_k = \frac{14230 P}{d_k^2} T_Q^{(2 - m_3 - m_4)} \dots (6.50a)$$

$$D_v E_v = \frac{1854.4 P}{d_v^2} T_Q^{(2 - m_3 - m_4)} \dots (6.50b)$$

The mean values of constants are summarised in Tables 6.11 and 6.12.

A careful study of mean values of 'constants' and their deviations from the corresponding individual observation clearly indicates that the deviations are within experimental errors. A glance at Table 6.11 and 6.12 shows that,

$$D = AB \dots (6.51)$$

$$AP = \frac{DE}{R} \dots (6.52)$$

$$E = \frac{C}{D} \dots (6.53)$$

From tables 6.3 and 6.4 we have,

$$\frac{C_k}{C_v} = \frac{\bar{H}_k}{\bar{H}_v} \text{ for all temperatures.}$$

Thus for all loads in HLR for Knoop and Vickers indenters, the variation of hardness number H and the variation of hardness constant a_2 with quenching temperature and also with each other follow the equation,

$$H T_Q^k = C = \text{Constant} \quad \dots (6.55)$$

$$a_2 T_Q^r = D = \text{Constant} \quad \dots (6.56)$$

$$a_2 H^s = F = \text{Constant} \quad \dots (6.57)$$

where k , r and s are different and numerically less than unity. The signs for these constants decide the nature of the crystal. For sodium nitrate they are negative as shown above. Further quenching can also be carried out by bringing a crystal from very low temperature to room temperature. Thus for $T_Q = 1^\circ\text{K}$,

$$H = \text{Constant} \quad \dots (6.58)$$

$$a_2 = \text{Constant} \quad \dots (6.59)$$

These values can be considered to characterise a crystalline material. Thus for sodium nitrate, the quench hardness number and quench hardness constant

are given by,

$$H_k = 6.95 \text{ Kg} - \text{mm}^{-2} \dots\dots (6.60)$$

and

$$H_v = 6.95 \text{ Kg} - \text{mm}^{-2} \dots\dots (6.61)$$

$$a_k = 1.804 \times 10^{-3} \text{ Kg} - \text{mm}^{-2} \dots\dots (6.62)$$

and

$$a_v = 10.46 \times 10^{-3} \text{ Kg} - \text{mm}^{-2} \dots\dots (6.63)$$

6.3.2 Relation between microhardness and electrical conductivity

There are several temperature dependent crystal properties. One such property is electrical conductivity which varies in an exponential fashion with temperature. The comparison of electrical conductivity measured at temperature T to the microhardness value determined for the same quenching temperature could provide a clue about the possible relation between two quantities, hardness and electrical conductivity.

The values of electrical conductivity, σ_c , are given in Table 6.13 (taken from a paper of C. Ramasastry and V.V.G.S. Murti⁸).

Table 6.13*

Temperature T °K	Electrical conductivity σ_c mho cm^{-1}	Log $\sigma_c T$	$10^3/T$
373	1×10^{-12}	$\overline{10.5717}$	2.68
398	7.5×10^{-12}	$\overline{9.4749}$	2.512
423	5×10^{-11}	$\overline{8.3253}$	2.364
448	1×10^{-10}	$\overline{8.6512}$	2.232
473	7×10^{-10}	$\overline{7.5199}$	2.114
498	2×10^{-9}	$\overline{7.9982}$	2.008
533	4×10^{-8}	$\overline{6.3287}$	1.876

* The values of electrical conductivity of sodium nitrate crystals grown from melt are taken from a paper of C. Ramasastry and Y.V.G.S. Murti.⁸

It is clear from a study of electrical conductivity of sodium nitrate crystals⁸ that the activation energy is 0.94 eV for 100°C to 260°C. Beyond 260°C values of electrical conductivity are not dependable because of the onset of phase transformation in sodium nitrate. The same type of behaviour has been observed by present author in this laboratory. It should further be remarked that the data on electrical conductivity for solution-grown and melt grown crystals of sodium nitrate has shown that the former crystals were of inferior quality.⁹

It is known that the point defects which exists in crystal in thermal equilibrium, in contrast to thermodynamically unstable defects like dislocations and grain boundaries, may contribute to mechanical properties through diffusion, e.g. creep at high temperatures. Hence, it is desirable to review briefly the part played by point defects in 'hardening' crystalline materials. It is found that more direct effects of point defects on mechanical properties, e.g. an increase in the yield stress, are caused by non-equilibrium concentrations of point defects, and on formation of their aggregates. In the present case non-equilibrium concentrations of point defects in sodium nitrate are produced by rapid cooling from high temperatures, the resulting hardening is called 'quench hardening' as distinct from radiation hardening produced by irradiation. The quench

hardening is simpler amongst the two. The quenching experiments introduce the following few or all effects in a crystal.

- (i) Excess vacancies (equilibrium concentration of vacancies at higher temperature).
- (ii) Possible aggregation of some vacancies.
- (iii) Annihilation of vacancies.
- (iv) Quenching strains.
- (v) Pinning of vacancies at dislocations, grain boundaries and impurities.
- (vi) Effect of interstitials and their small aggregates.

The concentration and formation of energy of excess vacancies can be studied at low temperatures by measuring electrical resistivity. The main disadvantage in this procedure is possible aggregation or annihilation of some of the vacancies during quenching. Implicit in this method is the correction or avoidance of loss of vacancies together with any production of them e.g. by quenching strains and the effect of impurity and the formation of the more mobile vacancies. The quenching strains are associated with the production of vacancies. This will be clear from the following consideration.

During quenching of the specimen, the surface is

cooler than the inside and hence it is in tension while the inside is in compression. If the stress due to thermal gradient is large enough, the specimen will be deformed plastically. Since the yield stress is usually lower at higher temperature, the inside section of material will then undergo plastic deformation. When the quenching is completed and the temperature is again uniform, the plastically deformed inside material compresses the surface layers and vice versa. The thermal stresses thus set up are both axial and radial. Hence the deformation of the specimen is thus complex. Usually point defects are produced by deformation. Hence the production of vacancies by quenching strain must be taken into account in any assessment of the number of vacancies quenched into a crystal. Further the mechanical properties of a crystal are largely determined by the number, geometrical configurations, interactions and mobility of dislocations contained in it. The mobility of dislocations is mainly determined by their interactions with other defects, structural and/or otherwise. It is this interaction which produces 'hardening'. This production will now be reviewed briefly.

Non-conservative motion of jogs on dislocation and annihilation of two parallel edge dislocations of opposite

sign, one atomic plane apart, are the main mechanisms suggested for point defect formation during deformation by mechanical means or by quenching. The non-conservative motion of jogs is possible both on edge dislocations and screw dislocations. For deformation, however, jogs on screw dislocations are more important. Jogs on screw dislocation are geometrically short segments of edge dislocations. The slip plane of these jogs is not the slip plane of the parent screw dislocation. Hence as the screw dislocation moves, jogs should move in a non-conservative manner along the screw. These fundamental mechanisms of point defect formation are well established geometrically, but the theory cannot predict as yet how many of particular species of defect are produced under certain conditions. This is a very difficult problem because the number and behaviour of moving dislocations are very complicated functions of the deformation temperature, the strain rate as well as other conditions of the specimen. A complete understanding of work hardening is required to solve this problem. Thus quenching produces dislocations, grain boundaries segregation of impurities as well as point defects. It is also observed that a physical property suitable to detect the excess vacancies is also affected by plane and volume defects. Hence it is necessary to separate the effect of a particular kind of defect from the effect of others.

The procedure for effecting this discrimination varies in a finer way from specimen to specimen, materials to materials. This is not yet perfected for all types of materials. The interstitials act in somewhat similar fashion as mentioned for vacancies.

The above presents briefly the possible effects of quenching processes on materials. It is now interesting to consider the effect of these processes on crystals. It is observed that no noticeable increase or change in hardness is found for quenched and aged metallic crystals. This is in marked contrast with the pronounced change in yield stress. The reason for this apparent contradiction is found in the observed stress-strain curve of the quenched hardened crystal i.e. the effect of quenching on hardening disappears after a moderate amount of deformation. Since hardness is a measure of resistance to deformation, microhardness measurements using very small loads might detect quench hardening. However use of small loads would determine the hardness of only the surface layers probably few microns deep. It may be remarked that even in the low load region, local deformation will be severe. Since the vacancies escape to the surface during quenching, no hardening is to be expected in the thin surface layers. It is therefore imperative to remove the surface layers in order to detect hardening using small

load for microhardness measurements. It is from this view that Aust et al.,¹⁰ quenched zone-refined lead from near 300°C into water. Hardness was measured using a load of 1 gm., this resulted in a depth of indentation of about 3 μ . The specimen showed no hardening when tested without removing surface layers. Further hardening was observed when surface layers of 50 μ were removed. They also found that the region near the grain boundary showed no hardening. This is most likely to be due to the escape of vacancies to grain boundaries during quenching. Since the vacancies anneal out of the surface during quenching, the first few layers will not exhibit quenching effect. As sodium nitrate has a perfect cleavage, the quenched samples were cleaved and the hardness studies were carried out on these freshly cleaved specimens.

The graphs of $\log T_{Qd}$ versus $1/T_Q$ and $\log \sigma_c T$ versus $1/T$ (fig. 6.17) for sodium nitrate crystals showed close resemblance with one another (Fig. 6.18 ; 6.19, Tables 6.14 ; 6.15). Hence it appears that similar mechanisms are likely to operate in the crystal. Further, the plots of $\log T_{Qd}$ versus $1/T_Q$ are parallel to one another except for the load where maximum hardness is observed. Hence it can be conjectured that the point defects are mainly responsible for increased hardness of

Table 6.14 (KNOOP INDENTER)

QUENCHING TEMPERATURE T _Q °K	303	373	398	423	448	473	498	533
LOAD P gm	Log T _Q dk							
1.25	4.1713	4.2392	4.2636	4.2861	4.3088	4.3269	4.3412	4.3627
2.5	4.2504	4.2963	4.3337	4.3575	4.3691	4.3859	4.4150	4.4445
5.0	4.3276	4.4158	4.4198	4.4622	4.4819	4.5003	4.5173	4.5415
7.5	4.3662	4.4656	4.4893	4.5010	4.5219	4.5500	4.5866	4.6022
10	4.3931	4.4896	4.5116	4.5363	4.5598	4.5898	4.6175	4.6206
25	4.4723	4.5832	4.6049	4.6263	4.6417	4.6648	4.6841	4.7102
20	4.5604	4.6437	4.6669	4.6888	4.7112	4.7348	4.7550	4.7783
30	4.6624	4.7417	4.7787	4.7957	4.8158	4.8373	4.8622	4.8767
40	4.7011	4.8097	4.8317	4.8539	4.8747	4.8951	4.9142	4.9418
50	4.7623	4.8507	4.8826	4.9072	4.9303	4.9448	4.9640	4.9906
60	4.8077	4.8934	4.9238	4.9445	4.9660	4.9851	5.0120	5.0449
70	4.8412	4.9321	4.9633	4.9913	5.0101	5.0295	5.0514	5.0729
80	4.8768	4.9662	4.9901	5.0194	5.0429	5.0648	5.0850	5.1082
90	4.9076	4.9966	5.0261	5.0445	5.0626	5.0816	5.1002	5.1255
100	4.9309	5.0189	5.0452	5.0635	5.0829	5.1039	5.1247	5.1435

Table 6.15 (VICKERS INDENTER)

QUENCHING TEMPERATURE T _Q °K	303	373	398	423	448	473	498	533
LOAD P gm	Log T _Q d _V							
1.25	3.7154	3.8013	3.8264	3.8508	3.8703	3.8875	3.9067	3.9283
2.5	3.7732	3.8543	3.8825	3.9118	3.9293	3.9565	3.9704	3.9953
5.0	3.8554	3.9381	3.9663	3.9905	4.0115	4.0335	4.0536	4.0777
7.5	3.9352	4.0148	4.0411	4.0644	4.0847	4.1051	4.1240	4.1503
10	3.9746	4.0632	4.0901	4.1137	4.1364	4.1570	4.1770	4.2029
15	4.0501	4.1317	4.1537	4.1753	4.1963	4.2174	4.2368	4.2616
20	4.1091	4.1994	4.2241	4.2497	4.2726	4.2940	4.3147	4.3416
30	4.2093	4.2895	4.3143	4.3339	4.3560	4.3780	4.3977	4.4236
40	4.2682	4.3562	4.3831	4.4078	4.4295	4.4516	4.4725	4.4999
50	4.3306	4.4102	4.4358	4.4590	4.4799	4.5003	4.5205	4.5490
60	4.3766	4.4588	4.4846	4.5064	4.5267	4.5467	4.5672	4.5938
70	4.3980	4.4893	4.5067	4.5336	4.5577	4.5799	4.6012	4.6296
80	4.4265	4.5208	4.5484	4.5744	4.5983	4.6209	4.6409	4.6692
90	4.4594	4.5459	4.5741	4.5996	4.6236	4.6472	4.6679	4.6933
100	4.4777	4.5662	4.5934	4.6190	4.6421	4.6639	4.6844	4.7121
120	4.5234	4.6104	4.6337	4.6593	4.6769	4.6991	4.7254	4.7598

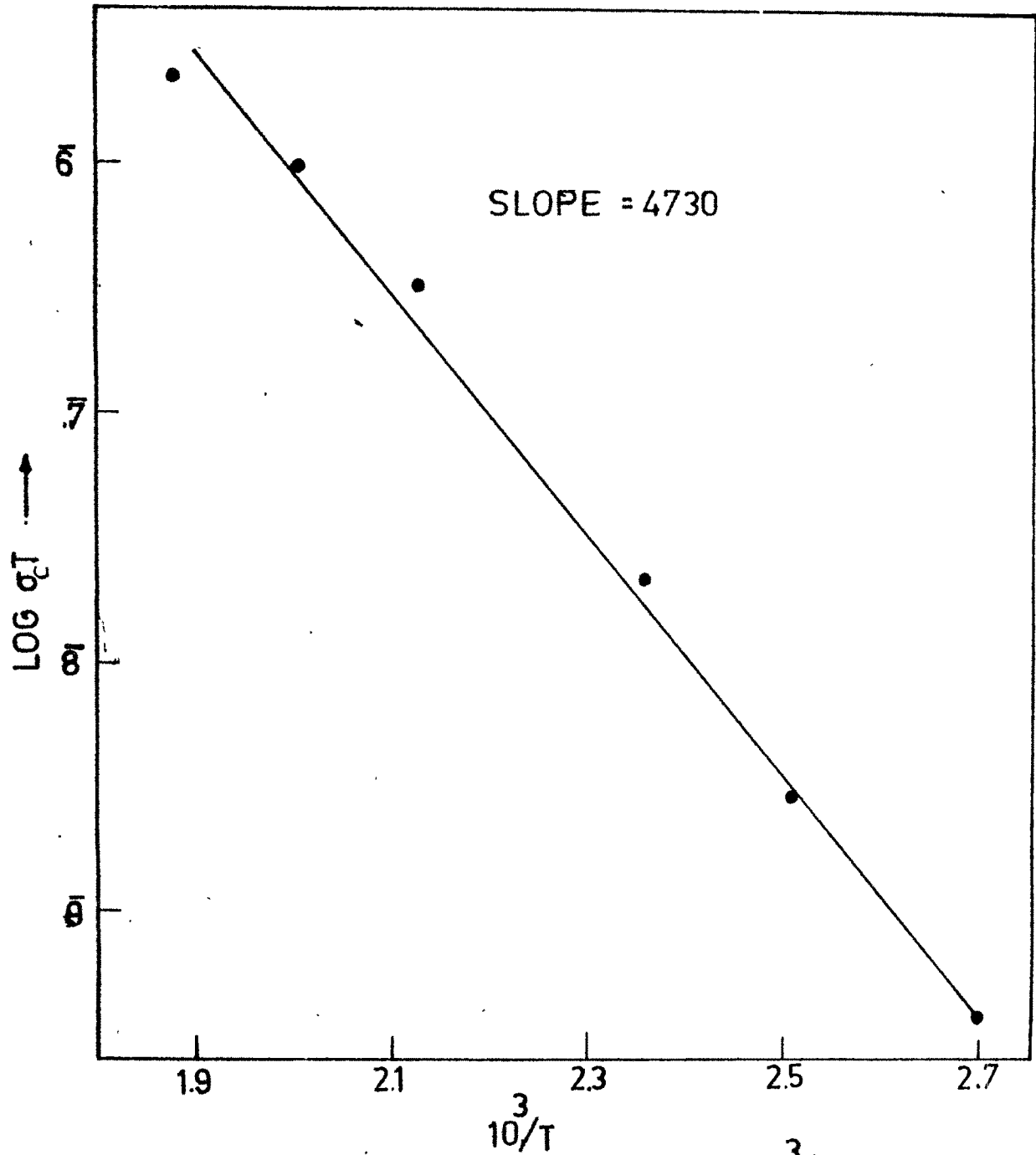


FIG 6.17 PLOT OF $\text{LOG } \sigma_c T$ VS $10^3/T$

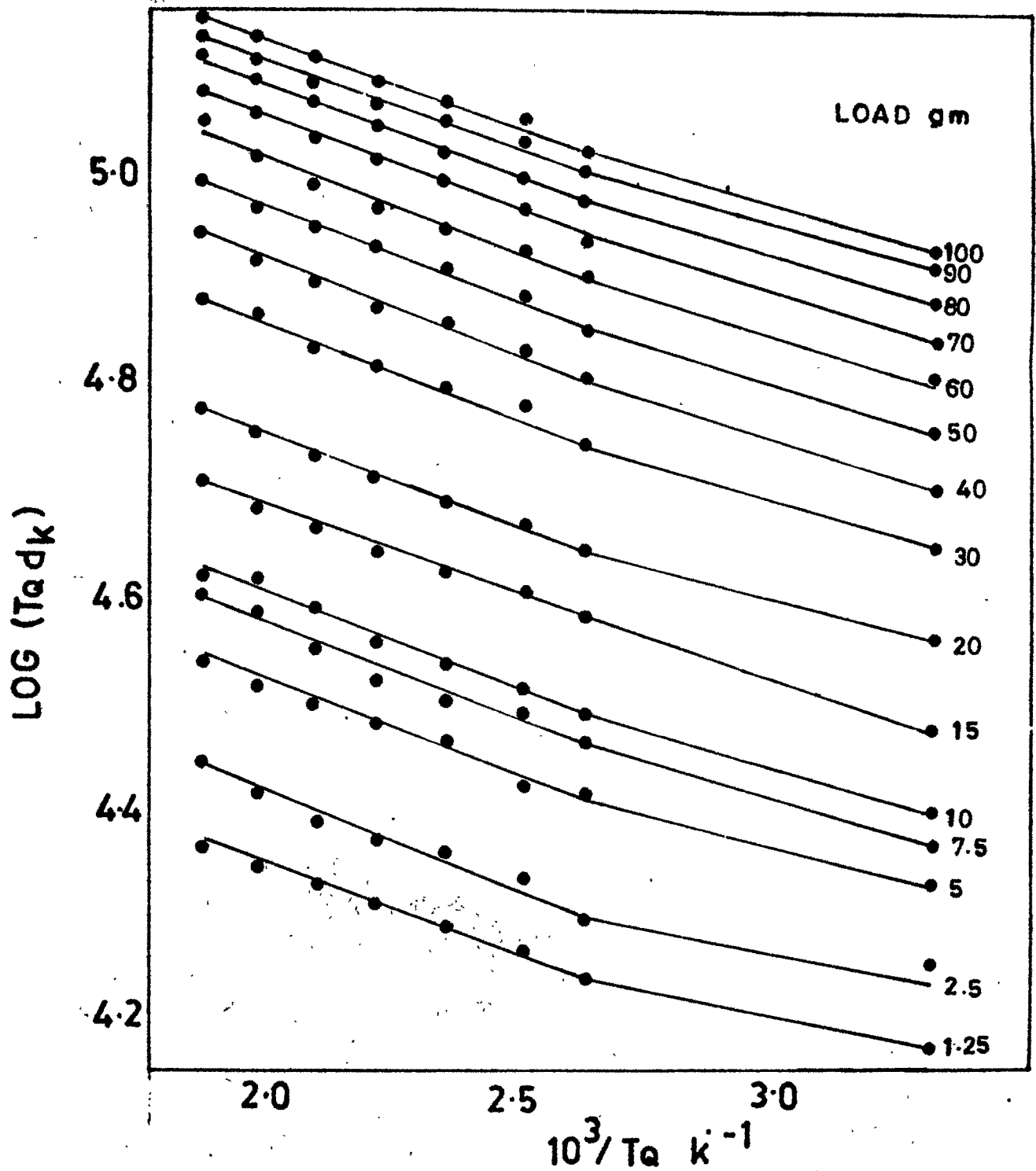


FIG 6-18 PLOT OF LOG Tad_k VS 10³ / Ta

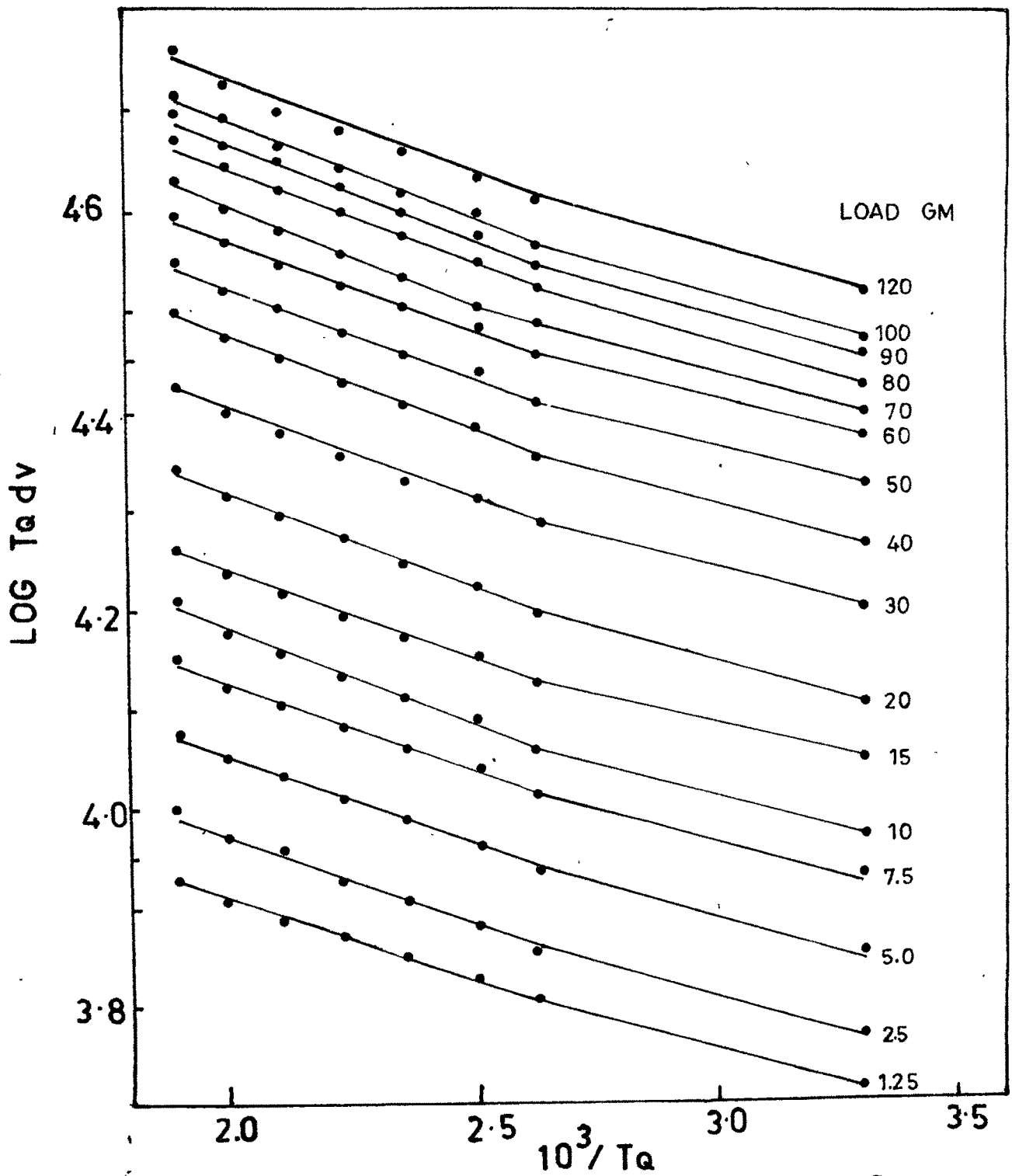


FIG 6-19 PLOT OF LOG T_{adv} VS $10^3 / T_a$

sodium nitrate crystals due to quenching. This is supported by the empirical relation between hardness and Schottky defects in alkali halides at room temperature.¹¹ With the increase of applied load dislocations which are produced on cleavage face by indentation would start interacting with quenched-in point defects. As a result the effect of load on indenter is reflected in the lost parallelism of graphs near the loads where kink in $\log P$ vs $\log D$ graphs is observed. For higher loads, the graphs of $\log T_Q d$ vs $1/T_Q$ are again parallel to one another. It is thus clear why the graph of hardness against load is divided into three regions. In the first region (AB) the quenched-in point defects operate through grown and aged dislocations ignoring to a greater extent the contribution of fresh dislocations introduced by indentations; at higher loads (CD portion of the graph) the freshly introduced dislocations are more active than grown and aged dislocations in 'hardening' the crystals. For intermediate loads (associated with portion BC of the graph) there appears to be a complicated interaction between quenched-in point defects, aged dislocations and freshly introduced dislocations, resulting in the non-linear behaviour of hardness versus load. It should be remarked here that the line of demarcation between low loads and intermediate loads, between intermediate loads and high loads is not well-defined.

The value of load at which hardness acquires a maximum value is not constant but changes with the quenching temperature. It has slight shift towards lower load value with higher quenching temperature. This is more clear from the graph of $\log P$ vs $\log d$ and can be inferred to a certain extent, from the plots of hardness versus load.

It is clear from the above discussion that the behaviour of hardness is similar to that of electrical conductivity for various quenching temperatures. Further the low load hardness values in the first region are governed by nature, ^{is} distribution and concentration of quenched-in point defects, and their interactions with grown and aged dislocations. Further the third region CD of the plot of hardness versus load is governed mainly by freshly introduced dislocations. Hence it is desirable to discuss the comparative behaviour of these two quantities with respect to temperature. Out of several combinations of these quantities to form different functions, the function $(\log \sigma_c / \bar{H}) / \log T$ has almost a constant value (Table 6.16) in a high load region (HLR). Hence the graph of $\log \sigma_c / \bar{H}$ versus $\log T$ are plotted for HLR (Fig. 6/20). The graph is a straight line for Knoop as well as Vickers hardness numbers. It is thus clear that for a given crystal σ_c / \bar{H} has a constant value at

Table 6.16

T_Q	$\text{Log } T_Q$	$\overline{H_K}$	$\overline{H_V}$	σ_C	$\text{Log } \sigma_C / \overline{H_K}$	$\text{Log } \sigma_C / \overline{H_V}$
373	2.5717	19.01	19.55	1×10^{-12}	14.7210	14.7088
398	2.5998	18.87	19.30	7.5×10^{-12}	13.5992	13.5895
423	2.6263	19.11	19.49	5.0×10^{-11}	12.4177	12.4097
448	2.6512	19.50	19.71	1×10^{-10}	12.7099	12.7053
473	2.6748	19.94	19.91	7×10^{-10}	11.5453	11.5460
498	2.6972	19.99	20.07	2×10^{-9}	10.0002	11.9984
533	2.7267	20.65	20.27	4×10^{-8}	9.2871	9.2952

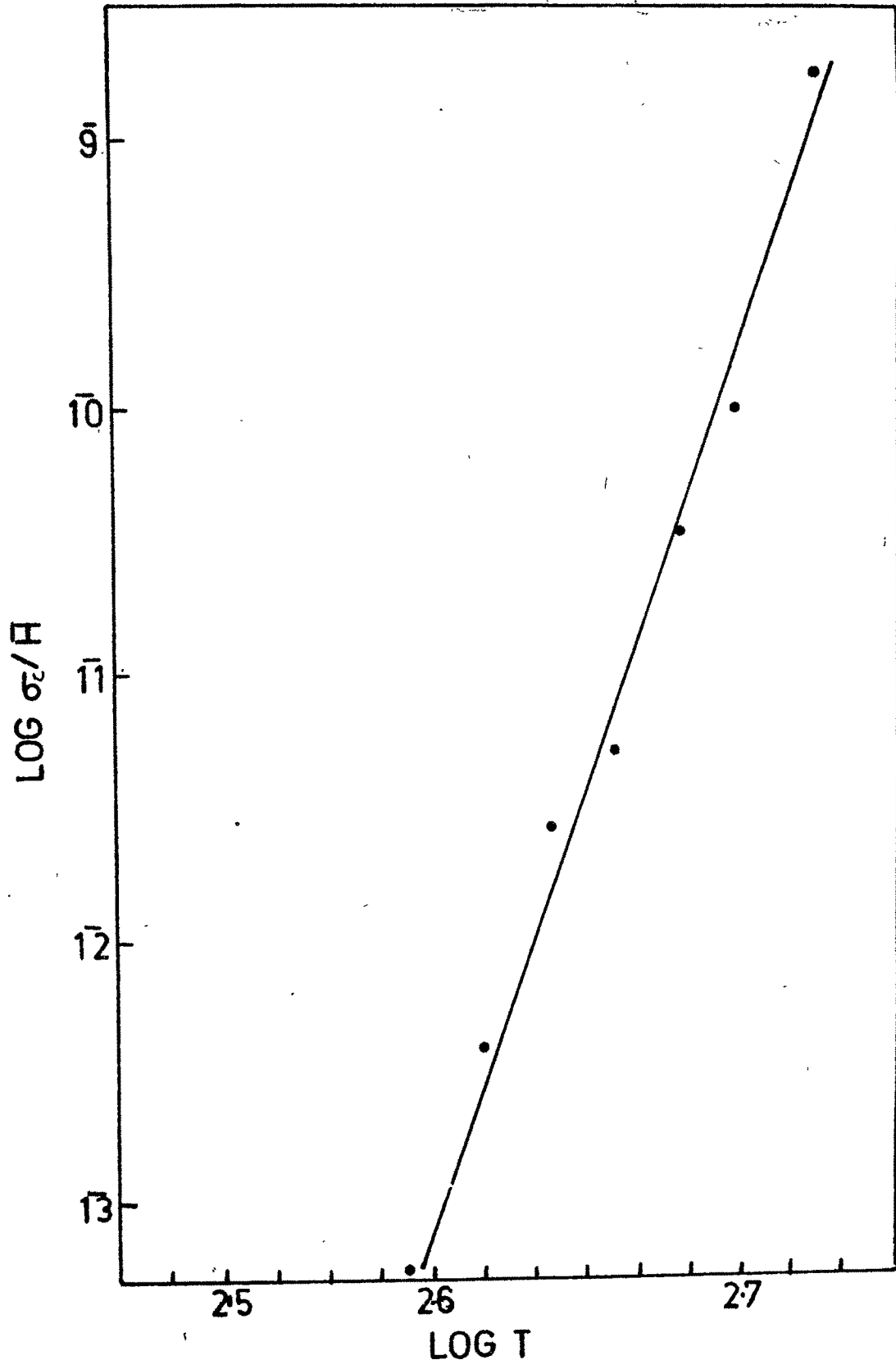


FIG. 6-20 PLOT OF LOG σ_c/H vs LOG T

a constant temperature for HLR. Since electrical conductivity is proportional to the diffusion constant (Nernst-Einstein equation) it can be concluded that for a given ionic crystal, the ratio of diffusion constant to hardness (number) at a constant temperature is constant in high load region. This also indicates that defect structure of the material in general and in particular equilibrium concentration of point defects at the quenching temperature for the same material for which two quantities are determined is more or less identical.

To verify the results obtained from hardness studies, the data on hardness is combined with the data on electrical conductivity. The electrical conductivity of sodium nitrate crystal is basically ionic in character. At temperature $T^{\circ}\text{K}$ it is given by

$$\sigma_c = \frac{\sigma_{oc}}{T} \exp(-E/KT) \quad \dots (6.64)$$

$$\log \sigma_c T = -\frac{E}{KT} \log_{10} e + \log \sigma_{oc} \quad \dots (6.64a)$$

where σ_{oc} is a constant independent of temperature, K is Boltzmann's constant and activation energy is 0.94 ev.

Combination of eqn. 6.64 with

$$H T^k = \text{Constant yields}$$

$$\frac{\sigma_c}{H T^k} = \frac{\sigma_{oc}}{T \times \text{constant}} \exp(-E/KT)$$

$$\begin{aligned} \log \frac{\sigma_c T^{(1-k)}}{H} &= (\log \sigma_{oc} - \log \text{Constant}) \\ &\quad - \frac{E}{KT} \log_{10} e \\ &= \log D - \frac{E}{KT} \log_{10} e \quad \dots (6.65) \end{aligned}$$

where $\log D = \log \sigma_{oc} - \log \text{Constant}$.

It is obvious that if the value of 'K' calculated from hardness studies is substituted in eqn. (6.65) a plot of

$$\log \frac{\sigma_c T^{(1-k)}}{H} \text{ versus } \frac{1}{T} \text{ (Fig. 6.21, Table 6.17)}$$

should be similar in all respects to that of conductivity plot except for the intercept. The slope of the graph (Tab 6.17) (Fig. 6.21) is 4880. It is equal to $E/K \log_{10} e$. This simplification gives the value of E to be 0.97 ev which is

Table 6.17

T_Q	σ_c	$\frac{\sigma_c T_Q}{H_k}^{1-k}$	$\frac{\sigma_c T_Q}{H_k}^{1-k}$	$\text{Log} \left(\frac{\sigma_c T_Q}{H_k} \right)^{1-k}$	$\text{Log} \left(\frac{\sigma_c T_Q}{H_k} \right)^{1-k}$	$1/T \times 10^{+3}$
373	1×10^{-12}	5.3678×10^{-11}	5.1475×10^{-11}	$\bar{11.7298}$	$\bar{11.7176}$	2.7021
398	7.5×10^{-12}	1.1010×10^{-10}	1.1010×10^{-10}	$\bar{10.0418}$	$\bar{10.0418}$	2.5125
423	5×10^{-11}	3.0938×10^{-9}	3.033×10^{-9}	$\bar{9.4905}$	$\bar{9.4819}$	2.3641
448	1×10^{-10}	6.4833×10^{-9}	6.4150×10^{-9}	$\bar{9.8118}$	$\bar{9.8072}$	2.2321
473	7×10^{-10}	4.7293×10^{-8}	4.7293×10^{-8}	$\bar{8.6748}$	$\bar{8.6755}$	2.1141
498	2×10^{-9}	1.4318×10^{-7}	1.4318×10^{-7}	$\bar{7.1559}$	$\bar{7.1541}$	2.0080
533	4×10^{-8}	3.0012×10^{-6}	3.0577×10^{-6}	$\bar{6.4773}$	$\bar{6.4854}$	1.8760

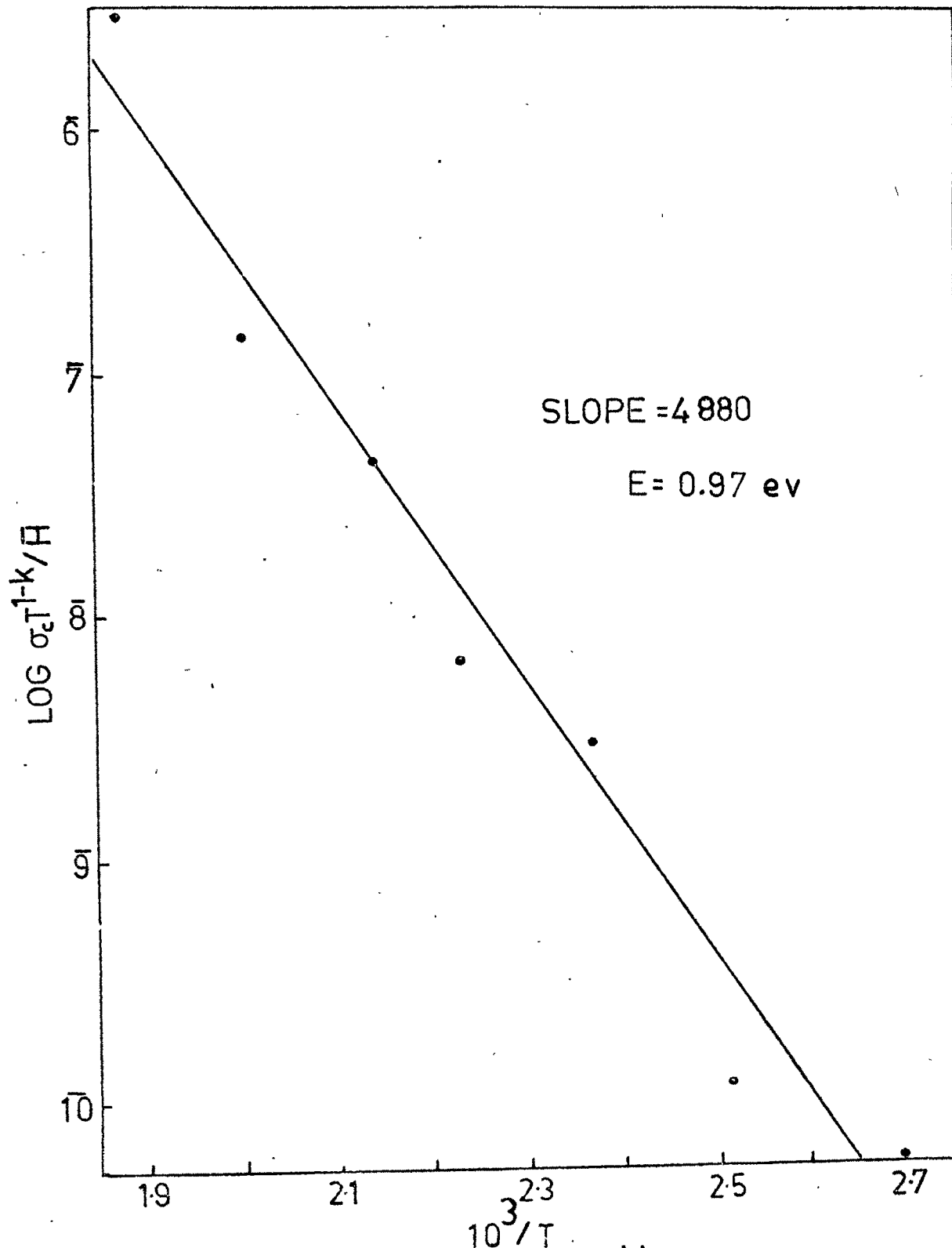


FIG.6-21 PLOT OF $\text{LOG } \sigma_c T^{1-k}/H$ vs $10^3/T$

almost equal to the observed from conductivity plot (fig. 6.17) of $\log \sigma_c T$ versus $1/T$ (eqn. 6.64a) in the temperature range of 100°C to 260°C . This result clearly supports the earlier empirical formula viz.

$$H T^k = \text{Constant},$$

in the high load region where hardness is constant and independent of applied load. The above procedure was followed while studying Quench hardness and electrical conductivity of KCl and KBr⁵ crystals.

6.4 CONCLUSIONS

- (1) The study of hardness of untreated and thermally treated specimens (quenched from different temperatures to room temperature) indicate that the plot between hardness and load can be qualitatively divided into three portions viz. low load region corresponding to linear part, intermediate load region corresponding to nonlinear part and high load region corresponding to linear portion of the graph.
- (2) Hardness depends upon quenching temperature. A relation between hardness and quenching temperature in the high load region is given by,
 - (a) $H T_Q^k = \text{Constant}$ where $K = -0.17$ for NaNO_3 crystals.

(b) $a_2 T_Q^r = \text{Constant}$ where $r = -0.07$ for NaNO_3 crystals.

(c) $a_2 H^s = \text{Constant}$ where $s = -0.75$ for NaNO_3 crystals.

- (3) Knoop hardness number has almost the same value as that of Vickers hardness number at any given temperature.
- (4) The mechanism of hardness and electrical conductivity in ionic crystals in general and sodium nitrate crystal in particular are more or less similar.
- (5) The ratio of hardness (Vickers or Knoop hardness number) to electrical conductivity of an ionic crystal in general and sodium nitrate crystal in particular is constant at constant temperature, in the high load region.

REFERENCES

1. Mott, B.L. 'Microindentation hardness testing', Butterworth Scientific Publications, London, Ch.1, 1956.
2. Saraf, C.L. Ph.D. Thesis, M.S. University of Baroda, Baroda, 1971.
3. Mehta, B.J. Ph.D. Thesis, M.S. University of Baroda, Baroda, 1972.
4. Shah, R.T. Ph.D. Thesis, M.S. University of Baroda, Baroda, 1976.
5. Acharya, C.T. Ph.D. Thesis, M.S. University of Baroda, Baroda, 1978.
6. Bhagia, L.J. Ph.D. Thesis, M.S. University of Baroda, Baroda, 1982.
7. Meyer, L. Quoted in 'Science of hardness Testing and its Research Applications', Amer. Soc. for metals, Ohio, 1973.
8. C. Ramasastry and Y.V.G.S. Murti Proc. Roy. Soc. A(GB), 305, 441-55 (1968).
9. Bhagat, S.D. M.Sc. Appl. Physics Dissertation, M.S. University of Baroda, Baroda, 1982.
10. Aust, K.T. ; Peat, A.J. and Westbrook, J.W. Act. Met., 14, 1469, 1966.
11. Shukla, M.S. and Bansigir, K.G. J. Phys. D. Appl. Phys., 9, 149, 1976.

CHAPTER - VII

GRAPHICAL ANALYSIS OF

EXPERIMENTAL OBSERVATIONS

CHAPTER - VII

GRAPHICAL ANALYSIS OF

EXPERIMENTAL OBSERVATIONS

		<u>PAGES</u>
7.1	Introduction	144
7.2	Analysis of Plot of Log P vs. Log d ..	144
7.3	Analysis of plot of Log $\bar{H} T_Q$ vs. Log T_Q	145
7.4	Analysis of plot of	
	Log $(\sigma T^{1-k}/\bar{H})$ vs. $10^3/T$	146
7.5	General remarks	147

7.1 INTRODUCTION

It is clear from the previous chapters V and VI on the studies of variation of diagonal length of indentation mark with applied load and of variation of hardness with applied load for thermally treated and untreated samples of synthetic single crystals of sodium nitrate that the high load region of the graph of hardness versus applied load and second part of the straight line plot of $\log P$ versus $\log d$ are amenable to interpretation to a certain extent and that it is possible to provide empirical relations between quench hardness (\bar{H}), quenching temperature (T_Q) and diagonal length of indentation (d) and T_Q and also to determine the value of exponent n . Hence the graphical analysis of the straight line plots corresponding to the high load region is presented here.

7.2 ANALYSIS OF PLOT OF LOG P vs. LOG d

It is obvious that for most of the quenching temperatures variations in the exponent value represented by the slope n_2 (cf. Table 5.3 and 5.4) in the high load region is small except for a few quenching temperatures. This is particularly most noticeable for indentation produced by Knoop indenter (e.g. percentage change in slope value for quenching temperatures 303° , 398° and 448°K

(Table 7.1)^{to 7.5}. It is difficult to account for these variations on the basis of a few factors only.

7.3 ANALYSIS OF PLOT OF $\text{LOG } \bar{H} T_Q$ vs. $\text{LOG } T_Q$

Tables 7.6 A, B, C, D, E are prepared to analyse the straight line plot of $\text{Log } \bar{H} T_Q$ versus $\text{log } T_Q$. Table 7.6A presents effect of the spread of the extreme observations on the slope. In the method of visual estimation of the best straight line the mean values of $\text{Log } \bar{H} T_Q$ and $\text{Log } T_Q$ (cf. Table 7.6A) are calculated for the Knoop and Vickers indenters used to determine quench hardness in the high load region from the table 6.3 and the graph (fig. 6.9). The extreme observations which indicate a large amount of scattering from the straight line plot are mentioned in table 7.6A. The slopes are determined from these pairs of observations and are compared with the slopes obtained from the graph. The percentage changes in the slopes from the graphical values are mentioned in the last column. It should be noted that except for a large percentage change (14.2%) in value of slope from actual graphical value (Table 7.6A) where a Knoop indenter was used for hardness work, the changes in the slope value calculated by applying various methods such as zero sum method (Table 7.6B), centroid method (Table 7.6C₁ and C2), data used in specific manner (Table 7.6D) and regression

Table 7.2 Zero sum method : Plot of $\log p$ vs. $\log d$ (Region II)
 (cf. equation 3.3 Chapter III)

Quenching Temperature T_Q °K	Knoop indenter			Vickers indenter		
	Calculated values of n_2	Values from graph n_2	% change in values of n_2	Calculated values of n_2^c	Values from graph n_2	% change in values of n_2
303	1.8425	1.87	1.47	1.9414	1.9	2.17
373	1.8916	1.87	1.15	1.8916	1.9	0.44
398	1.8929	1.87	1.22	1.8916	1.9	0.44
423	1.8766	1.87	0.35	1.8703	1.9	1.56
448	1.8593	1.87	0.57	1.8609	1.9	2.05
473	1.8804	1.87	0.55	1.8379	1.9	3.26
498	1.8646	1.87	0.29	1.8369	1.9	3.32
533	1.8589	1.87	0.59	1.8247	1.9	3.96

Table 7.3 Centroid method A for plot of Log P vs. Log d (Region II)

Quenching Temperature T_Q °K	Knoop indenter			Vickers indenter		
	Calculated value of slope n_2	Value of slope from graph n_2g	% change in n_2 from n_2g	Calculated value of slope n_2	Value of slope from graph n_2g	% change in n_2 from n_2g
303	1.8426	1.87	1.46	1.941	1.9	2.15
373	1.8917	1.87	1.11	1.891	1.9	0.47
398	1.8929	1.87	1.22	1.891	1.9	0.47
423	1.8766	1.87	0.35	1.87	1.9	1.57
448	1.8593	1.87	0.57	1.86	1.9	2.1
473	1.8804	1.87	0.55	1.837	1.9	3.3
498	1.8646	1.87	0.28	1.837	1.9	3.3
533	1.8589	1.87	0.59	1.826	1.9	3.89

* Centroid B method gives points on line of plot log P vs. log d hence the slope is almost the same.

Table 7.4 Data used in a specific manner : Plot of $\log P$ vs. $\log d$ (Region II)
 (cf. equations 3.20 Chapter III)

Quenching Temperature T_Q °K	Knoop indenter		Vickers indenter		
	Calculated values of n_2	Values from graph n_2	Calculated values of n_2	Values from graph n_2	
		% change in values of n_2		% change in values of n_2	
303	1.8111	1.87	3.14	1.9	5.41
373	1.9088	1.87	2.07	1.9	1.38
398	1.9181	1.87	2.57	1.9	1.72
428	1.9173	1.87	2.52	1.9	2.92
448	1.8579	1.87	0.64	1.9	1.789
473	1.8904	1.87	0.01	1.9	1.87
498	1.8787	1.87	0.46	1.9	7.47
533	1.8808	1.87	0.57	1.9	4.79

Table 7.5 Regression Coefficients : Plot of $\log P$ vs. $\log d$ (Region II)
 (Ref. eqns. 3.30, 3.35 Chapter III)

Quenching Temperature T_Q $^{\circ}K$	Knoop indenter			Vickers indenter			
	Calculated slope m_1	Calculated slope $1/m_2$	Value of % change in m_1 and $1/m_2$ from graph mg	Calculated slopes m_1	Calculated slopes $1/m_2$	Value of slope from graph mg	% change in value of m_1 and $1/m_2$ from mg
303	1.8906	1.8914	1.87	1.8568	1.8975	1.9	0.12
373	1.8826	1.8857	1.87	1.7549	1.8828	1.9	0.90
398	1.8702	1.8726	1.87	1.8790	1.8814	1.9	0.89
423	1.8646	1.8204	1.87	1.8709	1.8419	1.9	3.05
448	1.8460	1.8477	1.87	1.8946	1.8688	1.9	1.64
473	1.8797	1.8747	1.87	1.9107	1.8946	1.9	0.28
498	1.8679	1.8712	1.87	1.9117	1.8882	1.9	0.62
533	1.8414	1.8986	1.87	1.8546	1.8208	1.9	4.166

coefficients (Table 7.6E) are small (2 to 3%) and within experimental errors. The relatively large change in value (14.2%) suggests not only the reexamination of the extreme observations but also the considerations of several experimental errors and physical and chemical properties of the crystal. Since this remark is of general nature, it is considered in detail in article 7.5.

7.4 ANALYSIS OF PLOT OF $\text{LOG} \left(\frac{\sigma T^{1-k}}{\bar{H}} \right)$ vs. $10^3/T$

The graph of $\text{Log} \left(\sigma T^{1-k} / \bar{H} \right)$ vs. $10^3/T$ is to determine the activation energy for conduction of electricity through sodium nitrate. The activation energy calculated by employing method of visual estimation (Table 7.7A), Zero-sum method (Table 7.7B), Centroid method (Table 7.7C) and statistical method (Table 7.7D) is shown in respective tables along with its percentage deviation from the actual plot (fig. 6.21). The variation is from 12 to 19%. This indicates that the mechanism of conduction of electricity is not completely identical with that of hardness. Since the scattering of points around the actual plot is tolerable, the mechanisms are likely to be similar in certain respects.

7.5 GENERAL REMARKS

It is worthwhile to consider in general the analysis of straight line plots made above by employing the known

methods of fitting the lines. Besides personal errors, there are errors which could creep in due to physical properties of sodium nitrate crystal and due to certain basic requirements for taking observations with the help of microscope and indenter.

While carrying out the indentation work several precautions are required to be taken e.g. the surface to be tested should be normal to the axis of the indenter and the microscope. The specimen should be firmly fixed on the glass slide. The centre of gravity of the applied load should be on the vertical axis of the indenter and microscope. The vibrations due to fan etc. should be stopped during the experimental work of indentation and measurement of the diagonal length. The micrometer eyepiece divisions should be set on one of the ends of a diagonal of indentation mark without introducing error due to backlash. The region to be indented should be free from cleavage lines, cracks, twins etc. for carrying out the entire hardness work, which is normally spread over a period of about 6 hrs. The speed of fine motion should be constant and maintained at $0.13 \frac{\text{mm}}{\text{sec}}$ per second so as to maintain the static nature of the test. The clearance of the indenter should be $\frac{1}{10}$ revolution. Strict count of the revolution should be made as fine motion is advanced. The contact of the indenter with the specimen

surface should be maintained for a fixed period (15 sec.) for all applied loads. On removing the indenter speed should be identical with the forward speed towards the specimen. When a series of indentations are to be made the distance between any two consecutive indentations should not be less than twice the length of diagonal. In the present case this distance is kept about eight times the diagonal length. As a result plastic flow around an indentation is not affected by that of other indentation. The indentation mark should be a square or a rhombus depending upon the use of the indenter, namely Vickers or Knoop. If an errors exists in the axial setting of the pyramid or the levelling of the sample to be tested, it should be checked first.

There are certain difficulties in working with the single crystals of sodium nitrate. It has a perfect rhombohedral cleavage. Hence with a little pressure along a cleavage direction, cleavage surface can be easily produced. It is soft, can be shattered into pieces by a small blow and sensitive to the little touches made unintentionally while fixing it on a glass slide by araldite or galva cement. Further its power to absorb water vapour from atmosphere at ordinary temperatures is more noticeable ; its surface is therefore easily affected by the water vapoure present in the atmosphere. The literature survey

reveals that not much work has been reported on this crystal. This is likely to be due to such fundamental natural difficulties. To overcome these difficulties, the experimental work was confined for about eight months in a year. Further studies were carried out in a small room (about 8 ft x 8 ft) which was not exposed directly to the atmosphere. The exhaust fans, room heaters, vapour absorbers like calcium chloride were used to control the humidity in the room.

The author has taken extra care to avoid difficulties associated with the preparation of the specimen (crystal) and with the indentation work described above. However there is a distinct possibility that enough attention might not have been given to one or a couple of factors mentioned above, leading to large percentage deviation from the actual graphical plot, observed in some of the tables mentioned above. It should also be remarked here that a large number of observations give results which, when analysed by various methods are within experimental errors. This is more so in view of the fact that the requirements of a particular method of analysis are not completely satisfied by the sets of observations.